

Distribution Agreement

In presenting this thesis or dissertation as a partial fulfillment of the requirements for an advanced degree from Emory University, I hereby grant to Emory University and its agents the non-exclusive license to archive, make accessible, and display my thesis or dissertation in whole or in part in all forms of media, now or hereafter known, including display on the world wide web. I understand that I may select some access restrictions as part of the online submission of this thesis or dissertation. I retain all ownership rights to the copyright of the thesis or dissertation. I also retain the right to use in future works (such as articles or books) all or part of this thesis or dissertation.

Signature:

Maria A. Briscione

Date

Abnormal dopamine signaling in a mouse model of dystonia

By

Maria A. Briscione
Doctor of Philosophy

Graduate Division of Biological and Biomedical Science
Neuroscience

[Advisor's signature]

Ellen J. Hess, PhD
Advisor

John Hepler, PhD
Committee Member

Yoland Smith, PhD
Committee Member

H.A. Jinnah, MD/PhD
Committee Member

David Weinschenker, PhD
Committee Member

Machelle Pardue, PhD
Committee Member

Accepted:

Lisa A. Tedesco, Ph.D.
Dean of the James T. Laney School of Graduate Studies

Date

Abnormal dopamine signaling in a mouse model of dystonia

By

Maria A. Briscione
B.S., American University, 2012

Advisor: Ellen J. Hess, PhD

An abstract of
A dissertation submitted to the Faculty of the
James T. Laney School of Graduate Studies of Emory University
in partial fulfillment of the requirements for the degree of
Doctor of Philosophy
in Neuroscience
2019

Abstract

Abnormal dopamine signaling in a mouse model of dystonia

By Maria A. Briscione

Dystonia is a neurological movement disorder characterized by involuntary twisting movements and unnatural postures. Current treatment options for dystonia are palliative or inadequate for many patients. The limited effectiveness of current treatment options highlights our incomplete understanding of underlying pathomechanisms. Studies of acquired, inherited, and idiopathic dystonias have led to the identification of some common etiologies, specifically, abnormal dopamine signaling in the basal ganglia. Historically, dystonia has been viewed as a disorder of the basal ganglia and studies also directly support a role for postsynaptic dopamine dysfunction in the striatum, the primary input nucleus of the basal ganglia, in many forms of dystonia. Dopamine exerts opposite physiological effects on neural activity via activation of dopamine D1 (D1Rs) or D2 receptors (D2Rs), which are expressed on the primary output neurons of the striatum, so-called medium spiny neurons. However, the precise nature of abnormal postsynaptic dopamine-mediated intracellular signaling pathways in dystonia is unknown. Until recently, it was not possible to study abnormal postsynaptic dopamine-mediated signaling pathways in dystonia because suitable animal models that exhibit dystonia caused by dysfunction in dopamine neurotransmission were not available. However, studies in a recently developed mouse model of dystonia (DRD mice) have identified specific abnormalities in dopamine-mediated signaling implicated in dystonia. I utilized the DRD mouse model to determine the precise nature of striatal dysfunction that may distinguish dystonia from other abnormal motor phenotypes. My findings showed that dysfunction of both D1Rs and D2Rs is necessary for the expression of dystonia. I determined that DRD mice exhibit blunted striatal D2R-mediated intracellular signaling and supersensitive striatal D1R-mediated intracellular signaling. My results suggest that abnormal striatal D1R-mediated signaling may be necessary, but not sufficient, for the expression of dystonia. Determining the relationship between D1R- and D2R-mediated effects of abnormal striatal intracellular signaling may ultimately reveal the precise nature of dysfunction in dopamine neurotransmission that gives rise to dystonia.

Abnormal dopamine signaling in a mouse model of dystonia

By

Maria A. Briscione
B.S., American University, 2012

Advisor: Ellen J. Hess, PhD

A dissertation submitted to the Faculty of the
James T. Laney School of Graduate Studies of Emory University
in partial fulfillment of the requirements for the degree of
Doctor of Philosophy
in Neuroscience
2019

Acknowledgments

During my time in graduate school, I have been fortunate to have a community of inspiring mentors and supportive colleagues, friends, and family.

I would first like to thank my advisor, Dr. Ellen Hess, who embodies the level of intellectual curiosity, effectiveness, and thoughtfulness that I hope to emulate.

I would next like to thank the members of my committee, an inspiring group of scientists whom I have had the immense privilege to work with. Dr. “Buz” Jinnah provided a unique clinical perspective that not only helped guide my research, but also put a human face to my research and made me a more compassionate scientist. Dr. John Hepler’s thoughtful discourse helped develop my confidence and ultimately further my research. Dr. Mabelle Pardue’s long-time support and mentorship provided stability and direction throughout graduate school and for what comes next. Dr. Yolanda Smith’s enthusiasm and technical insight have been great sources of support. Dr. David Weinshenker has helped me navigate many challenges, both within and outside the lab, throughout my time in graduate school.

I also thank Drs. Victor Faundez and Malu Tansey for their valuable guidance. I would also like to thank Gary Longstreet for his positivity and support navigating graduate school.

I would also like to thank my current and former labmates: Dr. Gamze Kilic Berkmen, Sofia Bonno, Doug Bernhard, Simone Campbell, MS, Adam Cotton, Tony Downs, Dr. Xueliang Fan, Maggie Fagan, Dr. Rong Fu, Wendy Hughes, Jordan Ingram, Radhika Kadakia, Trisha Lala,

Lucy Outtrim, Dr. Jose Manuel Lopez Blanco, Kaitlyn Roman, Tejas Sardar, Diane Sutcliffe, MPH, and Yunmiao Wang. Thank you for your camaraderie and technical assistance. I would like to thank Christine Donsante, MS, for helping me develop the skills to conduct this research and for her constant support. Alec Shannon was a fantastic undergraduate student that I had the privilege to mentor, and I appreciate his contributions to this research.

I would like to thank my friends and family. Dr. Elizabeth Kline is a true professional enthusiast, and I am privileged to know her as a friend and colleague. Kristie Garza and Ashley McCullough Pilato, MSW, have been great sources of support throughout graduate school. My parents, Marge and Jay, and my in-laws, Cindy and Paul Sr., have provided unwavering encouragement and support. My husband, Paul, has shared in the ups and downs and makes it all worthwhile.

Finally, I would like to thank Dr. Ashok Dinasarapu, Laura Fox-Goharioon, Kaylor Kelly, and Dr. Dave Gutman for their technical support. I would also like to acknowledge the support of the Emory University Institutional Training Grant and the Training and Translational Research in Neurology Grant, which have supported my research and afforded me unique training opportunities.

Table of Contents

Chapter 1: Introduction

1.1. Historical perspective	1
1.2. Epidemiology	2
1.3. Phenomenology	2
1.3.1. Clinical characteristics	3
1.4. Treatments	4
1.4.1. Botulinum toxin	4
1.4.2. Small molecule medications	5
1.4.3. Surgical procedures	7
1.5. Etiology	8
1.5.1. Brain areas involved in dystonia	9
1.5.2. Evidence supporting basal ganglia dysfunction in dystonia	10
1.5.3. Evidence supporting dopamine signaling dysfunction in dystonia	11
1.6. Anatomy of the basal ganglia	15
1.7. Dopamine signaling in the striatum	17
1.7.1. Second messenger-dependent protein phosphorylation signaling	20
1.7.2. Transcriptional regulation	22
1.8. Abnormal postsynaptic dopamine-mediated signaling pathways in dystonia	23
1.9. Overall objective	28

Chapter 2: A novel method using QuPath to automate counts of immunoreactive cells and define striatal regions

2.1. Abstract	30
2.2. Introduction	31
2.3. Methods	32
2.4. Results	34
2.4.1. Confirmation of 6-OHDA-lesion	34
2.4.2. Immunoreactive cell count automation	35
2.4.3. Defining striatal regions	39
2.5. Discussion	39

**Chapter 3: Abnormal dopamine receptor-mediated intracellular signaling in a mouse
model of DOPA-responsive dystonia**

3.1. Abstract	41
3.2. Introduction	42
3.3. Methods	43
3.4. Results	50
3.4.1. Behavioral analysis of DRD mice expressing fluorescent reporter proteins	50
3.4.2. Distribution of D1R-tdTom and D2R-EGFP striatal neurons	51
3.4.3. D1R agonist-mediated signaling	53
3.4.4. D2R agonist-mediated signaling	59
3.4.5. D2R antagonist-mediated signaling	63
3.5. Discussion	69
3.5.1. Distribution of D1R- and D2R-MSNs	70
3.5.2. Regional differences in dopamine signaling in the dorsal striatum	70

3.5.3. D1R-mediated signaling	71
3.5.4. D2R-mediated signaling	73
3.5.5. Implications of blunted D2R inhibition in DRD mice	74
3.5.6. Conclusions	75

**Chapter 4: Determining the therapeutic mechanism of L-DOPA in a mouse model of
DOPA-responsive dystonia**

4.1. Abstract	76
4.2. Introduction	77
4.3. Methods	77
4.4. Results	79
4.4.1 L-DOPA-induced p-PKA-sub immunoreactivity	79
4.4.2 L-DOPA-induced p-ERK immunoreactivity	81
4.4.3. L-DOPA-induced c-Fos immunoreactivity	83
4.4.3. Correlation of L-DOPA-induced p-PKA-sub, p-ERK, and c-Fos immunoreactivity	85
4.5. Discussion	87
4.5.1. L-DOPA-induced postsynaptic intracellular signaling cascades	87
4.5.2. Regional differences in L-DOPA-induced ERK phosphorylation	89
4.5.3. Conclusions	90

**Chapter 5: Determining the role of D1Rs and D2Rs in the therapeutic mechanism of L-
DOPA in a mouse model of DOPA-responsive dystonia**

5.1. Abstract	92
5.2. Introduction	93
5.3. Methods	93
5.4. Results	96
5.4.1. Role of D1Rs in L-DOPA-induced abnormal striatal signaling in DRD mice	96
5.4.2. Role of D2Rs in L-DOPA-induced abnormal striatal signaling in DRD mice	98
5.4.3 Effects of dopamine receptor antagonist treatment on baseline behaviors	100
5.4.4. Role of D1Rs in L-DOPA-induced behavioral effects	102
5.4.5. Role of D2Rs in L-DOPA-induced behavioral effects	103
5.4.6. Role of D1R plus D2R-activation in L-DOPA-induced behavioral effects	105
5.5. Discussion	106
5.5.1. Role of D1Rs and D2Rs in the therapeutic effect of L-DOPA	107
5.5.2. Significance of D1R-antagonism in dystonia	108
5.5.3. Significance of D2R-antagonism in dystonia	108
5.5.4. Conclusions	109

Chapter 6: General discussion

6.1. Blunted D2R-mediated signaling in DRD mouse striatum	111
6.2. Supersensitive D1R-mediated signaling in DRD mouse striatum	114
6.3. Significance of L-DOPA-induced abnormal signaling in dystonia	115
6.4. Mechanism of L-DOPA-induced abnormal signaling in dystonia	119
6.5. Regional differences in postsynaptic intracellular signaling cascades in dystonia	121
6.6. Conclusions and future directions	123

**Appendix: Assessment of the striatal proteome in a mouse model of DOPA-responsive
dystonia**

A.1. Abstract	124
A.2. Introduction	125
A.3. Methods	125
A.4. Results	130
A.5. Discussion	140

References

References	145
------------	-----

List of Figures

Chapter 1: Introduction

Figure 1.1. Schematic of the functional anatomy of the basal ganglia	18
Figure 1.2. Dopamine-mediated second messenger signaling in MSNs	21
Figure 1.3. Schematic of postsynaptic dopamine signaling in the striatum	29

Chapter 2: A novel method using QuPath to automate counts of immunoreactive cells and define striatal regions

Figure 2.1. TH immunostaining	35
Table 2.1. Final positive cell counting parameters	37
Figure 2.2. Positive cell counts for p-ERK immunoreactivity in dorsal striatum	38
Table 2.2. Effect of p-ERK antibody dilution on positive cell counts in the dorsal striatum	38
Figure 2.3. Striatal regions	39

Chapter 3: Abnormal dopamine receptor-mediated intracellular signaling in a mouse model of DOPA-responsive dystonia

Figure 3.1. Cell type specificity analysis	49
Figure 3.2. Abnormal movement in DRD mice with RFPs	50
Figure 3.3. Representative fluorescent micrographs of DRD and normal mouse striatum	52
Figure 3.4. D1R-expressing and D2R-expressing cell density in normal and DRD mouse striatum	52
Figure 3.5. Effects of SKF 81297 treatment on striatal p-PKA-sub immunoreactivity in normal and DRD mice	54

Figure 3.6. Effects of SKF 81297 treatment on striatal p-ERK immunoreactivity in normal and DRD mice	56
Figure 3.7. Correlation of p-PKA-sub and p-ERK immunoreactivity following SKF 81297 treatment in DRD mice	57
Figure 3.8. Effects of SKF 81297 treatment on striatal c-Fos immunoreactivity in normal and DRD mice	58
Figure 3.9. Effects of quinpirole treatment on striatal p-PKA-sub immunoreactivity in normal and DRD mice	60
Figure 3.10. Effects of quinpirole treatment on striatal p-ERK Immunoreactivity in normal and DRD mice	61
Figure 3.11. Effects of quinpirole treatment on striatal c-Fos immunoreactivity in normal and DRD mice	63
Figure 3.12. Effects of raclopride treatment on striatal p-PKA-sub immunoreactivity in normal and DRD mice	64
Figure 3.13. Effects of raclopride treatment on striatal p-ERK immunoreactivity in normal and DRD mice	66
Figure 3.14. Effects of raclopride treatment on striatal c-Fos immunoreactivity in normal and DRD mice	68
Table 3.1. Summary of immunohistochemistry results	70

Chapter 4: Determining the therapeutic mechanism of L-DOPA in a mouse model of DOPA-responsive dystonia

Figure 4.1. Effects of L-DOPA treatment on striatal p-PKA-sub immunoreactivity in	80
---	----

normal and DRD mice	
Figure 4.2. Effects of L-DOPA treatment on striatal p-ERK immunoreactivity in normal and DRD mice	82
Figure 4.3. Effects of L-DOPA treatment on striatal c-Fos immunoreactivity in normal and DRD mice	84
Figure 4.4. Correlation of p-PKA-sub, p-ERK and, and c-Fos immunoreactivity following L-DOPA treatment in DRD mice	86
Chapter 5: Determining the role of D1Rs and D2Rs in the therapeutic mechanism of L-DOPA in a mouse model of DOPA-responsive dystonia	
Figure 5.1. Effects of SCH 23390 pretreatment on L-DOPA-induced abnormal striatal signaling in DRD mice	97
Figure 5.2. Effects of raclopride pretreatment on L-DOPA-induced abnormal striatal signaling in DRD mice	100
Figure 5.3. Effects of dopamine receptor antagonists on baseline behaviors	101
Figure 5.4. Effects of SCH 23390 pretreatment on L-DOPA-mediated abnormal movements and locomotor activity in DRD mice	103
Figure 5.5. Effects of raclopride pretreatment on L-DOPA-mediated abnormal movements and locomotor activity in DRD mice	104
Figure 5.6. Effects of combined SCH 23390 and raclopride pretreatment on L-DOPA-mediated abnormal movements and locomotor activity in DRD mice	106

Chapter 6: General discussion

Figure 6.1. Potential mediators of blunted D2R-mediated signaling in D2R-MSNs	113
Figure 6.2. Schematic of D1R supersensitivity in the DRD mouse striatum and its relationship to locomotor hyperactivity and dystonia	117
Figure 6.3. Proposed mechanism of sensitized PKA/p-ERK/c-Fos signaling in D1R-MSNs in the dorsal striatum of DRD mice	121

Appendix: Assessment of the striatal proteome in a mouse model of DOPA-responsive dystonia

Figure A.1. Volcano plot of the significance levels of the expression difference between normal and DRD mice versus the mean difference in protein expression levels	131
Figure A.2. Differentially regulated proteins in the striatum of DRD compared to normal mice	133
Figure A.3. Heat map of proteins upregulated and downregulated in the striatum of normal and DRD mice	134
Table A.1. Differentially regulated proteins ($p < 0.05$) previously associated with dystonia	136
Figure A.4. Cytoscape enriched pathways of differentially expressed proteins ($p < 0.05$)	137
Table A.2. Cytoscape enriched pathways of differentially expressed proteins ($p < 0.05$)	138
Figure A.5. Cytoscape enriched KEGG pathways of differentially expressed proteins ($p < 0.05$)	139
Table A.3. Cytoscape enriched KEGG pathways of differentially expressed proteins ($p < 0.05$)	140

Chapter 1: Introduction

1.1. Historical perspective

Dystonia is a neurological movement disorder characterized by involuntary twisting movements and unnatural postures. The first description of dystonia dates back to 1911, when neurologist Hermann Oppenheim coined the term, “Dystonia Musculorum Deforms” to describe abnormal posturing in four unrelated children (Oppenheim 1911, Klein and Fahn 2013). An accurate historical account of this movement disorder is difficult to obtain prior to the advent of a unifying nomenclature (Newby, Thorpe et al. 2017). However, some accounts speculate Alexander the Great’s (356-23 BC) abnormal neck posture, which was portrayed in various statues and described in texts, was ocular torticollis (Lascaratos and Damanakis 1996), a form of cervical dystonia characterized by an abnormal neck rotation to the left or right.

Oppenheim, in his initial account of dystonia, recognized dystonia to be an organic disease of the nervous system (Klein and Fahn 2013). However, in the 1900s, Sigmund Freud’s psychoanalytical theories were popularized and supported a psychogenic model of dystonia (Newby, Thorpe et al. 2017). Freud’s psychoanalytical theories supported symbolic interpretations of the disorder; for example, twisting of the neck was interpreted as turning away from stressful situations (Newby, Thorpe et al. 2017). It was not until 1944, when Ernst Herz published a triad of articles, which described the symptoms (Herz 1944a), outlined the clinical classification (Herz 1944b), and proposed an underlying pathology of dystonia (Herz 1944c), that dystonia was reestablished as an organic disorder (Klein and Fahn 2013). In a statement from Herz in the final paper of the series (Herz 1944c), he captures the ultimate goal and struggle of translational research,

“In the establishment of a disease entity, the correlation of a clinical with a pathologic entity is an ideal demand which has not yet been fulfilled in the majority of instances.”

Our understanding of dystonia has rapidly developed. Oppenheim’s contemporaries reported similar cases in three affected siblings, which suggested the disease was heritable (Klein and Fahn 2013). In 1959, the heritability of dystonia was definitively argued (Zeman, Kaelbling et al. 1959), and less than a decade later an animal model of dystonia was created by lesioning the basal ganglia (Denny-Brown 1965). Today, scientists appreciate that dystonia occurs as a result of an underlying neurological pathology; however, many questions remain unanswered. In the following dissertation, I present an appraisal of the current knowledge in the field of dystonia research, and discuss the results of my experiments involving abnormal dopamine-mediated intracellular signaling in a mouse model of dystonia and its contribution to our greater understanding of this disorder.

1.2. Epidemiology

Current estimates place the number of patients with dystonia at 3 million worldwide, ranking dystonia as the third most prevalent movement disorder behind essential tremor and Parkinson’s disease (Defazio, Abbruzzese et al. 2004, Cloud and Jinnah 2010). However, the actual number of people with dystonia is likely much higher because a diagnosis requires access to a highly trained neurologist.

1.3. Phenomenology

In 2013, an international panel of experts published the following consensus classification of dystonia (Albanese, Bhatia et al. 2013): “Dystonia is a movement disorder characterized by sustained or intermittent muscle contractions causing abnormal, often repetitive, movements, postures, or both. Dystonic movements are typically patterned, twisting, and may be tremulous.”

1.3.1. Clinical characteristics

The clinical characteristics of dystonia are defined by four key phenomenological classifications: 1) body distribution, 2) age at onset, 3) temporal pattern, 4) and additional features (Albanese, Bhatia et al. 2013).

Body distribution. Many different body regions can be affected in dystonia; these include muscles in the cranial region, cervical region, larynx, trunk, and limbs. Affected regions may be involved individually or in different combinations. For example, affected regions may be singular (focal) or may include two or more contiguous regions (segmental), two or more noncontiguous regions (generalized), or regions that are restricted to one side of the body (hemidystonia). Dystonia can also progress to previously unaffected regions over time.

Age at onset. Dystonia can occur in a variety of different age ranges, including infancy (birth to 2 years), childhood (3-12 years), adolescence (13-20 years), early adulthood (21-40 years), and late adulthood (>40 years). The age at onset can generally inform the diagnosis and prognosis; for example, dystonia that begins in childhood is more likely to have an identifiable cause and develop into the more severe generalized dystonia.

Temporal pattern. Dystonia can occur consistently or can display variability. For example, dystonia can be task-specific and only occur only during a certain activity. Paroxysmal dystonia describes a sudden, limited dystonia that is usually induced by a trigger and can persist for a period of time even after the trigger has ended. Dystonia can also be diurnal, such that the occurrence and severity has a circadian fluctuation. Further, the disease course of dystonia can be static or progressive.

Additional features. Dystonia can be isolated or combined with other movement disorders. For example, dystonia is sometimes observed in patients with Parkinson's disease, a neurodegenerative movement disorder. Dystonia can also coexist with other neurological or systemic manifestations. Dystonia can be associated with non-motor symptoms including changes in mood, cognition, and sleep (Soeder, Kluger et al. 2009). Some patients may also experience pain, which can be unrelated to the severity of the motor symptoms (Kuyper, Parra et al. 2011).

1.4. Treatments

Current treatment options for dystonia are palliative or inadequate for many patients and vary based on the clinical manifestation of dystonia and the underlying etiology, if it is known.

Treatments available for dystonia include botulinum toxin injections, small molecule medications, and surgical procedures.

1.4.1. Botulinum toxin

The most common treatment for dystonia is botulinum toxin injected into the affected muscles to

chemically reduce activity at the neuromuscular junction. Botulinum toxin, which is produced by the bacterium, *Clostridium botulinum*, is highly effective at treating dystonia. For example, botulinum toxin injections can be effective for the treatment of blepharospasm (Defazio, Hallett et al. 2017), which is characterized by spasms of the orbicularis oculi muscles that close the eyelid, and laryngeal dystonia, which is characterized by intermittent airway obstruction due to laryngeal muscle spasms (Woisard, Liu et al. 2017). The use of botulinum toxin injections can be limited by improper selection of dosing and/or muscle groups, and less commonly due to intolerable side effects (Jinnah, Goodmann et al. 2016). Side effects are primarily localized and include bruising, excess weakness, and more rarely flu-like symptoms (Baizabal-Carvallo, Jankovic et al. 2013, Thenganatt and Jankovic 2014). The development of neutralizing antibodies and associated resistance is a potential concern associated with frequent or long-term use of botulinum toxin; however, newer formulations reduce an associated immune response (Jankovic, Vuong et al. 2003). Botulinum toxin injections are typically not utilized in generalized dystonia due to the complexity of contributing muscle groups.

1.4.2. Small molecule medications

Drugs used to treat dystonia have not been rigorously tested in large-scale, double-blinded, placebo-controlled trials; instead, evidence for efficacy comes from small-scale studies, retrospective reviews, and observational or anecdotal experience (Jinnah and Factor 2015). Many current drugs are only effective in a subset of patients and may be intolerable due to side effects.

Anticholinergic drugs are frequently prescribed to treat many types of dystonia (Jinnah and Factor 2015); however, the underlying mechanism of cholinergic dysfunction has yet to be fully determined (Pisani, Bernardi et al. 2007). Trihexyphenidyl (THP), a nonselective

muscarinic acetylcholine receptor antagonist, is one of the only small molecule medications proven effective using a prospective, double-blind study for the treatment of dystonia (Burke, Fahn et al. 1986). THP is poorly tolerated due to cholinergic central and peripheral side effects including dry mouth, blurred vision, constipation, urinary retention, and cognitive impairment. Thus, few patients take THP, despite its efficacy (Thenganatt and Jankovic 2014).

Administration of L-DOPA, the precursor to dopamine, can be an effective treatment when dystonia is caused by dysfunction in dopamine biosynthesis. This type of dystonia, DOPA-responsive dystonia, is in fact characterized by the dramatic symptom reduction after L-DOPA administration. L-DOPA is rarely effective in other forms of dystonia (Jinnah and Factor 2015); however, dopamine agonists may be effective in cases of dystonia where dopamine synthesis is not affected. Selective dopamine D2 receptor (D2R) agonists have been effective in reducing dystonia when assessed in various small-scale studies; however, more rigorous, controlled trials have not been conducted (Fan, Donsante et al. 2018). A recent analysis of published trials of dopamine receptor agonists in patients with idiopathic dystonia demonstrated apomorphine, an indirect dopamine D1 receptor (D1R) and D2R agonist, effectively reduced dystonia in two-thirds of treated patients. While coactivation of D1Rs and D2Rs may be effective in alleviating dystonia, apomorphine use is limited due to its side effects, which include nausea, psychosis, headache, sweating, and dizziness (Fan, Donsante et al. 2018). Further, apomorphine is delivered via subcutaneous injection due to its poor bioavailability, which contributes to its limited use. Dopaminergic agonists are not commonly prescribed to treat dystonia given the limited effectiveness in some populations and untoward side effects (Fan, Donsante et al. 2018).

Dopamine depleting agents and dopamine antagonists can also be effective in treating dystonia. Case report findings and small trials have demonstrated that clozapine, an atypical

neuroleptic that antagonizes D2Rs and dopamine D4 receptors (D4Rs), can be effective in treating dystonia (Trugman, Leadbetter et al. 1994, Karp, Goldstein et al. 1999). The use of both dopamine agonists and antagonists to treat dystonia may appear somewhat paradoxical, but in fact, this highlights the diverse etiology and associated difficulty in identifying appropriate treatment for patients.

Various other small molecule medications show some efficacy in treating dystonia (for a review see Cloud and Jinnah 2010, Thenganatt and Jankovic 2014, Jinnah and Factor 2015). For example, benzodiazepines, which function by enhancing inhibitory γ -aminobutyric acid (GABA) activity and are commonly used to treat anxiety, can also be effective in treating dystonia. Muscle relaxants can be used to address pain associated with muscle spasms. Baclofen, a GABA receptor agonist, can also be used to treat dystonia (Greene and Fahn 1992). Potential side effects of baclofen include sedation, dizziness, and hypotonia, and abrupt discontinuation of baclofen can result in withdrawal seizures. These side effects are exacerbated by the large doses necessary for oral administration. Intrathecal pumps, which deliver baclofen directly to the cerebrospinal fluid, and more recently intraventricular administration, which delivers baclofen directly to the brain via the lateral ventricle, may reduce the doses required and the associated side effects (Brennan and Whittle 2008, Turner, Nguyen et al. 2012). However, these routes of administration also incur additional drawbacks including risks of infection and withdrawal due to pump failure.

1.4.3. Surgical procedures

In addition to delivering drugs (i.e. intraventricular baclofen), surgical procedures can be used as last resort for the treatment of dystonia (for a review see Cloud and Jinnah 2010, Thenganatt and

Jankovic 2014, Jinnah and Factor 2015). Ablating the parts of the ventral motor thalamus (thalamotomy) or the internal globus pallidus (pallidotomy) can alleviate dystonia, which supports the involvement of these brain areas in dystonia. Ablative procedures, or surgical lesioning, are imprecise and irreversible and accordingly have largely been replaced with deep brain stimulation (DBS), also termed neuromodulation. Neuromodulation involves modulation of brain activity by an implanted electrical impulse generator (Jinnah and Factor 2015). The internal segment of the globus pallidus, the primary output structure of the basal ganglia, is the most common target of neuromodulation in dystonia (for a review see Ostrem and Starr 2008). In addition to neuromodulation, peripheral denervation is also utilized as a last resort in patients with cervical dystonia (Ravindran, Ganesh Kumar et al. 2019). While these last resort measures can be effective, the use of such procedures may also be limited by patients' overall health and access to procedures, whether due to financial reasons or the availability of highly trained neurosurgeons (Warnke 2015).

1.5. Etiology

The limited effectiveness of current treatment options highlights the etiological heterogeneity of dystonia and our incomplete understanding of underlying pathomechanisms. For example, there are more than 200 genes associated with dystonia (Lohmann and Klein 2017). These genetic alterations can follow dominant, recessive, X-linked, or mitochondrial patterns of inheritance (Albanese, Bhatia et al. 2013, Balint and Bhatia 2015, Jinnah and Hess 2018) and are involved in diverse biological processes (Lohmann and Klein 2017, Siokas, Aloizou et al. 2018, Jinnah and Sun 2019). For example, pathogenic variants in *TOR1A*, which encodes the protein, torsinA, a member of the AAA+ protein family (Hanson and Whiteheart 2005), causes nuclear envelope

abnormalities (Goodchild and Dauer 2004) and is associated with an early-onset isolated dystonia (Ozelius, Hewett et al. 1997, Klein 2014). Mutations in genes associated with dopamine biosynthesis have also been extensively studied (Jinnah and Hess 2018, Siokas, Aloizou et al. 2018). Dystonia can also be acquired as a result of infections, exposure to certain drugs and chemicals, and physical trauma (Jinnah and Hess 2018). Acquired, inherited, and idiopathic dystonias have led to the identification of some common etiologies, specifically, dopamine signaling in the basal ganglia.

1.5.1. Brain areas involved in dystonia

However, basal ganglia abnormalities are not responsible for all dystonias. Brain imaging studies of patients with dystonia reveal abnormalities in the cerebral cortex, basal ganglia, cerebellum, thalamus, midbrain, and brainstem (for a review see Neychev, Gross et al. 2011). Additionally, multiple lines of evidence support dysfunction of the cerebellum in dystonia (for a review, see Shakkottai, Batla et al. 2017). There are a number of genes causative for dystonia related to dysfunction of the cerebellum (Nibbeling, Delnooz et al. 2017). Studies of animal models of dystonia have also been instrumental in showing cerebellar dysfunction is integral in the expression of dystonia. Cerebellectomy abolishes dystonia in the DT rat model, in which a naturally occurring autosomal recessive pathogenic variant causes spontaneous dystonia (Lorden, McKeon et al. 1984, LeDoux 2011). Further, abnormal cerebellar metabolism has been identified in a mouse model that recapitulates a pathogenic variant in *TORIA*, which, as discussed, in humans is associated with an early-onset dystonia (Ozelius, Hewett et al. 1997, Zhao, Sharma et al. 2011, Klein 2014). Microinjection of low doses of kainic acid, a glutamate receptor agonist, in the cerebellar vermis induces dystonia in mice (Pizoli, Jinnah et al. 2002). Basal ganglia and

cerebellar outputs also interact in a number of ways, for example, at the level of cortical motor areas (for a review, see Shakkottai, Batla et al. 2017). Abnormal activity in the cerebellum may therefore alter basal ganglia function or vice versa. Together, these data support a role for abnormal cerebellar signaling in dystonia.

Dystonia may also be viewed as a disorder of the motor network (Jinnah, Neychev et al. 2017). In addition to dysfunction occurring in one of the aforementioned brain areas, abnormal communication between brain regions can also cause dystonia (Prudente, Hess et al. 2014). Further, the affected pathways may differ according to type of dystonia (Neychev, Gross et al. 2011). Nonetheless, a large body of evidence from many forms of dystonia supports a role for dopamine signaling in the basal ganglia.

1.5.2. Evidence supporting basal ganglia dysfunction in dystonia

Historically, dystonia has been viewed as a disorder of the basal ganglia. Even prior to Oppenheim's coining of the term dystonia, the basal ganglia were associated with movement disorders. In 1890, Hammond described pathology of the basal ganglia in an individual with athetosis, an abnormal movement disorder that historically overlapped with dystonia (Hammond 1890, Neychev, Gross et al. 2011). In the 1940s, Herz published a seminal paper that helped reestablish dystonia as a neurological disorder (Herz 1944c, Klein and Fahn 2013). In the paper, Herz proposed an underlying pathology of dystonia, which included abnormalities in basal ganglia regions. Multiple lines of evidence from more modern studies also support the role of the basal ganglia in dystonia.

While the incidence of overt neurological damage in dystonia is rare, dystonia has been observed after lesions, or structural damage, to the basal ganglia and related circuitry (Bhatia and

Marsden 1994). Moldy sugarcane poisoning in children in China is one such example. Children with moldy sugarcane poisoning initially present with gastrointestinal symptoms and noninflammatory encephalopathy, and notably, delayed-onset dystonia, which can persist for years (He, Zhang et al. 1995, Raïke, Jinnah et al. 2005). The main pathogen in moldy sugarcane, *Arthrinium* spp., produces the neurotoxin 3-nitropropionic acid (3-NPA), which causes degeneration of the basal ganglia. Lesions within the basal ganglia are, in fact, observed in affected children (Liu, Luo et al. 1992, He, Zhang et al. 1995, Ming 1995). Further, a study using computerized tomography (CT) scans of 28 patients presenting with focal or hemi-dystonia identified neuropathology within the caudate nucleus, putamen, thalamus, or a combination of these structures, which comprise the basal ganglia and related circuitry (Marsden, Obeso et al. 1985). More subtle dysregulations in the basal ganglia have been identified by sophisticated imaging techniques including voxel-based morphometry (VBM), [¹⁸F]-fluorodeoxyglucose positron-emission tomography (FDG-PET), and functional magnetic resonance imaging (fMRI) to list a few (for a review see Lehericy, Tijssen et al. 2013, Jinnah, Neychev et al. 2017). As briefly discussed, treatments targeting the basal ganglia are effective in individuals with dystonia. In fact, neuromodulation of the internal segment of the globus pallidus, which comprises the primary output nuclei of the basal ganglia, is effective in individuals with both acquired and inherited dystonias (Damier, Thobois et al. 2007, Ostrem and Starr 2008).

1.5.3. Evidence supporting dopamine signaling dysfunction in dystonia

Dopamine signaling, which modulates basal ganglia function, is implicated in dystonia. As briefly discussed, dystonia can be observed in patients with Parkinson's disease, a hypokinetic movement disorder caused by neurodegeneration of midbrain dopamine neurons and subsequent

dopamine depletion in the basal ganglia (Jankovic and Tintner 2001). Symptoms of Parkinson's disease include bradykinesia, akinesia, rigidity, postural abnormalities, and tremor (Bastide, Meissner et al. 2015). A dystonic foot is often the first symptom of Parkinson's disease, and blepharospasm and cervical dystonia may also be observed (Tolosa and Compta 2006).

Further, L-DOPA-induced motor complications occur in the vast majority of patients with Parkinson's disease who take L-DOPA, the "gold-standard" treatment for the management of parkinsonian symptoms (Bastide, Meissner et al. 2015, Rascol, Perez-Lloret et al. 2015). L-DOPA-induced dyskinesia (LID) is the most debilitating of the motor sequelae that commonly occurs after chronic L-DOPA use, and is characterized by abnormal involuntary movements. LID includes peak-dose dyskinesia, which describes the abnormal involuntary movements that occur when L-DOPA plasma concentrations peak. LID can also refer to the abnormal involuntary movements that arise after L-DOPA concentrations subside; this is termed OFF period dystonia. The pathomechanisms of the dystonia observed in LID involve states of both peak and low dopamine levels; however, this paradoxical relationship nonetheless supports a role of dysregulated dopamine neurotransmission in dystonia.

A number of pathogenic variants causative for dystonia involve genes associated with dopamine biosynthesis (Jinnah and Hess 2018, Siokas, Aloizou et al. 2018). Briefly, dopamine and other catecholamines, which include norepinephrine and epinephrine, are synthesized from the amino acid tyrosine. Tyrosine is derived primarily from dietary sources and is converted to L-3,4-dihydroxy-phenylalanine (L-DOPA) by tyrosine hydroxylase (TH), the rate-limiting enzyme in catecholamine synthesis (Nagatsu, Levitt et al. 1964). TH requires several cofactors, including tetrahydrobiopterin (BH₄), iron, and molecular oxygen. L-DOPA is then decarboxylated by the enzyme aromatic acid decarboxylase (AADC) to dopamine.

In 1994, four independent pathogenic variants in the gene coding GTP cyclohydrolase 1 (*GCH1*), which is required for the synthesis of BH₄, were reported (Ichinose, Ohye et al. 1994). To date, over 100 different pathogenic variants in *GCH1* coding and noncoding regions have been identified (Klein 2014, Lohmann and Klein 2017). Pathogenic variants in *GCH1* result in childhood onset dystonia characterized by a diurnal pattern of symptoms, in which symptoms are partially alleviated in the morning and worsen throughout the course of the day (Ichinose, Ohye et al. 1994). In 1971, Segawa and colleagues originally discovered this presentation of dystonia, often referred to as Segawa disease, and observed a drastic reduction in symptoms after administration of low-doses of L-DOPA (Segawa 2011), which had suggested the underlying cause was related to catecholamine synthesis dysfunction. The term DOPA-responsive dystonia was ultimately adopted to describe patients with dystonia resulting from heterogeneous etiologies that all respond to L-DOPA and often exhibit a similar phenotype as observed in Segawa disease (for a review see Wijemanne and Jankovic 2015). For example, in 1995, a substitution in *TH* that causes autosomal recessive DOPA-responsive dystonia was discovered in two siblings (Knappskog, Flatmark et al. 1995). This pathogenic variant (p.381Q>K) resulted in reduced TH protein stability and an ~85% reduction in enzymatic activity (Knappskog, Flatmark et al. 1995).

Further, dystonia is observed as a prominent feature in other disorders in which presynaptic dopamine regulation is abnormal. Abnormalities in dopamine nerve terminals and cell bodies are observed in Lesch-Nyhan disease, an inherited disease caused by pathogenic variants affecting purine synthesis (Nyhan, O'Neill et al. 1993, Ernst, Zemetkin et al. 1996, Gottle, Prudente et al. 2014). Lesch-Nyhan disease is a multisystem disease, and the clinical presentation consists of a number of severe neurological symptoms, including dystonia (Nyhan,

O'Neill et al. 1993). Children with hereditary dopamine transporter deficiency syndrome, which is caused by pathogenic variants in the gene encoding the dopamine transporter, display diminished dopamine reuptake and increased dopamine metabolites in cerebrospinal fluid, which may ultimately result in subsequent downregulation or desensitization of postsynaptic dopamine receptors. Clinically, dopamine transporter deficiency syndrome is characterized by dystonic, hypokinetic, parkinsonian, and pyramidal tract features (Kurian, Li et al. 2011).

Multiple studies also directly support postsynaptic dopamine dysfunction in many forms of dystonia. Drug-induced dystonia, or tardive dyskinesia, can occur as a result of treatment with typical antipsychotics, which antagonize D2Rs. In 1952, chlorpromazine was serendipitously shown to be effective in treating psychosis, and two years later drug-induced side effects including dystonia, parkinsonism, akathisia, were reported (Shen 1999). There is not a clear understanding of how these motor symptoms develop after chronic (Sethi, Hess et al. 1990), and more rarely acute (Mehta, Morgan et al. 2015), administration of typical antipsychotics, but given their antagonism of D2Rs (Laruelle, Frankle et al. 2005), dysregulations related to D2R-mediated signaling are likely involved (Prosser, Pruthi et al. 1989, Seeman, Weinshenker et al. 2005). Further, reduced striatal D2R availability is observed in writer's cramp (Berman, Hallett et al. 2013), blepharospasm (Horie, Suzuki et al. 2009), torticollis (Naumann, Pirker et al. 1998), and carriers of *TOR1A* pathogenic variants (Asanuma, Ma et al. 2005, Klein 2014). Increased striatal D1R availability is also associated with writer's cramp and laryngeal dystonia (Simonyan, Cho et al. 2017).

Evidence from multiple studies supports abnormalities in dopamine neurotransmission, including postsynaptic dopamine-mediated signaling, as a common underlying mechanism across diverse dystonias (Wichmann 2008). Postsynaptic dopamine-mediated signaling in the

basal ganglia is well characterized, and understanding the precise nature of dysfunction could lead to the development of drugs that target a common underlying pathology. This would facilitate the ultimate goal of developing novel therapeutics for dystonias that involve dopamine dysfunction for which current treatment options are limited.

1.6. Anatomy of the basal ganglia

The basal ganglia are involved in the execution of movement and motor learning and were first described by Thomas Willis in the 1600s (Sarikcioglu, Altun et al. 2008). The basal ganglia receive and process information from the cortex and project information back to the cortex via the thalamus. The basal ganglia are in fact not ganglia, but are a group of interconnected subcortical nuclei located within the basal regions of the cerebrum (Sarikcioglu, Altun et al. 2008). Individual basal ganglia nuclei include the striatum, globus pallidus, and the subthalamic nucleus (STN, DeLong and Wichmann 2010).

The striatum, named for the striated or striped appearance of interspersed grey and white matter, is the primary input nucleus of the basal ganglia. The striatum is comprised of ventral and dorsal divisions. The ventral striatum, or the nucleus accumbens (NAc), plays a central role in reward circuitry. The dorsal striatum consists of the caudate nucleus and the putamen. In humans these are distinct structures, but in rodents, the caudate nucleus and putamen are joined in a single structure, the caudoputamen (Grillner and Robertson 2016). The caudal putamen in humans, and the dorsolateral caudoputamen in rodents, is predominantly involved in motor control.

The striatum receives glutamatergic input from the entire cortex, which forms segregated anatomical and functional circuits between the cortex and striatum (McGeorge and Faull 1989,

Hintiryan, Foster et al. 2016, Hunnicutt, Jongbloets et al. 2016). Excitatory glutamatergic inputs also arise from the thalamus, preferentially from the intralaminar nuclei (Smith, Raju et al. 2004), and to a lesser extent from the STN (Gonzales and Smith 2015). Interneurons make up approximately 5-10% of striatal neurons and include GABAergic interneurons and large, aspiny cholinergic interneurons (Tepper and Bolam 2004, Gonzales and Smith 2015).

The primary output neurons of the striatum are medium spiny neurons (MSNs) or spiny projection neurons, which are named for the dense spinous morphology of their dendrites (Wilson and Groves 1980). MSNs are inhibitory, GABA producing projection neurons. In rodents, MSNs compose 90-95% of neurons in the striatum (Kemp and Powell 1971, Keefe and Gerfen 1995, Gerfen and Surmeier 2011). Two distinct, approximately equal subpopulations of MSNs give rise to the direct and indirect pathways of the basal ganglia (Graybiel 2000, Gerfen and Surmeier 2011). Direct pathway MSNs form monosynaptic projections to the substantia nigra pars reticulata (SNr), and the internal segment of the globus pallidus (GPi), which correspond to the rodent endopenduncular nucleus (EPN). Activation of the direct pathway facilitates the cortico-basal ganglia-thalamic transmission (DeLong and Wichmann 2010). As the name implies, indirect pathway MSNs indirectly project to the SNr/GPi (EPN), via the external segment of the globus pallidus (GPe), which corresponds to the rodent globus pallidus, and the STN. Activation of the indirect pathway results in inhibition of cortico-basal ganglia-thalamic transmission (DeLong and Wichmann 2010). There are also glutamatergic projections from the cerebral cortex that bypass the striatum and directly project to the STN, termed the hyper-direct pathway (Nambu, Tokuno et al. 2002). Selective optogenetic stimulation of direct pathway MSNs does increase movement, while stimulation of indirect pathway MSNs inhibits movement in mice (Kravitz, Freeze et al. 2010). However, the basal ganglia output and behavior is more

complex than this classic model suggests, and in fact, concurrent activation of direct and indirect pathways MSNs has been shown to precede initiation of movement in mice (Cui, Jun et al. 2013).

1.7. Dopamine signaling in the striatum

In addition to these projection pathways, direct and indirect MSNs can be differentiated based on neuropeptide and dopamine receptor expression. Direct pathway MSNs express substance P, dynorphin, and D1Rs, whereas indirect pathway MSNs express enkephalin and D2Rs (Gerfen, Engber et al. 1990), and only a small percentage of MSNs co-express D1Rs and D2Rs (Bertran-Gonzalez, Herve et al. 2010). Dopamine exerts opposite effects on D1Rs and D2Rs, thereby increasing the activity of the direct pathway and decreasing the activity of the indirect pathway (Mink and Thach 1993, Surmeier, Ding et al. 2007). Excitatory cortical inputs to the striatum are regulated by dopamine, and dendritic spines are the main site of interaction between glutamatergic and dopaminergic inputs to the striatum (Gerfen and Surmeier 2011).

Dopaminergic projections from the substantia nigra pars compacta (SNc, Peterson, Sejnowski et al. 2010) modulate MSNs within the dorsal striatum, while dopaminergic projections from the ventral tegmental area (VTA) modulate MSNs within the ventral striatum (Gangarossa, Espallergues et al. 2013).

Dopamine exerts its effects by binding to five dopamine receptor subtypes (D1R-D5R). While mRNA for all five receptor subtypes are expressed in the striatum, D1Rs and D2Rs are the most abundant (Boyson, McGonigle et al. 1986, Araki, Sims et al. 2007), with D2Rs exhibiting a greater affinity for dopamine than D1Rs (Richfield, Penney et al. 1989). D2R autoreceptors expressed on presynaptic dopaminergic terminals regulate dopamine synthesis and release (Ford

2014). All dopamine receptor subtypes belong to the superfamily of seven-transmembrane G protein-coupled receptors (GPCRs) and exert intracellular effects through second messenger signaling via G protein coupling.

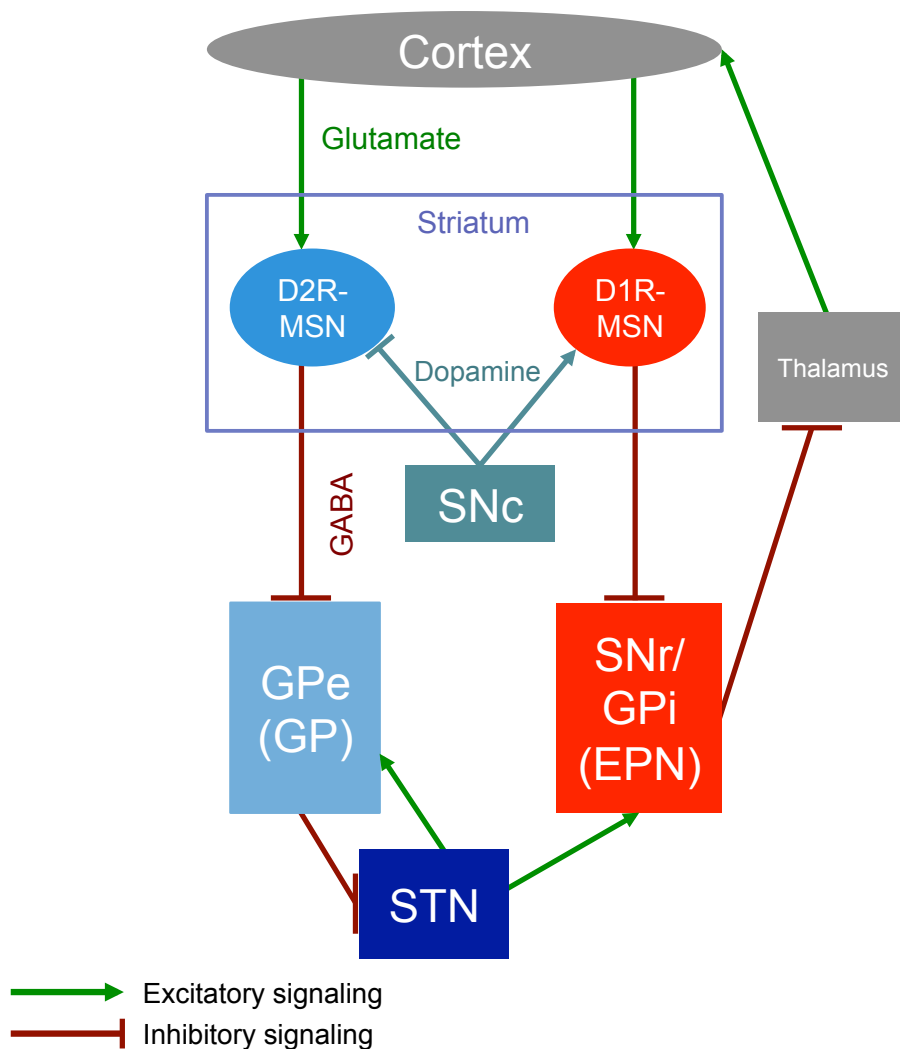


Figure 1.1. Schematic of the functional anatomy of the basal ganglia. Two distinct subpopulations of MSNs give rise to the direct and indirect output pathways of the basal ganglia. D1R-MSNs are segregated within the direct pathway. This pathway facilitates cortico-basal ganglia-thalamic transmission via disinhibition of the thalamus and promotes motor movement. D2R-MSNs are segregated within the

indirect pathway. Activation of the indirect pathways inhibits cortico-basal ganglia-thalamic transmission and reduces locomotor activity.

G proteins, or guanine nucleotide-binding proteins, are GTPases that function as molecular switches, transmitting extracellular signals to intracellular downstream signaling molecules, or effector proteins. G proteins are heterotrimeric, consisting of α , β , and γ subunits, and are active when bound to guanosine triphosphate (GTP) and are inactive when bound to guanosine diphosphate (GDP, Marinissen and Gutkind 2001). When bound by the associated neurotransmitter, GPCRs catalyze the exchange of G protein-bound GDP to GTP (Bos, Rehmann et al. 2007). The first G protein was discovered for its role as a stimulatory regulator of adenylyl, or adenylyl, cyclase and was accordingly termed $G_{\alpha s}$ (Jiang and Bajpayee 2009). Adenylyl cyclase is an enzyme necessary for the synthesis of cyclic AMP (cAMP), which was discovered by Earl Sutherland as a second messenger in epinephrine-mediated signaling (Blumenthal 2012). The family of G proteins that inhibit adenylyl cyclase consists of $G_{\alpha i}$ (Katada and Ui 1982, Jiang and Bajpayee 2009) and an additional form of $G_{\alpha i}$, termed $G_{\alpha o}$, or “other” (Neer, Lok et al. 1984, Sternweis and Robishaw 1984, Jiang and Bajpayee 2009).

Dopamine receptors can be categorized into two groups, D1-like receptors and D2-like receptors, on the basis of second messenger signaling via G protein coupling (Sibley and Monsma 1992, Vallone, Picetti et al. 2000, Xie and Martemyanov 2011). D1-like dopamine receptors, which includes D1Rs and D5Rs, couple to $G_{\alpha s}$, and the related $G_{\alpha olf}$, and stimulate adenylyl cyclase, which promotes the subsequent production of cAMP (Herve, Levi-Strauss et al. 1993, Neve, Seamans et al. 2004). In the striatum, expression of $G_{\alpha olf}$, an isoform of $G_{\alpha s}$, predominates over $G_{\alpha s}$ (Largent, Jones et al. 1988). $G_{\alpha olf}$ was originally discovered in olfactory epithelium and stimulates adenylyl cyclase type 5 (Herve 2011). In contrast, D2-like dopamine

receptors, which includes D2Rs, D3Rs, and D4Rs, couple to the G α i/o family and inhibit adenylylase and subsequent cAMP production (Bonci and Hopf 2005).

Dopamine receptors can activate various signaling pathways (Hernandez-Lopez, Tkatch et al. 2000, Jin, Goswami et al. 2003, Rashid, So et al. 2007). For example, GTP binding to the α subunit causes dissociation from the $\beta\gamma$ complex, and the free $\beta\gamma$ complex can modulate G protein signaling and activate unique signal transduction pathways (Smrcka 2008).

Neurotransmitter binding also initiates G protein-independent signaling pathways including GPCR binding of β -arrestins, which are adaptor proteins. β -arrestins are involved in GPCR desensitization and internalization and can also activate unique signal transduction pathways (Lefkowitz and Shenoy 2005, Smith and Rajagopal 2016, Rose, Pack et al. 2018). However, the signaling pathways downstream of dopamine-mediated stimulation or inhibition of cAMP are well characterized and are the principal, or canonical, mode of action (Vallone, Picetti et al. 2000).

1.7.1. Second messenger-dependent protein phosphorylation signaling

Dopamine exerts opposite effects on cAMP signaling in D1R- and D2R-MSNs. Activation of D1-like receptors stimulates adenylylase and subsequent cAMP, whereas activation of D2-like receptors inhibits adenylylase and subsequent cAMP production (Figure 1.2, Xie and Martemyanov 2011). Regulation of protein phosphorylation is the mechanism by which cAMP, and second messengers in general, exert their effects. The major target of cAMP is the cAMP-dependent protein kinase A (PKA), a serine-threonine kinase. In general, protein kinases add phosphate groups to specific amino acid residues, and these large, negatively charged phosphate groups alter the function of a protein by altering its charge and conformation.

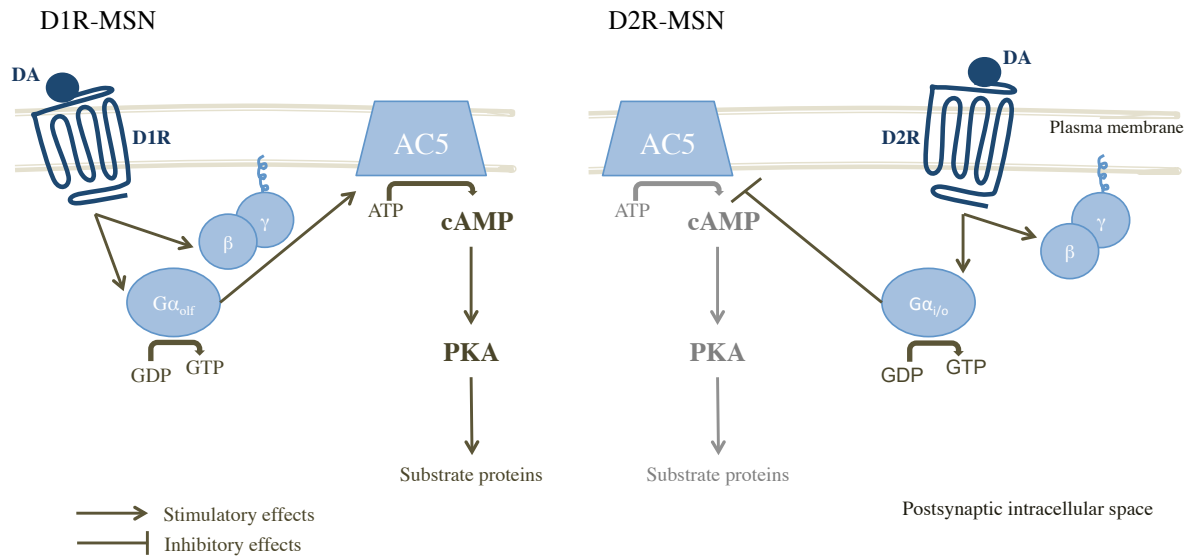


Figure 1.2. Dopamine-mediated second messenger signaling in MSNs. When neurotransmitters, including dopamine (DA), activate GPCRs, the α subunit undergoes a conformational change resulting in release of GDP and subsequent GTP binding to the α subunit. The α subunit then disassociates, and the free α subunit bound to GTP can regulate adenylate cyclase, the enzyme that catalyzes cAMP production. In MSNs, D1Rs couple to $G\alpha_{olf}$, and, when bound by dopamine, stimulate adenylate cyclase type 5 (AC5). D2Rs couple to $G\alpha_{i/o}$, and, when bound by dopamine, inhibit AC5. Adenylate cyclase catalyzes the synthesis of cAMP. Two molecules of cAMP bind to each regulatory subunit of PKA causing subsequent dissociation and activation of the catalytic subunit. Activated PKA can then phosphorylate downstream substrate proteins.

PKA-mediated signaling can be regulated in a number of ways. For example, PKA-mediated signaling can be limited by phosphodiesterases (PDEs), which are enzymes that break down cyclic nucleotides, including cAMP. Inhibitors of specific PDE isoforms, including PDE10A, which is enriched in the striatum, have demonstrated the role of specific PDE isoforms in mediating striatal signaling (Threlfell and West 2013). The effects of PKA can be amplified

by the dopamine and cAMP regulated phosphoprotein of Mr 32 kDa (DARPP-32, Walaas, Aswad et al. 1983, Fienberg, Hiroi et al. 1998, Svenningsson, Nishi et al. 2004, Cahill, Salery et al. 2014). DARPP-32 amplifies the effects of PKA via inhibition of protein phosphatase 1 (PP1), a serine-threonine phosphatase that reverses the actions of PKA. DARPP-32 has various residues, and phosphorylation by PKA at a specific threonine residue (Thr34) converts DARPP-32 into a potent inhibitor of PP1 (Hemmings, Greengard et al. 1984, Svenningsson, Lindskog et al. 1998).

PKA alters cellular responses through phosphorylation of various target proteins. Activated PKA can phosphorylate substrate proteins that serve as third messengers or can regulate the gating and trafficking of ion channels. One example of the latter involves dopamine mediated glutamatergic signaling (Surmeier, Ding et al. 2007). PKA phosphorylation of the glutamatergic NMDA-type ionotropic receptor (NMDAR), which is named for its affinity for the synthetic agonist, *N*-methyl-D-aspartate (NMDA), alters receptor calcium permeability and subsequent changes in synaptic strength (Skeberdis, Chevaleyre et al. 2006, Traynelis, Wollmuth et al. 2010).

1.7.2. Transcriptional regulation

Through passive diffusion into the nucleus, activated PKA can also regulate gene transcription (Yapo, Nair et al. 2018). Changes in gene transcription are necessary to maintain long-term cellular adaptations in response to altered extracellular stimuli and altered intracellular signaling (Matamales and Girault 2011). In general, activated PKA can regulate neuronal gene transcription via transcriptional regulation of immediate early genes, which regulate neuronal activity. Specifically, activated PKA can translocate to the nucleus and phosphorylate the cAMP

response element binding protein (CREB) family of transcription factors. CREB is constitutively expressed and bound by the cAMP response element (CRE), which is present in a number of genes, including the immediate early gene *c-Fos*. Phosphorylation of CREB at a specific serine residue (Ser133) is necessary for transcription, and multiple signaling cascades converge on Ser133 to regulate transcription. Unlike CREB, which is constitutively expressed, basal c-Fos expression is low and activation requires de novo transcription and translation. CREB activation is therefore necessary for regulation of immediate early genes. For example, CREB phosphorylation via D1R-mediated activation of PKA has been shown to mediate amphetamine-induced cellular alterations (Konradi, Cole et al. 1994). Immediate early genes encode proteins that compose a transcription factor termed activator protein-1 (AP-1), which serves as key regulator of neuronal gene expression. AP-1 consists of Fos (i.e. c-Fos) and Jun proteins, which when assembled bind their cognate regulatory sequence, the AP-1 sequence, as hetero- or homodimers. Expression of immediate early genes, including *c-Fos*, can then serve as reporters of neuronal activity given their rapid activation.

1.8. Abnormal postsynaptic dopamine-mediated signaling pathways in dystonia

Until recently, it was not possible to study abnormal postsynaptic striatal dopamine-mediated signaling pathways in dystonia because suitable animal models that exhibit dystonia caused by dysfunction in dopamine neurotransmission were not available. However, studies in a recently developed mouse model of DOPA-responsive dystonia, *Th^{tm1Ehes}* mice, have identified specific abnormalities in dopamine-mediated signaling implicated in dystonia (Rose, Yu et al. 2015). *Th^{tm1Ehes}* mice, termed DRD mice, are the first well-studied model of dystonia with construct, face, and predictive validity. If a mouse model satisfies the criterion of construct validity, then

the causative factor of the model mimics the etiology of the human condition. Face validity refers to whether the animal model resembles the presentation of the human condition. Predictive validity can be established when treatments that are effective in the model are also effective in humans or when treatments known to be effective in humans are shown to be effective in the model (Geyer and Markou 1995, Jinnah, Hess et al. 2005).

DRD mice are a knock-in mouse model that recapitulates the substitution in *TH* (p.381Q>K; c.1141C>A) that causes autosomal recessive DOPA-responsive dystonia (Knappskog, Flatmark et al. 1995). DRD mice are homozygous for the p.381Q>K substitution and thus truly model the genetic etiology of DOPA-responsive dystonia identified in humans. Reduced TH protein content and activity is observed in DRD mice and dopamine levels in the striatum are less than 1% of normal. DRD mice are unique in that they display overt abnormal involuntary movements that increase during the active period, consistent with patients' symptoms worsening throughout the day (Rose, Yu et al. 2015). Treatments that are effective in alleviating dystonia in humans, notably L-DOPA and THP, alleviate the abnormal movements in DRD mice. Peripheral administration, as well as microinjections of L-DOPA directly into the striatum, ameliorates the dystonia. Cerebellar microinjections of L-DOPA had no effect on abnormal movements, which suggests L-DOPA exerts its therapeutic effects via regulation of striatal dopamine-mediated signaling.

In regards to abnormal postsynaptic dopamine-mediated signaling, DRD mice exhibit supersensitive striatal adenylate cyclase activation in response to D1R-activation, and a corresponding behavioral supersensitivity (Rose, Yu et al. 2015). Activation of D2Rs, which inhibits locomotor activity in normal mice, increased locomotor activity and failed to inhibit striatal adenylate cyclase signaling in DRD mice (Rose, Yu et al. 2015). While these results

highlight postsynaptic dopamine-mediated signaling abnormalities in dystonia, the specific abnormalities that underlie dystonia are still unknown.

In DRD mice, the chronic dopamine deficit that occurs throughout development is associated with dystonia; therefore, dysregulated postsynaptic dopamine-mediated signaling pathways following chronic dopamine depletion observed in other animal models may inform our understanding of how these pathways are dysregulated in dystonia. The effects of dopamine deficiency on postsynaptic dopamine-mediated signaling in a rodent 6-hydroxydopamine (6-OHDA)-lesion model of Parkinson's disease have been particularly well characterized. 6-OHDA is a neurotoxin that causes degeneration of nigral dopamine neurons, which mimics the underlying etiology of Parkinson's disease in humans. Adult rodents given 6-OHDA lesions develop the typical motor features of Parkinson's disease including akinesia, rigidity, tremor, and postural abnormalities. Abnormal postsynaptic dopamine-mediated signaling has also been studied in dopamine-deficient (DD) mice. DD mice do not have dystonia but model early life dopamine depletion (Zhou and Palmiter 1995, Kim, Szczypka et al. 2000). Specifically, *Th* knockout mice were first generated in 1995, but these mice died prior to birth (Zhou, Quaipe et al. 1995) due to cardiac failure associated with the noradrenergic deficiency secondary to TH depletion (Thomas, Matsumoto et al. 1995). Targeting *Th* to one allele of the *Dbh* promoter enabled catecholamine synthesis to be restricted to noradrenergic neurons, or those expressing DBH. This rescued the noradrenergic deficiency and associated cardiac failure (Zhou and Palmiter 1995). The mice, termed dopamine-deficient, or DD mice, mice survive to birth; however, a few weeks after birth, these mice become severely hypoactive and hypophagic and die without daily administration of L-DOPA (Zhou and Palmiter 1995). This genetic etiology

does not precisely mimic *TH* mutations observed in humans; however, it does recapitulate early life dopamine depletion, which is a core feature of DOPA-responsive dystonia.

In both the 6-OHDA-lesioned rodent model (Gerfen, Keefe et al. 1995, Berke, Paletzki et al. 1998, Gerfen, Miyachi et al. 2002) and the DD mouse model (Kim, Szczypka et al. 2000), D1R-mediated expression of c-Fos is abnormally elevated. Administration of a partial D1R agonist or a low dose of a full D1R agonist induces c-Fos in the dopamine-depleted, but not the normal, striatum (Gerfen, Miyachi et al. 2002). In rodents with intact dopamine systems, the expression of immediate early genes in the striatum, specifically c-Fos, occurs only after administration of high doses of a full D1R agonist (Gerfen, Miyachi et al. 2002), administration of psychostimulants such as cocaine (Valjent, Corvol et al. 2000), or direct stimulation of the nigrostriatal dopamine pathway (Gerfen, Miyachi et al. 2002).

In DD and 6-OHDA-lesioned animals, extracellular signal-regulated kinase (ERK) phosphorylation is also abnormal. ERK is phosphorylated (p-ERK) via D1R-activation in the dorsal striatum of DD and 6-OHDA-lesioned animals, whereas D1R-activation does not induce p-ERK in the dorsal striatum of rodents with intact dopamine systems (Kim, Szczypka et al. 2000, Gerfen, Miyachi et al. 2002, Kim, Palmiter et al. 2006). Previous work also demonstrates that D2R-activation inhibited p-ERK induction, and that antagonism of D2Rs induced p-ERK in D2R-MSNs in the dopamine-intact, but not the dopamine-depleted, striatum of 6-OHDA rats (Gerfen, Miyachi et al. 2002).

ERK is phosphorylated via the mitogen-activated protein kinase (MAPK) cascade, which consists of four levels of signaling proteins. First, small GTPases, including Ras, function in the same manner as other GTPases (i.e. G-proteins) and serve as molecular switches to transmit and amplify extracellular signals to downstream signaling events. Ras activates MAPK kinase kinase

(Raf-1 or MEKK), which in turn phosphorylates and activates the downstream MAPK kinase (MEK), which subsequently phosphorylates and activates MAPK, which is synonymous with ERK (Wang, Fibuch et al. 2007, Kim and Choi 2010). MEKs are dual-function kinases, and phosphorylate both the threonine and tyrosine residues required to activate ERK (Dhanasekaran and Premkumar Reddy 1998, Girault, Valjent et al. 2007). In proliferative cells, MAPK signaling generally functions to mediate cellular growth, differentiation, and survival (for a review see Pearson, Robinson et al. 2001). In neurons, ERK is activated via a unique, calcium-dependent mechanism that is yet to be fully elucidated (Thomas and Huganir 2004). Once activated, p-ERK can exert many downstream effects, which can ultimately alter cellular excitability and regulate gene transcription (Thomas and Huganir 2004).

Despite the chronic dopamine deficiency and associated dysregulated postsynaptic dopamine-mediated signaling responses, dystonia is not observed in either 6-OHDA-lesioned or DD animals. The timing and extent of striatal dopaminergic loss are likely relevant factors for the development of dystonia. Only rodents given 6-OHDA lesions as adults exhibit a parkinsonian phenotype, whereas neonates lesioned with 6-OHDA that have comparable dopamine loss exhibit hyperactivity (Ungerstedt 1971, Shaywitz, Yager et al. 1976, Breese, Baumeister et al. 1984). In DRD and DD mice, dopamine loss occurs throughout development; however, unlike DD mice, dopamine levels in DRD mice are low, but not abolished (Zhou and Palmiter 1995, Rose, Yu et al. 2015). Typically patients with GCH1 deficiency develop DRD when they are ten years old; however, patients who have an age of onset of over 20 years old can exhibit parkinsonian symptoms (Tadic, Kasten et al. 2012). This example further supports the importance of the timing of dopamine loss in the development of dystonia. The fact that a dystonic foot is observed in the early stages of Parkinson's disease, when there is only moderate

dopaminergic degeneration (Tolosa and Compta 2006), also supports that the extent of dopamine loss is an important factor. Ultimately, these factors likely contribute to the development of specific abnormalities in postsynaptic dopamine-mediated signaling pathways that may lead to the development of dystonia.

1.9. Overall objective

The DRD mouse model allows for the identification of the precise nature of the striatal dysfunction that may distinguish dystonia from other abnormal motor phenotypes. Given the potentiated adenylate cyclase response to D1R-activation and the absence of adenylate cyclase inhibition in response to D2R-activation in DRD mice, we sought to further determine the specific striatal abnormalities that underlie dystonia by examining both postsynaptic dopamine-mediated signaling and the striatal proteome. More specifically, in normal and DRD mice I examined alterations in dopamine-mediated regulation of

- 1) PKA, the main target of canonical cAMP-mediated signaling,
- 2) ERK phosphorylation, which may reflect aberrant signaling, and
- 3) c-Fos expression, a marker of transcriptional regulation (Figure 1.3).

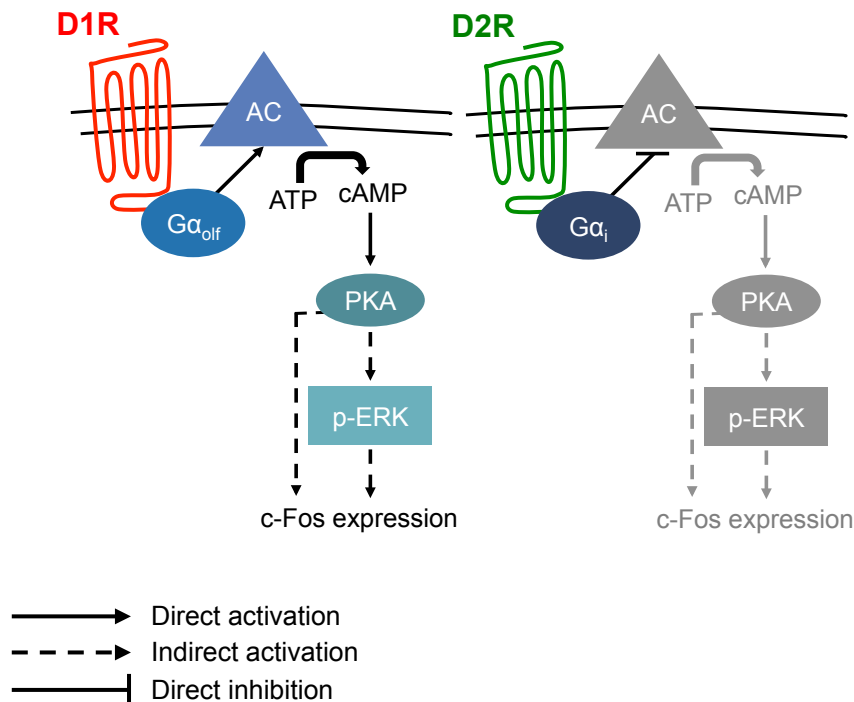


Figure 1.3. Schematic of postsynaptic dopamine signaling in the striatum. In the normal mouse striatum, when dopamine binds to D1Rs, it stimulates $G\alpha_{olf}$, which acts as a molecular switch, and stimulates adenylyl cyclase (AC). Adenylyl cyclase promotes the subsequent production of cAMP. The major target of cAMP is PKA. PKA alters cellular responses through phosphorylation of various target proteins. PKA can regulate changes in gene transcription and PKA can also indirectly facilitate the phosphorylation of ERK. When phosphorylated, ERK can alter cell excitability and regulate gene transcription. In contrast, when dopamine binds to D2Rs, it stimulates $G\alpha_{i/o}$, which inhibits adenylyl cyclase-mediated signaling.

Chapter 2: A novel method using QuPath to automate counts of immunoreactive cells and define striatal regions

2.1. Abstract

Dopamine-mediated signal transduction pathways are differentially regulated throughout regions of the striatum. However, the striatum, which is organized in a somatotopic manner, lacks obvious anatomical boundaries that can serve as landmarks for consistent section-to-section quantitation, and previous methods for overcoming this limitation are imperfect. Therefore, to rigorously and reproducibly quantify cells immunostained for signaling proteins within the striatum, a novel method to automate counts of immunoreactive cells and to define striatal regions for analysis was developed using QuPath, an open source software for whole slide image analysis.

2.2. Introduction

Dopamine-mediated signal transduction pathways are differentially regulated throughout regions of the striatum. For example, differential regulation of p-ERK has been reported in the dorsal and ventral striatum of 6-OHDA-lesioned rodents. In the intact striatum, D1R-activation induces p-ERK only in the ventral striatum, whereas in the dopamine-depleted striatum, p-ERK is induced only in the dorsal striatum (Gerfen, Miyachi et al. 2002). Further, cocaine treatment results in ERK phosphorylation in only a relatively small subset of MSNs in the dorsal striatum, but p-ERK is induced in a large proportion of cells in the ventral striatum (Valjent, Corvol et al. 2000).

It is, perhaps, not surprising that the anatomical distribution of signaling cascades is not uniform across the striatum given glutamatergic inputs to the striatum project in a somatotopic manner forming segregated loops and distinct functional territories within the striatum (Redgrave, Rodriguez et al. 2010, Hintiryan, Foster et al. 2016, Anderson, Krienen et al. 2018). However, in general, the functional and somatotopic organization of the basal ganglia is less obvious in rodents compared to humans (Shakkottai, Batla et al. 2017). The dorsolateral striatum receives input from cortical sensorimotor regions and is responsible for habit formation, and the dorsomedial striatum, which is responsible for cognitive function and goal-directed behavior, receives input from cortical regions responsible for associative functions (Redgrave, Rodriguez et al. 2010, Graybiel and Grafton 2015).

The somatotopic organization of the striatum, as well as evidence from these previous studies, suggests that assessing regional differences in striatal signal transduction pathways may be necessary to fully understand abnormal striatal signaling pathways. However, there are no obvious observable anatomical boundaries separating dorsolateral and dorsomedial striatum and previous methods of delineating striatal regions are either difficult to reproduce or are restricted

to limited sample areas (Westin, Vercammen et al. 2007, Alcacer, Andreoli et al. 2017).

Therefore, I developed a novel workflow for automating counts of immunoreactive cells and delineating striatal regions for analysis in a rigorous and reproducible way using QuPath (version 0.1.2), an open source software for whole slide image analysis (Bankhead, Loughrey et al. 2017). Specifically, this methodology was developed to examine regional differences in cells immunostained for markers of p-ERK, c-Fos, and PKA activity in the striatum of DRD mice compared to normal mice.

To develop this novel approach for the analysis of striatal immunostaining, I used a mouse model that received a unilateral 6-OHDA lesion of the nigrostriatal dopaminergic pathway. Abnormal striatal signaling, including p-ERK, c-Fos, and PKA activity, has been well documented in this model (Gerfen, Keefe et al. 1995, Berke, Paletzki et al. 1998, Gerfen, Miyachi et al. 2002, Alcacer, Andreoli et al. 2017), which facilitated the refinement of the cell counting parameters. This approach is in line with more recent reports that highlight the importance of assessing multiple striatal regions when determining mechanisms of neurotransmitter signaling (Hintiryan, Foster et al. 2016, Yalcin-Cakmakli, Rose et al. 2018).

2.3. Methods

Mice. One male adult (4 month) mouse on a mixed C57BL/6J and DBA/2J background received a unilateral injection of 20 mM 6-OHDA in 0.02% ascorbic acid in the medial forebrain bundle. Specifically, 1 μ l was injected at the following coordinates (in millimeters relative to bregma, sagittal suture, and dural surface): anterior-posterior = -1.2, lateral = -1.3, dorsoventral = -4.75 (Heiman, Heilbut et al. 2014). Xueliang Fan, PhD, performed the lesion surgeries. Three weeks post surgery, the 6-OHDA-lesioned mouse was subcutaneously injected with L-DOPA (20

mg/kg) and benserazide (2.5 mg/kg, all from Sigma-Aldrich, St. Louis, MO) in 2.5 mg/ml ascorbic acid in normal saline (0.9% NaCl)) and sacrificed 45 min later.

Immunohistochemistry. The 6-OHDA-lesioned mouse was deeply anesthetized with isoflurane and perfused with a 4% ice-cold, buffered paraformaldehyde solution (pH 7.2). The brain was rapidly removed and post fixed overnight in the perfusion solution at 4°C, transferred to 20% buffered sucrose overnight, and then transferred to 30% buffered sucrose solution overnight at 4°C. The brain was stored at 4°C in 30% buffered sucrose until it was sectioned (30 µm) in the coronal plane using a freezing microtome. Free-floating sections were stored in a cryoprotective solution at -20°C.

Striatal sections were immunostained for TH using the rabbit anti-tyrosine hydroxylase (1:1,000; #P40101-0 Pel-Freez) primary antibody (Rose, Yu et al. 2015). Striatal sections were immunostained for phosphorylated ERK1/2 using the phospho-(Thr202/Tyr204)-ERK1/2 rabbit monoclonal (p-ERK; 1:5,000; #4370 Cell Signaling) primary antibody that detects ERK1/2 when dually phosphorylated at Thr202 and Tyr204 of ERK1 (Thr185 and Tyr187 of ERK2), and singly phosphorylated at Thr202 (Gerfen, Miyachi et al. 2002). ERK1 and ERK2 (ERK1/2) exhibit 90% homology, are well characterized, and are important for synaptic plasticity (Thomas and Huganir 2004, Girault, Valjent et al. 2007). Striatal sections were immunostained for c-Fos using the c-Fos rabbit polyclonal (1:20,000; PC38 EMD Millipore) primary antibody (Jinnah, Egami et al. 2003). Striatal sections were immunostained for the phosphorylated PKA substrate using the phospho-(Ser/Thr) PKA substrate rabbit polyclonal (p-PKA-sub; 1:5,000; #9621 Cell Signaling) primary antibody. The p-PKA-sub antibody recognizes the phosphorylated PKA substrate, phospho-serine/threonine residue with arginine at the -3 position, and has been

validated as a marker of PKA signaling in mice (Sindreu, Scheiner et al. 2007, Alcacer, Andreoli et al. 2017).

Floating sections were treated with 0.5% Triton-X in Tris-buffered saline (TBS) for 30 min and then blocked with 5% normal goat serum, 5% bovine serum albumin, 0.1 % bovine gelatin, 0.05% Tween-80, and 0.01% sodium azide in TBS for two hrs. Floating sections were then reacted for 16-24 hrs at 4°C with the primary antibody. Sections were then incubated for 2 hrs at 4°C with a biotinylated goat anti-rabbit IgG secondary antibody (1:800, Vector Laboratories) in 5% normal goat serum in 0.1% Triton-X-100 in TBS. Sections were incubated with avidin-biotin complex (Vector Labs, Burlingame, CA) for 1 h, and developed using a peroxidase-based detection method and 3-3'-diaminobenzidine (DAB; Sigma-Aldrich, St. Louis, MO) as the chromogen.

Imaging and software. One striatal section was selected for TH immunostaining and was mounted on glass slides and imaged using an Olympus BX51 microscope with a 2X objective. For p-ERK, c-Fos, and p-PKA-sub immunostaining, one striatal section was selected for each antibody. Sections were mounted on glass slides and were digitized by the Emory Neuroscience NINDS Core Facilities (ENNCF) Neuropathology Core using a slide scanner (Aperio AT2 Scanner; Leica Biosystems). QuPath was used to automate counts of immunoreactive cells and to delineate striatal regions for analysis.

2.4. Results

2.4.1. Confirmation of 6-OHDA-lesion

In order to confirm the loss of nigrostriatal dopamine fibers on the lesion side, striatal samples from the 6-OHDA-lesioned mouse striatum were immunostained for TH. Qualitative assessment of TH immunostaining revealed a reduction in TH immunostaining only on the lesion side, which confirmed loss of dopamine fibers on the lesion side and demonstrated intact dopamine fibers on the control side (Figure 2.1).

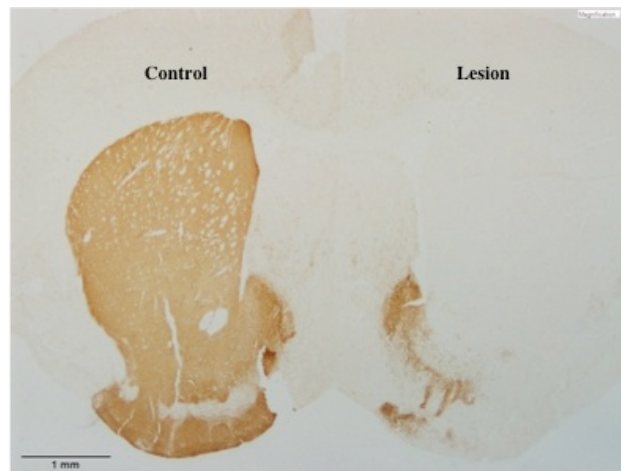


Figure 2.1. TH immunostaining. TH immunostaining was qualitatively decreased in the dorsal striatum of the lesion compared to the control side.

2.4.2. Immunoreactive cell count automation

Consistent with previous literature, after L-DOPA treatment, an increase in p-ERK (Figure 2.1, Gerfen, Miyachi et al. 2002) and c-Fos (Gerfen, Keefe et al. 1995, Berke, Paletzki et al. 1998, Gerfen, Miyachi et al. 2002) immunoreactivity was observed in the dorsal striatum of the lesion side compared to the control side. Increased p-PKA-sub immunoreactivity was also observed in the dorsal striatum of the lesion compared to the control side. Therefore, the unilateral 6-OHDA-lesioned striatal sections were used to optimize the cell counting parameters for p-ERK, c-Fos, and p-PKA-sub immunostaining using QuPath.

To quantify immunostained cells, first, background was adjusted for each image. QuPath automatically sets the background to white; however, most slides vary slightly from this default background. The ‘estimate stain vectors’ function within QuPath was used to set a background equivalent to that of the corpus callosum to account for variation in background staining intensities between the images. Further, detected cells occurring on a background greater than a default maximum background intensity were excluded from final cell counts. The ‘positive cell detection’ function was used to automate counts of immunoreactive cells. The counting parameters for the ‘positive cell detection’ function were optimized for each primary antibody (Table 2.1) to ensure the final parameters reliably identified the p-ERK, c-Fos, and p-PKA-sub immunoreactivity observed within the striatum of the lesion side compared to the control side. Within the ‘setup parameters’, ‘detection image’ was changed from ‘hematoxylin OD’ to ‘optical density sum’ to reflect that DAB, not hematoxylin, was used for immunostaining. Within the ‘nucleus parameters’, the ‘minimum area’ and ‘maximum area’ were adjusted to approximate MSN perikarya area to 30-100 μm^2 and to exclude large, cholinergic interneurons (Gagnon, Petryszyn et al. 2017). Within ‘intensity parameters’, the ‘threshold’ was adjusted to reflect the intensity of immunostaining for each antibody.

Figure 2.2 shows representative images comparing detections of positive cell counts for p-ERK immunoreactivity in dorsal striatum using original and refined parameters. The default parameters show delineation of the nucleus and the cell body for the positive detections, whereas the final cell counting parameters identify the entire positive cell (Figure 2. 2). To ensure that cell counting was not affected by staining intensity, several different dilutions of primary antibody were tested and did not considerably alter the positive cell counts from the dorsal striatum of the lesion or control side (Table 2.2).

Table 2.1. Final positive cell counting parameters

	Default Parameters	p-ERK Parameters	c-Fos Parameters	p-PKA-sub Parameters
Setup parameters				
Choose detection image*	Hematoxylin OD	Optical density sum	Optical density sum	Optical density sum
Requested pixel size (μm)	0.5	0.5	0.5	0.5
Nucleus parameters				
Background radius (μm)	8	8	8	8
Median filter radius (μm)	0	0	0	0
Sigma (μm)	1.5	1.5	1.5	1.5
Minimum area (μm^2)*	10	30	30	20
Maximum area (μm^2)*	400	100	100	100
Intensity parameters				
Threshold*	0.1	0.25	0.15	0.15
Max background intensity	2	2	2	2
Split by shape	ON	ON	ON	ON
Exclude DAB (membrane staining)	OFF	OFF	OFF	OFF
Cell parameters				
Cell expansion (μm)*	5	0	0	0
Include cell nucleus*	ON	OFF	OFF	OFF
General parameters				
Smooth boundaries	ON	ON	ON	ON
Make measurements	ON	ON	ON	ON
Intensity threshold parameters				
Score compartment*	Nucleus: DAB OD mean	Nucleus: DAB OD max	Nucleus: DAB OD max	Nucleus: DAB OD max
Threshold 1+*	0.2	0.2	0.1	0.1
Threshold 2+	0.4	0.4	0.4	0.4
Threshold 3+	0.6	0.6	0.6	0.6
Single threshold	ON	ON	ON	ON

*indicates a parameter that was adjusted from the default value

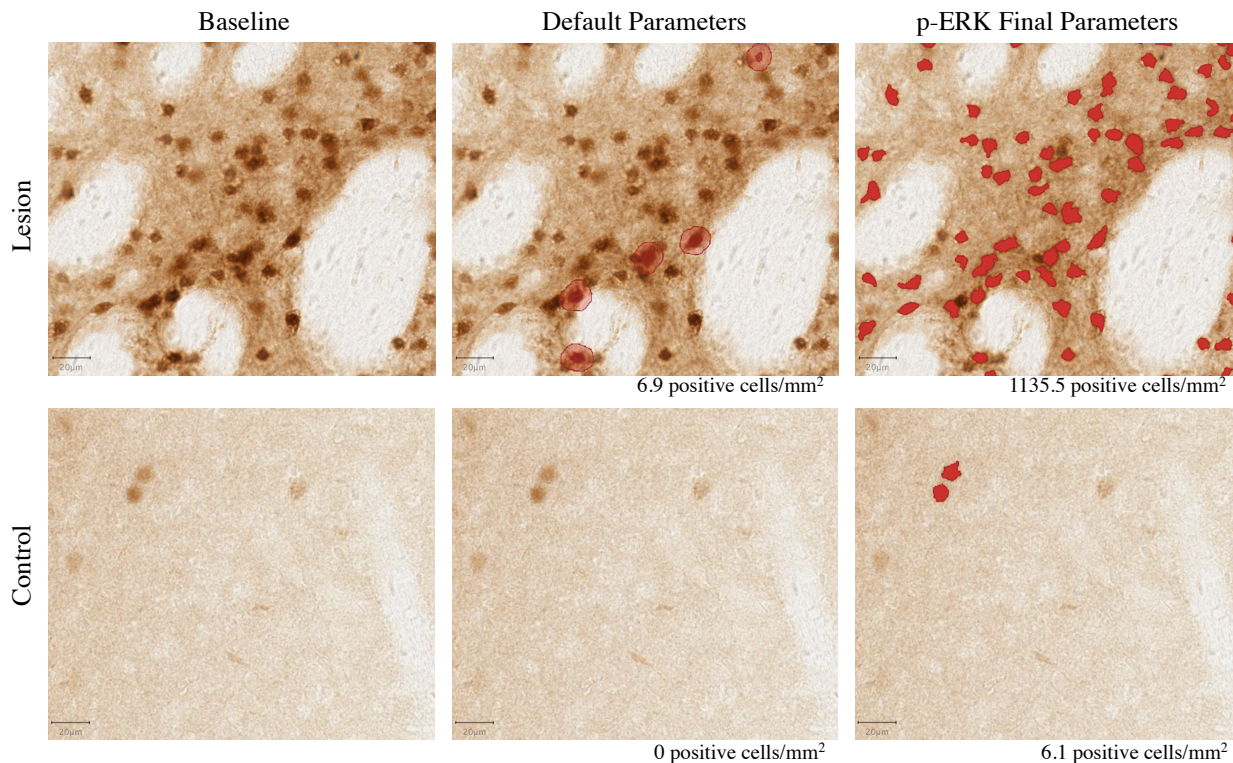


Figure 2.2. Positive cell counts for p-ERK immunoreactivity in dorsal striatum. Representative images from QuPath of p-ERK (1:5,000 dilution) immunostaining in the dorsal striatum of the lesion and control side, illustrating the unprocessed image (baseline), the p-ERK-positive cells detected using the default parameters in QuPath and p-ERK-positive cells detected after determining optimal detection parameter (final parameters).

Table 2.2. Effect of p-ERK antibody dilution on positive cell counts

		p-ERK antibody dilution		
		1:2,000	1:5,000	1:10,000
Control	Lesion	1531.4 positive cells/mm ²	1937.9 positive cells/mm ²	1360.5 positive cells/mm ²
	Control	50.2 positive cells/mm ²	47.4 positive cells/mm ²	16.6 positive cells/mm ²

2.4.3. Defining striatal regions

Striatal regions were defined using QuPath to develop a reproducible method for generating regions of analysis in order to determine if signaling cascades were differentially affected across the striatum. First, the entire striatum was outlined for each hemisphere using The Allen Mouse Brain Atlas (Coronal) as a reference. The midpoint of each striatum was defined by QuPath by a center x and y coordinate. Then, a line was drawn to connect the midpoint of the left with the right striatum. This line defined the boundary between dorsal and ventral striatum. A line perpendicular to the dorsal-ventral boundary was drawn from the center x,y coordinate of each region to define a boundary between medial and lateral striatum (Figure 2.3). This protocol ensured that the dorsomedial and dorsolateral regions would be parallel and perpendicular to the midpoint of the striatum and that the ventral striatum would be parallel to the midpoint of the striatum for every section analyzed. This novel workflow was utilized for all immunohistochemical experiments assessing p-ERK, c-Fos, and p-PKA-sub immunoreactivity in the DRD and normal mouse striatum.

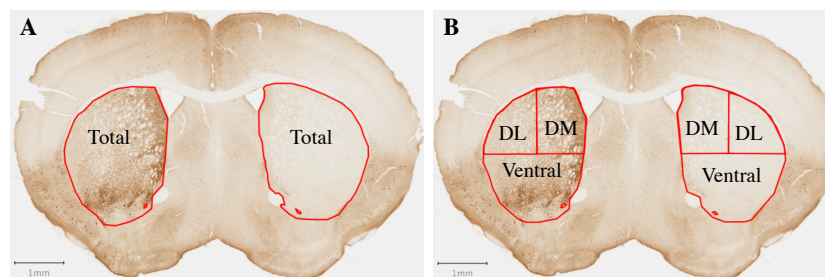


Figure 2.3. Striatal regions. (A) Total striatum was subdivided into (B) dorsomedial (DM), dorsolateral (DL), and ventral striatum.

2.5. Discussion

A novel method to automate counts of immunoreactive cells and define striatal regions was developed using QuPath. Refined cell counting parameters reliably detected the increased p-ERK, c-Fos, and p-PKA-sub immunoreactivity observed within the dopamine-depleted compared to the control striatum in mice with unilateral 6-OHDA-lesions. Further, a reproducible method for generating dorsomedial, dorsolateral, and ventral striatal regions was developed using QuPath. The relationship between dorsomedial, dorsolateral, and ventral striatum to the total striatum is clearly defined, and employment of this protocol ensures that striatal regions can be reliably demarcated between striatal sections.

This workflow overcomes previous limitations including the lack of obvious anatomical boundaries within the striatum that can serve as landmarks for consistent quantitation of striatal regions. Further, previous methods of delineating striatal regions are either difficult to reproduce or were also restricted to limited sample areas (Westin, Vercammen et al. 2007, Alcacer, Andreoli et al. 2017). QuPath is also freely available, which allows for similar studies to be easily conducted by others. Thus, this methodology was used in the following chapters to determine abnormal dopamine-mediated signal transduction pathways that may be differentially regulated throughout regions of the striatum.

Chapter 3: Abnormal dopamine receptor-mediated intracellular signaling in a mouse model of DOPA-responsive dystonia

3.1. Abstract

The work in this chapter identifies abnormalities in postsynaptic D1R- and D2R-mediated signaling pathways in the striatum of DRD mice. Immunohistochemistry was used to examine changes in D1R- and D2R-mediated regulation of PKA activity, ERK phosphorylation, and c-Fos expression in the striatum of normal and DRD mice. I demonstrated that abnormalities in dopamine-mediated signaling pathways did not arise from alterations in the number of D1R- or D2R-MSNs in the DRD mouse striatum. In DRD mice, potentiated striatal D1R-mediated signaling was observed, as evidenced by increased PKA activity and ERK phosphorylation. The response to D2R-antagonism was blunted or abolished in DRD mice, as evidenced by increased c-Fos expression throughout the striatum of normal but not DRD mice in response to D2R-antagonism. Potentiated D1R-mediated signaling has been observed in other rodent models of dopamine depletion; however, blunted D2R-mediated signaling may be specific to dystonia. Therefore, understanding the precise nature of D2R-mediated signaling may inform our understanding of dystonia.

3.2. Introduction

Although dopamine neurotransmission in the basal ganglia is abnormal in many different forms of dystonia, the precise nature of abnormal dopamine-mediated signaling pathways are unknown. In DRD mice, the chronic dopamine deficit that occurs throughout development is associated with dystonia. However, a chronic dopamine deficit per se is not sufficient to cause dystonia as neither 6-OHDA-lesioned mice nor DD mice exhibit dystonia, despite profound long-term reductions in dopamine neurotransmission (Gerfen, Keefe et al. 1995, Zhou and Palmiter 1995, Berke, Paletzki et al. 1998, Kim, Szczypka et al. 2000, Gerfen, Miyachi et al. 2002). Therefore, the development of dystonia is likely due to the result of dopamine depletion along with very specific abnormalities in dopamine-mediated signaling pathways. Until recently, it was not possible to identify the dysregulated pathways because animal models that exhibit dystonia caused by underlying defects in dopamine neurotransmission were not available. However, recent studies in DRD mice, which have face, etiologic, and predictive validity, have demonstrated that specific abnormalities in dopamine-mediated adenylyate cyclase activation may distinguish dystonia from other abnormal motor phenotypes (Rose, Yu et al. 2015).

Adenylyate cyclase activation is necessary for the synthesis of cAMP and subsequent PKA-mediated signaling. In normal mice, activation of D1Rs stimulates adenylyate cyclase activity, whereas activation of D2Rs inhibits adenylyate cyclase activity (Bertran-Gonzalez, Bosch et al. 2008). In DRD mice, D1R-stimulated adenylyate cyclase activity is greatly potentiated compared to normal mice, whereas the response to D2R agonists is blunted (Rose, Yu et al. 2015). These results suggest that abnormal downstream D1R- and D2R-mediated signaling responses in the DRD mouse striatum may underlie the expression of dystonia. Therefore, to identify the precise abnormalities in postsynaptic dopamine-mediated signaling

pathways in DRD mice, I utilized immunohistochemistry to examine changes in dopamine-mediated changes in 1) PKA activity using an indirect assessment of PKA substrate phosphorylation, 2) ERK phosphorylation, and 3) c-Fos expression in the striatum of normal and DRD mice.

Given previous work has shown D1R-stimulated striatal adenylate cyclase activity is potentiated in DRD mice compared to normal mice (Rose, Yu et al. 2015) and adenylate cyclase activation is necessary for the synthesis of cAMP and subsequent PKA-mediated signaling, I hypothesized that D1R-mediated striatal PKA activity is potentiated in DRD mice. PKA can also regulate changes in gene transcription and can indirectly facilitate the phosphorylation of ERK, which when phosphorylated can regulate gene transcription. Further, previous studies have shown ERK phosphorylation and c-Fos expression are potentiated in response to D1R agonist treatment after chronic dopamine depletion (Gerfen, Keefe et al. 1995, Berke, Paletzki et al. 1998, Kim, Szczypka et al. 2000, Gerfen, Miyachi et al. 2002, Kim, Palmiter et al. 2006). Therefore, I hypothesized that that D1R-mediated striatal ERK phosphorylation and c-Fos expression are also potentiated in DRD mice.

3.3. Methods

Mice. Male and female adult (3-6 month) mice homozygous for the c.1160C>A *Th* mutation (DRD; drd/drd) and littermates carrying two wild-type alleles (normal; +/+) were used for all experiments. Because DRD mice do not survive inbred on C57BL/6J, most DRD mice were produced by crossing +/drd mice coisogenic with C57BL/6J with +/drd mice congenic on DBA/2J. Prior to the completion of the inbreeding of the drd allele onto the DBA/2J strain, a two generation cross was used, as previously described (Rose, Yu et al. 2015), whereby +/drd mice

coisogenic with C57BL/6J were crossed with normal DBA/2J. The +/drd mice generated from this cross were then bred to create DRD mice. There were no differences in abnormal movement in the mice generated by these two breeding schemes (data not shown), so these groups were combined.

BAC reporter fluorescent transgenes were bred onto the DRD strain to identify D1R-expressing (*Drd1a*-tdTomato; JAX) or D2R-expressing (*Drd2*-EGFP; Heintz, Rockefeller University) MSNs (Ade, Wan et al. 2011, Chan, Peterson et al. 2012). Christine Donsante, MS, generated all mice used in the experiments described.

Housing conditions were in accordance with Emory University's Institutional Animal Care and Use Committee (IACUC). The light period was 7am to 7pm. All procedures were conducted in accordance with Emory's IACUC and Division of Animal Resources guidelines and were approved by IACUC. Mice were maintained as previously described (Rose, Yu et al. 2015). DRD and normal control mice received a daily injection subcutaneously (s.c.) of 5 mg/kg L-DOPA and 2.5 mg/kg benserazide (all from Sigma-Aldrich, St. Louis, MO) in 2.5 mg/ml ascorbic acid in normal saline (0.9% NaCl). L-DOPA supplementation was terminated >24 h prior to all experiments.

Behavioral assessment. Mice were tested in a behavioral suite separate from the location of home cages. Abnormal movements were tested in activity cages (29 x 50 cm). Prior to all testing periods, mice were habituated to the behavior suite for > 3 hrs. A behavioral inventory was used to identify abnormal movements including tonic flexion (forelimbs, hindlimbs, trunk, head), tonic extension (forelimbs, hindlimbs, trunk, head), clonus (forelimbs and hindlimbs), twisting (trunk, head), and tremor (forelimbs, hindlimbs, trunk, head; Raike, Pizoli et al. 2013). Testing

began at 2 pm, and abnormal movements were observed and scored for 30 sec at 10 min intervals for 1 h. Abnormal movements were scored as present (1) or absent (0) for each body region during each time bin. An abnormal movement score was calculated by summing all scores.

Drug challenges. Drugs were injected s.c. in normal saline (0.9% NaCl) in a volume of 10 ml/kg unless otherwise noted. The D1-like receptor agonist, SKF 81297 hydrobromide (SKF 81297); the D2-like receptor agonist (-)-quinpirole hydrochloride (quinpirole); and the D2R antagonist, raclopride were obtained from Tocris Biosciences (Minneapolis, MN). Drug doses were chosen based on previous reports demonstrating they are behaviorally active in DRD mice. SKF 81297 (0.2 mg/kg) and quinpirole (0.1 mg/kg) at the doses selected alleviate abnormal movement and increase locomotor activity in DRD mice (Rose, Yu et al. 2015). The dose of raclopride (1 mg/kg) chosen worsens dystonia in DRD mice (Rose, Yu et al. 2015). Mice were treated with drug between 12-4 pm and were sacrificed 45 min later because qualitative assessment of preliminary data confirmed p-PKA-sub, p-ERK, and c-Fos immunoreactivity was increased in the dopamine-depleted striatum of 6-OHDA-lesioned mice 45 min after L-DOPA treatment (data not shown).

Immunohistochemistry. Mice were deeply anesthetized with isoflurane and perfused with a 4% ice-cold, buffered paraformaldehyde solution (pH 7.2). Brains were rapidly removed and post fixed overnight in the perfusion solution at 4°C. Brains were transferred to 20% buffered sucrose overnight and were then transferred to 30% buffered sucrose solution overnight at 4°C. Brains were stored at 4°C in 30% buffered sucrose until sectioning. Brains were sectioned (30 µm) in

the coronal plane using a freezing microtome. Free-floating sections were stored in a cryoprotective solution at -20°C until further processing.

Sections were immunostained using the following primary antibodies as described in Chapter 2: Phospho-(Thr202/Tyr204)-ERK1/2 rabbit monoclonal antibody (1:5,000; #4370 Cell Signaling); c-Fos rabbit polyclonal antibody (1:20,000; PC38 EMD Millipore), anti-mCherry antibody (1:5,000; #AB167453; Abcam), GFP tag polyclonal antibody (1:20,000; A-11122; Invitrogen) and phospho-(Ser/Thr) PKA substrate (p-PKA-sub) rabbit polyclonal antibody (1:5,000; #9621 Cell Signaling).

Bright-field immunohistochemistry. Floating sections were treated with 0.5% Triton-X in Tris-buffered saline (TBS) for 30 min and then blocked with 5% normal goat serum, 5% bovine serum albumin, 0.1% bovine gelatin, 0.05% Tween-80, and 0.01% sodium azide in TBS for 2 hrs. Floating sections were then reacted for 16-24 hrs at 4°C with the primary antibody. Sections were then incubated for 2 hrs at 4°C with a biotinylated goat anti-rabbit IgG secondary antibody (1:800, Vector Laboratories) in 5% normal goat serum in 0.1% Triton-X-100 in TBS. Sections were incubated with avidin-biotin complex (Vector Labs, Burlingame, CA) for 1 h, and developed using a peroxidase-based detection method and 3-3'-diaminobenzidine (DAB; Sigma-Aldrich, St. Louis, MO) as the chromogen.

Immunofluorescence. Floating sections were treated with 0.5% Triton-X in Tris-buffered saline (TBS) for 30 min and then blocked with 5% normal goat serum, 5% bovine serum albumin, 0.1% bovine gelatin, 0.05% Tween-80, and 0.01% sodium azide in TBS for 2 hrs. Floating sections were then reacted for 16-24 hrs at 4°C with the primary antibody. Sections were then

incubated for 1 hr at 4°C with goat anti-rabbit IgG (H+L) highly cross-adsorbed secondary antibody, Alexa Fluor 59 (1:500; Vector Laboratories) in 5% normal goat serum in 0.1% Triton-X-100 in TBS.

Bright-field image analysis and cell counts. One striatal section from Bregma +1.145 to 0.145 was selected for immunostaining. The Allen Coronal Mouse Brain Atlas was used as a reference. Analysis was carried out in dorsomedial, dorsolateral, and ventral regions of the striatum as previously described (Chapter 2). To determine positive counts for the dorsomedial, dorsolateral, and ventral regions, positive cell counts and total area for each region from the left and right striatum were summed. The total number of positive cells from the DM, DL, or ventral region was divided by total area of the respective regions to determine the number of cells positive per square mm. This was completed for each region of interest. Because the dorsal striatum is predominantly involved in motor control, dorsomedial and dorsolateral regions were the focus.

Fluorescent image analysis and cell counts. Immunofluorescence was used to determine the cell type specificity of p-PKA-sub, p-ERK, and c-Fos positive cells. Images were collected using a Leica SP8 confocal microscope at a 40X objective. NIH ImageJ software (1.52a) was used to create a merged color image. Analysis was carried out on one side of the brain in an equivalent area within the dorsomedial and dorsolateral region of one section from the mid-rostrocaudal level of the striatum. QuPath software was used to automate positive counts of immunofluorescence. Striatal sections from Bregma +1.145 to 0.145 were selected for assessing immunofluorescence. Fluorescent images were not adjusted for quantification, but the brightness has been adjusted for presentation purposes.

Given approximately 95% of neurons in the striatum are MSNs and less than 2% of MSNs express both receptors (Gagnon, Petryszyn et al. 2017), positive immunostaining for p-PKA-sub, p-ERK, or c-Fos (secondary antibody Alexa Fluor 59, red) that overlapped with D2R-MSNs (EGFP, green) was considered specific to D2R-MSNs, and positive immunostaining for p-PKA-sub, p-ERK, or c-Fos (secondary antibody Alexa Fluor 59, red) that did not overlap with D2R-MSNs (EGFP, green) was considered specific to D1R-MSNs. Positive cells were counted independently on a red and green channel and the overlap was then determined in the merged image (Figure 3.1). The percentage of D2R-MSNs and D1R-MSNs immunostained for p-PKA-sub, p-ERK, or c-Fos was determined by using the following formulas:

%D2R-MSNs immunostained for p-PKA-sub, p-ERK, or c-Fos =

$$(\# \text{ of 'red' and 'green' cells} / \# \text{ of 'red' cells}) * 100$$

%D1R-MSNs immunostained for p-PKA-sub, p-ERK, or c-Fos =

$$100\% - \% \text{D2R-MSNs immunostained for p-PKA-sub, p-ERK, or c-Fos}$$

The percentage of D2R-MSNs immunostained for p-PKA-sub, p-ERK, or c-Fos (secondary antibody Alexa Fluor 59, red) was determined by dividing the number of 'overlap' cells by the number of 'red' cells, or cells positive for p-PKA-sub, p-ERK, or c-Fos (secondary antibody Alexa Fluor 59, red) but not endogenous EGFP (green) and multiplying that by 100. 'Overlap' cells refers to cells positive for p-PKA-sub, p-ERK, or c-Fos (secondary antibody Alexa Fluor 59, red) and endogenous EGFP (green, D2R-MSNs). The percentage of D2R-MSNs immunostained for p-PKA-sub, p-ERK, or c-Fos was subtracted from 100% to determine the

percentage of D1R-MSNs immunostained for p-PKA-sub, p-ERK, or c-Fos (secondary antibody Alexa Fluor 59, red) that did not co-localize with endogenous EGFP (green, D2R-MSNs).

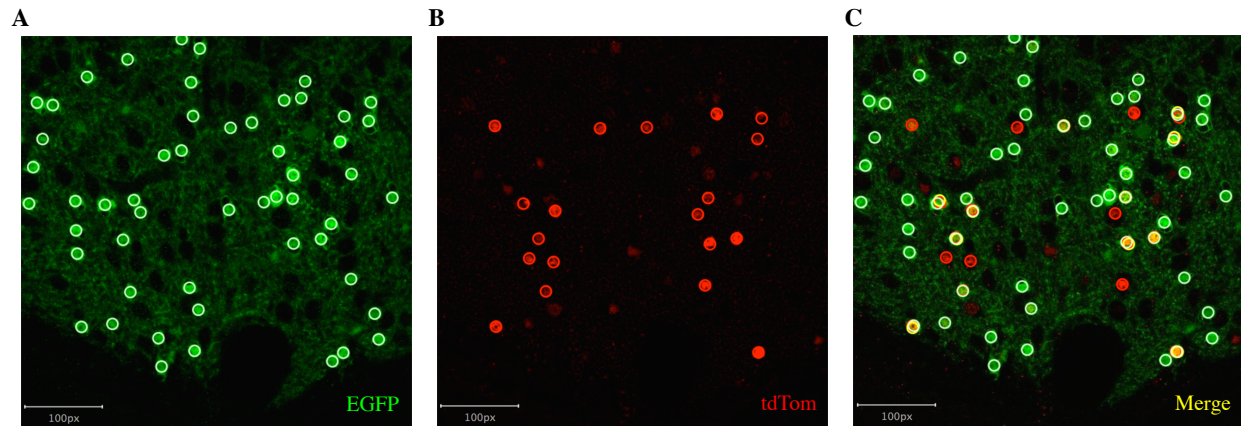


Figure 3.1. Cell type specificity analysis. (A) D2R-MSNs were identified by counting cells positive for endogenous EGFP. Green circles identify D2R-MSNs (endogenous EGFP). (B) Cells immunostained for primary antibodies (p-PKA-sub, p-ERK, or c-Fos) were identified by counting cells positive for the goat anti-rabbit IgG (H+L) highly cross-adsorbed secondary antibody Alexa Fluor 59 (red). This example shows c-Fos immunoreactivity in the striatum of a normal mouse treated with raclopride. Red circles identify cells immunostained for primary antibodies (p-PKA-sub, p-ERK, or c-Fos) and positive for the goat anti-rabbit IgG (H+L) highly cross-adsorbed secondary antibody Alexa Fluor 59. (C) Yellow circles identify overlap (red and green circles) on the merged image.

Statistics. Prism 8 was used for all analyses. Detailed statistical results are presented in the figure legends. Counts of p-PKA-sub, p-ERK and c-Fos positive cells per square mm in dorsomedial and dorsolateral striatum were analyzed using a treatment x region x genotype ANOVA. Given the dorsal striatum is predominantly involved in motor control, results in ventral striatum were analyzed separately using a two-way treatment x genotype ANOVA.

3.4. Results

3.4.1. Behavioral analysis of DRD mice expressing fluorescent reporter proteins

As discussed, DRD mice were crossed with mouse lines in which neurons ‘report’ D1R-MSNs or D2R-MSNs by expressing tdTomato (tdTom) or EGFP, respectively. Abnormal movement was assessed in DRD mice carrying *Drd1a*-tdTomato (tdTom), *Drd2*-EGFP (EGFP), or both transgenes (tdTom, EGFP) in order to determine whether abnormal movement was altered by the presence of the transgenes. Student’s *t* tests revealed abnormal movements in DRD mice carrying tdTom, EGFP, or both tdTom and EGFP, did not differ from DRD mice without reporter fluorescent proteins (no RFP). These results demonstrate that the presence of these reporter fluorescent transgenes did not alter the phenotype of interest, abnormal movement, in DRD mice (Figure 3.2).

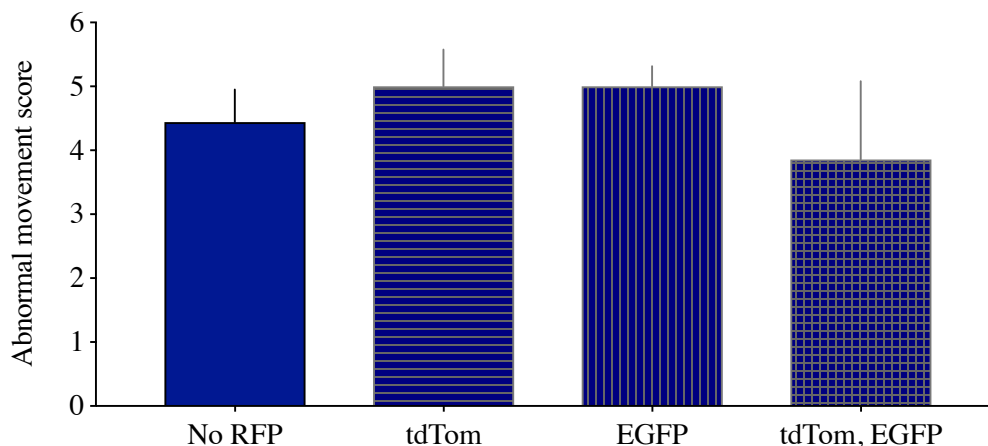


Figure 3.2. Abnormal movement in DRD mice with RFPs. Student’s *t* tests revealed abnormal movements in DRD mice carrying the RFPs, tdTom (D1R-MSNs; $n = 6$; $p > 0.1$), EGFP (D2R-MSNs; $n = 5$; $p > 0.1$), or both tdTom and EGFP (D1R- and D2R-MSNs; $n = 7$; $p > 0.1$) did not differ from DRD mice without the RFPs ($n = 27$). Values represent mean + SEM. *Data collected by Christine Donsante, MS, and analyzed by MAB.*

3.4.2. Distribution of D1R-tdTom and D2R-EGFP striatal neurons

Abnormalities in dopamine-mediated signaling pathways could arise from changes in the number of D1R-positive and D2R-positive MSNs caused by the lack of dopamine throughout development (Lieberman, McGuirt et al. 2018). Therefore, DRD mice expressing both tdTom (D1R-MSNs) and EGFP (D2R-MSNs) were used to compare the distribution of D1R-expressing and D2R-expressing striatal neurons between normal and DRD mice. Micrographs of EGFP and tdTom expression in DRD and normal mice are shown in Figure 3.3. To quantify D1R (tdTom)- and D2R (EGFP)-expressing MSNs, I performed immunostaining for tdTom (anti-mCherry antibody) and EGFP (GFP tag polyclonal antibody) followed by DAB development. Positive immunostained cells were quantified using the method described in Chapter 2. When examining the total striatum, the number of cells positive per square mm for tdTom (D1R-MSNs) and EGFP (D2R-MSNs) did not differ between normal and DRD mice (Figure 3.4). When examining the dorsomedial and dorsolateral striatum separately, the number of cells positive per square mm for tdTom (D1R-MSNs) and EGFP (D2R-MSNs) also did not differ between normal and DRD mice (data not shown). These data suggest that abnormalities in dopamine-mediated signaling pathways are likely not attributable to alterations in the population of MSN subtypes.

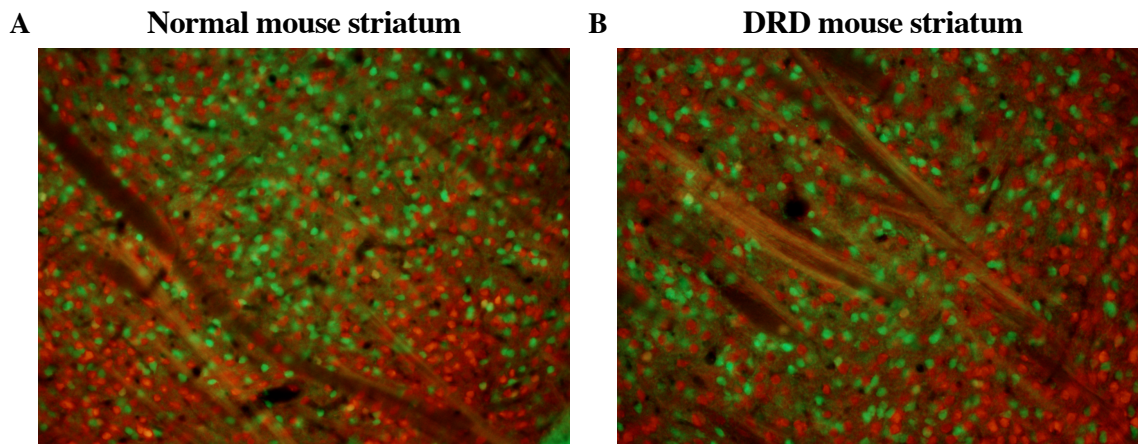


Figure 3.3. Representative fluorescent micrographs of DRD and normal mouse striatum. Micrographs of sagittal sections from normal (A) and DRD (B) mouse striatum with endogenous tdTom (D1R-MSNs) and EGFP (D2R-MSNs) fluorescent proteins. *Images generated by Yunmiao Wang, a Neuroscience graduate program rotation student.*

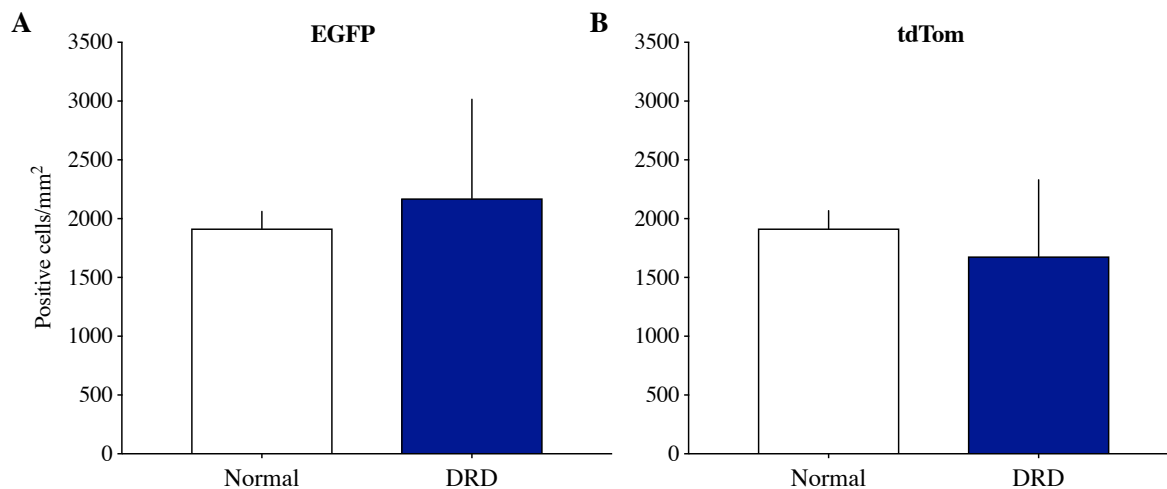


Figure 3.4. D1R-expressing and D2R-expressing cell density in normal and DRD mouse total striatum. EGFP positive cell counts (D2R-MSNs) did not differ between DRD (n = 3) and normal (n = 4) mice ($p > 0.1$; Student's t test). tdTom positive cell counts (D1R-MSNs) did not differ between DRD (n = 3) and normal (n = 3) mice ($p > 0.1$; Student's t test). Values represent mean + SEM. *Data generated by Alec Shannon, an undergraduate student supervised by MAB.*

3.4.3. D1R agonist-mediated signaling

D1R agonist-mediated p-PKA-sub immunoreactivity

In DRD mice, D1R-stimulated adenylate cyclase activity is potentiated compared to normal mice (Rose, Yu et al. 2015). Adenylate cyclase activation is necessary for the synthesis of cAMP and subsequent PKA-mediated signaling. As such, I hypothesized that D1R-mediated striatal PKA activation is potentiated in DRD mice. To test this hypothesis, the effects of treatment with the D1-like dopamine receptor agonist, SKF 81297 on p-PKA-sub immunoreactivity in dorsomedial and dorsolateral striatum of normal and DRD mice were assessed. The effects of SKF 81297 treatment on p-PKA-sub immunoreactivity in the ventral striatum of normal and DRD mice were also assessed.

In normal mice, SKF 81297 treatment did not change p-PKA-sub immunoreactivity in dorsomedial or dorsolateral striatum compared to saline treatment. However, in DRD mice, p-PKA-sub immunoreactivity was increased in response to SKF 81297 treatment compared to saline treatment in dorsomedial and dorsolateral striatum (treatment x genotype interaction effect, $p < 0.01$; Figure 3.5A). Dual immunofluorescence in the dorsomedial striatum of a DRD mouse revealed SKF 81297-induced p-PKA-sub immunoreactivity was expressed in only 5% of D2R-MSNs (Figure 3.5C) and in dorsolateral striatum, SKF 81297-induced p-PKA-sub immunoreactivity was not observed in D2R-MSNs (data not shown). This suggests that most p-PKA-sub immunoreactivity occurred in D1R-MSNs, as expected. In ventral striatum, p-PKA-sub immunoreactivity was increased by SKF 81297 treatment (main effect of treatment, $p < 0.01$) and p-PKA-sub immunoreactivity was increased in DRD mice compared to normal mice (main effect of genotype, $p < 0.05$; Figure 3.5B). There was a trend for a treatment x genotype

interaction effect ($p = 0.09$). Overall, these results suggest that in DRD mice, PKA-mediated signaling pathways in D1R-MSNs are potentiated.

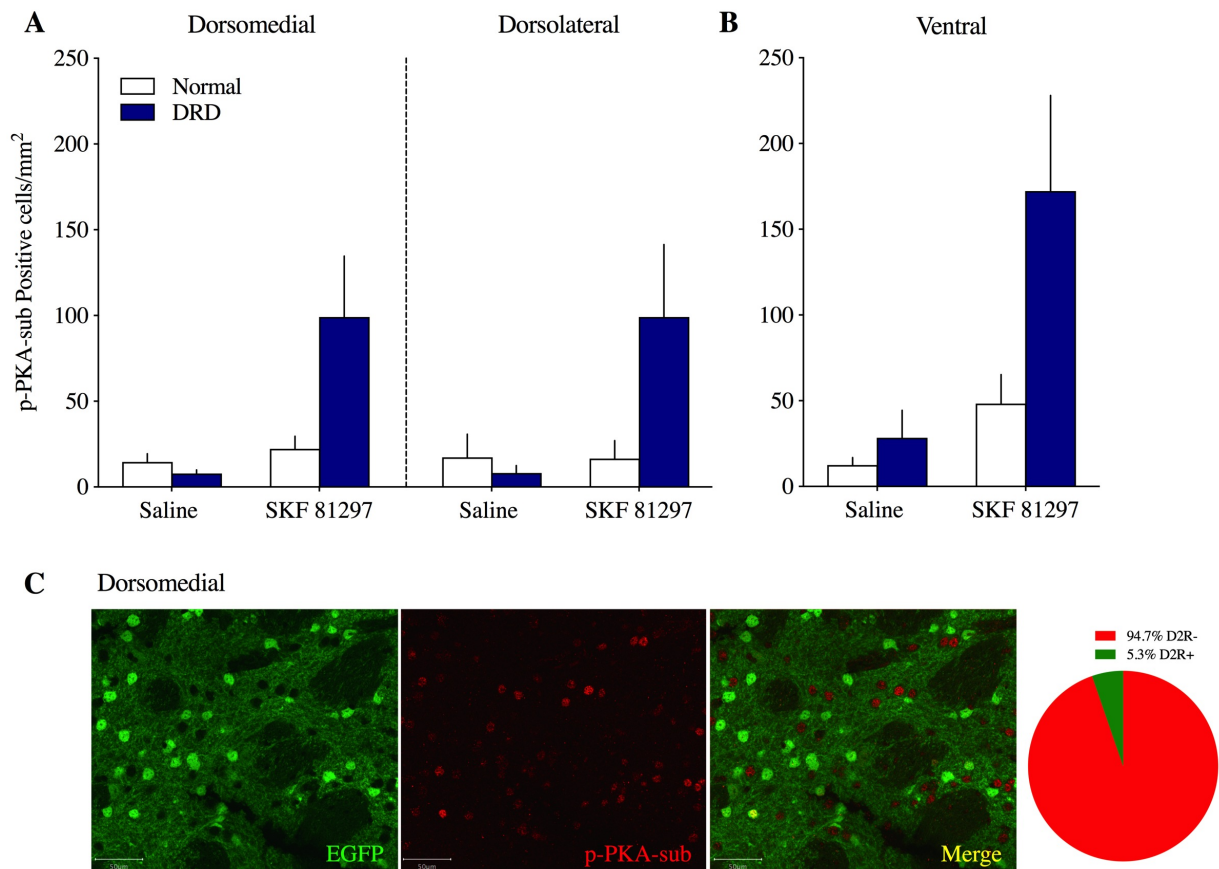


Figure 3.5. Effects of SKF 81297 treatment on striatal p-PKA-sub immunoreactivity in normal and DRD mice. (A) p-PKA-sub immunoreactivity in SKF 81297- and saline-treated normal and DRD mice in dorsomedial and dorsolateral striatum was tested using a genotype x treatment x region ANOVA. In normal mice, SKF 81297 treatment did not alter p-PKA-sub immunoreactivity in dorsomedial or dorsolateral striatum compared to saline treatment. In DRD mice, p-PKA-sub immunoreactivity was increased in response to SKF 81297 treatment compared to saline treatment in dorsomedial and dorsolateral striatum [treatment x genotype interaction effect, $F(1, 50) = 9.23$, $p < 0.01$]. (B) In ventral striatum, p-PKA-sub immunoreactivity in SKF 81297- and saline-treated normal and DRD mice was tested with a two-way ANOVA. SKF 81297 treatment increased p-PKA-sub immunoreactivity [main

effect of treatment, $F(1, 24) = 8.61, p < 0.01$] and p-PKA-sub immunoreactivity was increased in DRD mice compared to normal mice [main effect of genotype, $F(1, 24) = 5.22, p < 0.05$; there was a trend for a treatment x genotype interaction effect, $F(1, 24) = 3.12, p = 0.09$]. Values represent mean + SEM; $n = 6-8$ /group. (C) Dual immunofluorescence from the dorsomedial striatum of a DRD mouse revealed p-PKA-sub immunoreactivity was expressed in ~5% of D2R-MSNs.

D1R agonist-mediated p-ERK immunoreactivity

Previous studies have shown p-ERK pathways are abnormally activated in response to D1R agonist treatment after chronic dopamine depletion (Kim, Szczypka et al. 2000, Gerfen, Miyachi et al. 2002, Kim, Palmiter et al. 2006); therefore, I hypothesized that D1R-mediated striatal p-ERK signaling is potentiated in DRD mice. To test this hypothesis, the effects of SKF 81297 treatment on p-ERK immunoreactivity were assessed in the striatum of normal and DRD mice.

In DRD mice, there was an increase in p-ERK immunoreactivity in response to SKF 81297 treatment compared to saline treatment in dorsomedial, and to a lesser extent, dorsolateral, striatum (treatment x genotype interaction effect, $p < 0.05$; Figure 3.6A). In contrast, there was a decrease in p-ERK immunoreactivity in response to SKF 81297 treatment compared to saline treatment in dorsomedial, and to a lesser extent, dorsolateral, striatum, in normal mice (treatment x genotype interaction effect, $p < 0.05$; Figure 3.6A). There was a main effect of region ($p < 0.01$; Figure 3.6A), which suggests baseline differences in the regional regulation of ERK phosphorylation. Overall, there was lower expression of p-ERK in DRD mice and in DRD mice, there was lower expression of p-ERK in the dorsolateral compared to dorsomedial striatum. In ventral striatum, p-ERK immunoreactivity was increased in response to SKF 81297 treatment compared to saline treatment in DRD mice, but decreased in response to SKF 81297 treatment compared to saline treatment in normal mice (treatment x genotype interaction effect, $p < 0.01$;

Figure 3.6B). These results suggest that in DRD mice, striatal ERK is abnormally phosphorylated via D1R-activation whereas in normal mice, D1R-activation may inhibit ERK phosphorylation.

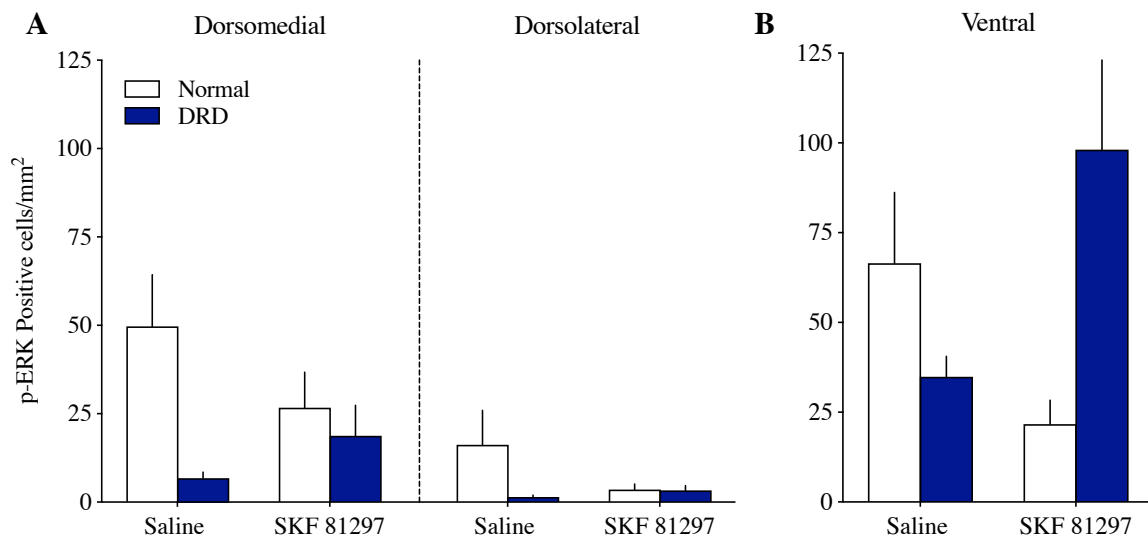


Figure 3.6. Effects of SKF 81297 treatment on striatal p-ERK immunoreactivity in normal and DRD mice. (A) p-ERK immunoreactivity in SKF 81297- and saline-treated normal and DRD mice in dorsomedial and dorsolateral striatum was tested using a genotype x treatment x region ANOVA. In DRD mice, there was an increase in p-ERK immunoreactivity in response to SKF 81297 treatment compared to saline treatment in dorsomedial and dorsolateral striatum [treatment x genotype interaction effect, $F(1, 50) = 9.23$, $p < 0.05$]. In normal mice there was a decrease in p-ERK immunoreactivity in response to SKF 81297 treatment compared to saline treatment in dorsomedial and dorsolateral striatum [treatment x genotype interaction effect, $F(1, 50) = 9.23$, $p < 0.05$]. In DRD mice, there was lower expression of p-ERK in dorsolateral compared to dorsomedial striatum [main effect of region [$F(1, 50) = 10.45$, $p < 0.01$]]. (B) In ventral striatum, p-ERK immunoreactivity in SKF 81297- and saline-treated normal and DRD mice was tested with a two-way ANOVA. p-ERK immunoreactivity was increased in response to SKF 81297 treatment compared to saline treatment in DRD mice, but decreased in response to SKF

81297 treatment compared to saline treatment in normal mice [treatment x genotype interaction effect, $F(1, 25) = 11.78, p < 0.01$]. Values represent mean + SEM; $n = 6-8/\text{group}$.

Correlation of D1R agonist-mediated p-PKA-sub and p-ERK immunoreactivity

There was a positive correlation between p-PKA-sub and p-ERK immunoreactivity in the dorsomedial ($r^2 = 0.82, p < 0.05$; Figure 3.7A), but not dorsolateral (Figure 3.7B), striatum of DRD mice. This suggests that D1R-mediated signaling, via supersensitive cAMP-mediated pathways, activates p-ERK in the dorsomedial striatum. This data further supports regional differences in the regulation of ERK phosphorylation in the dorsomedial and dorsolateral striatum.

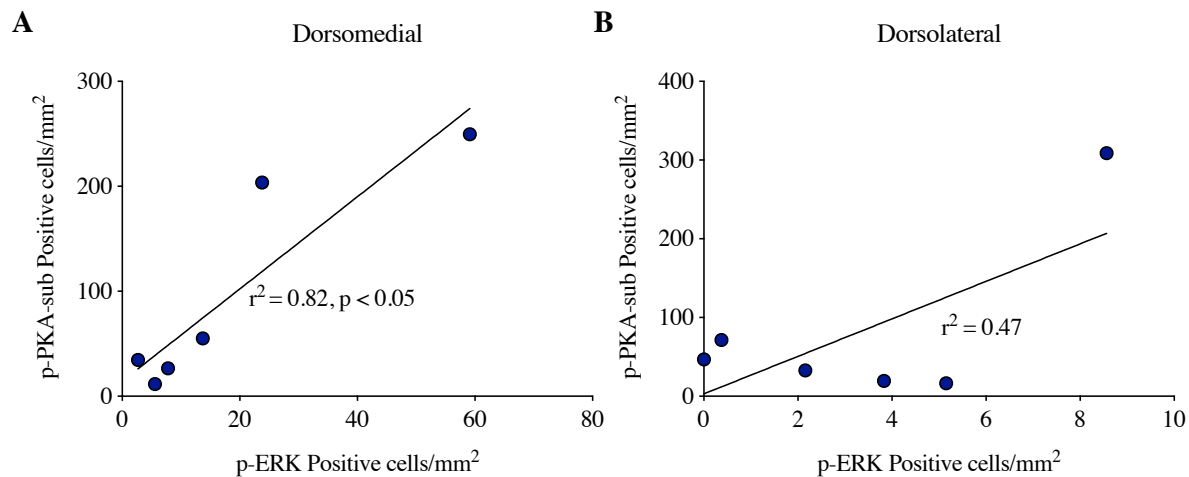


Figure 3.7. Correlation of p-PKA-sub and p-ERK immunoreactivity following SKF 81297 treatment in DRD mice. SKF 81297-induced p-PKA-sub and p-ERK immunoreactivity were correlated in the (A) dorsolateral striatum [$r(6) = 0.91, p < 0.05$], but not the (B) dorsolateral striatum [$r(6) = 0.68, p > 0.1$].

D1R agonist-mediated c-Fos immunoreactivity

PKA can regulate changes in gene transcription and can indirectly facilitate the phosphorylation of ERK, which when phosphorylated can regulate gene transcription. Further, previous studies have shown striatal c-Fos expression is abnormally induced in response to D1R-activation after chronic dopamine depletion (Gerfen, Keefe et al. 1995, Berke, Paletzki et al. 1998, Kim, Szczypka et al. 2000, Gerfen, Miyachi et al. 2002). Therefore, I hypothesized that that D1R-mediated striatal c-Fos expression is potentiated in DRD mice. To test this hypothesis, the effects of SKF 81297 treatment on c-Fos immunoreactivity in dorsomedial and dorsolateral striatum of normal and DRD mice were assessed. The effects of SKF 81297 treatment on c-Fos immunoreactivity in the ventral striatum of normal and DRD mice were also assessed. SKF 81297 treatment did not significantly affect c-Fos immunoreactivity in either normal or DRD mice in any striatal region (Figures 3.8A,B).

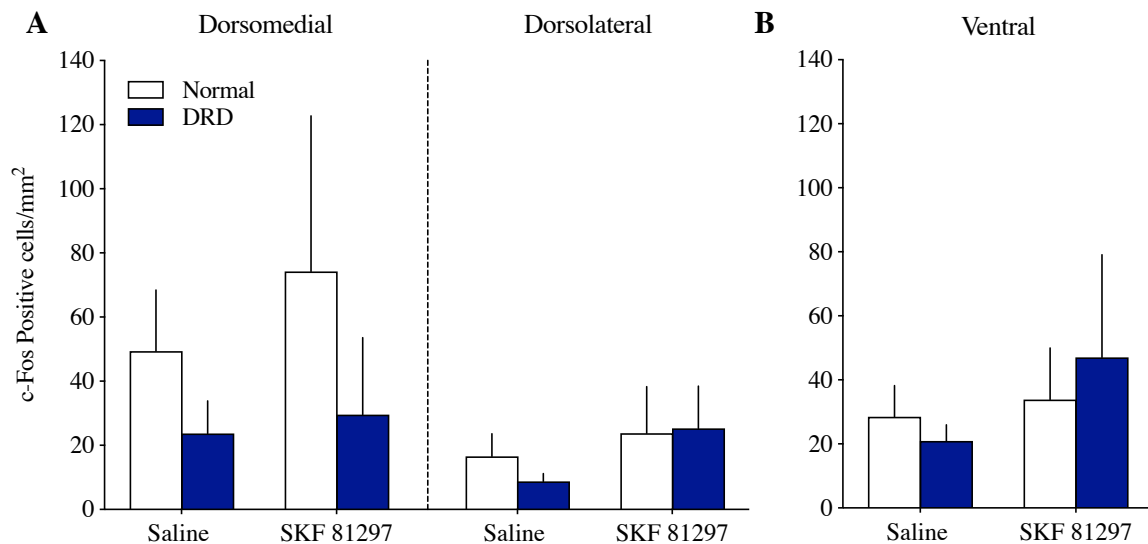


Figure 3.8. Effects of SKF 81297 treatment on striatal c-Fos immunoreactivity in normal and DRD mice. (A) c-Fos immunoreactivity in SKF 81297- and saline-treated normal and DRD mice in

dorsomedial and dorsolateral striatum was tested using a genotype x treatment x region ANOVA. SKF 81297 treatment did not significantly affect c-Fos immunoreactivity in either normal or DRD mice in dorsomedial or dorsolateral striatum [treatment x region x genotype interaction effect, $F(1, 52) = 0.19$, $p > 0.1$]. (B) In ventral striatum, c-Fos immunoreactivity in SKF 81297- and saline-treated normal and DRD mice was tested with a two-way ANOVA. SKF 81297 treatment did not significantly affect c-Fos immunoreactivity in either normal or DRD mice [treatment x genotype interaction effect, $F(1, 26) = 0.32$, $p > 0.1$]. Values represent mean + SEM; $n = 7-8/\text{group}$.

3.4.4. D2R agonist-mediated signaling

D2R agonist-mediated p-PKA-sub immunoreactivity

To determine whether D2R-mediated regulation of PKA, the main target of cAMP-mediated signaling, is dysregulated in DRD mice, the effects of treatment with a D2-like dopamine receptor agonist, quinpirole on p-PKA-sub immunoreactivity in dorsomedial and dorsolateral striatum of normal and DRD mice were assessed. The effects of quinpirole treatment on p-PKA-sub immunoreactivity in the ventral striatum of normal and DRD mice were also assessed.

Quinpirole treatment did not significantly affect p-PKA-sub expression in either normal or DRD mice in dorsomedial or dorsolateral striatum (Figure 3.9A). There was a trend for a treatment x genotype interaction effect ($p = 0.09$) in ventral striatum (Figure 3.9B). Overall, these results suggest that D2R-activation does not induce PKA in the dorsal striatum of DRD or normal mice.

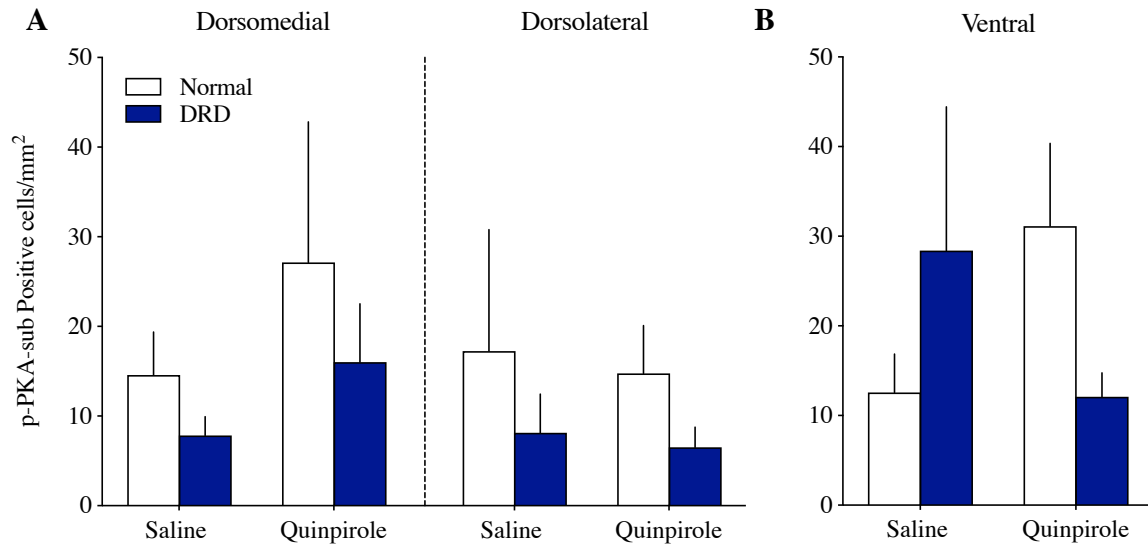


Figure 3.9. Effects of quinpirole treatment on striatal p-PKA-sub immunoreactivity in normal and DRD mice. (A) p-PKA-sub immunoreactivity in quinpirole- and saline-treated normal and DRD mice in dorsomedial and dorsolateral striatum was tested using a genotype x treatment x region ANOVA. Quinpirole treatment did not significantly affect p-PKA-sub expression in either normal or DRD mice in dorsomedial or dorsolateral striatum [treatment x region x genotype interaction effect, $F(1, 42) = 0.04$, $p > 0.1$]. (B) In ventral striatum, p-PKA-sub immunoreactivity in quinpirole- and saline-treated normal and DRD mice was tested with a two-way ANOVA. Quinpirole treatment did not significantly affect p-PKA-sub expression in either normal or DRD mice; however, there was a trend for a treatment x genotype interaction effect [$F(1, 20) = 3.21$, $p = 0.09$]. Values represent mean + SEM; $n = 5-7$ /group.

D2R agonist-mediated p-ERK immunoreactivity

To determine whether D2R-mediated regulation of p-ERK is dysregulated in DRD mice, the effects of quinpirole treatment on p-ERK immunoreactivity in dorsomedial and dorsolateral striatum of normal and DRD mice were assessed. The effects of quinpirole treatment on p-ERK immunoreactivity in the ventral striatum of normal and DRD mice were also assessed.

In dorsal striatum, quinpirole treatment had no effect of p-ERK immunoreactivity. Greater p-ERK immunoreactivity was observed in the dorsomedial striatum compared to the dorsolateral striatum of normal mice, whereas there were very low baseline levels of p-ERK immunoreactivity in both regions in DRD mice (region x genotype interaction, $p < 0.05$; Figure 3.10A). In ventral striatum, there was a main effect of treatment ($p < 0.05$; Figure 3.10B), with decreased p-ERK immunoreactivity in response to quinpirole treatment compared to saline treatment. These data suggest that in the ventral striatum, D2R-activation inhibits ERK phosphorylation.

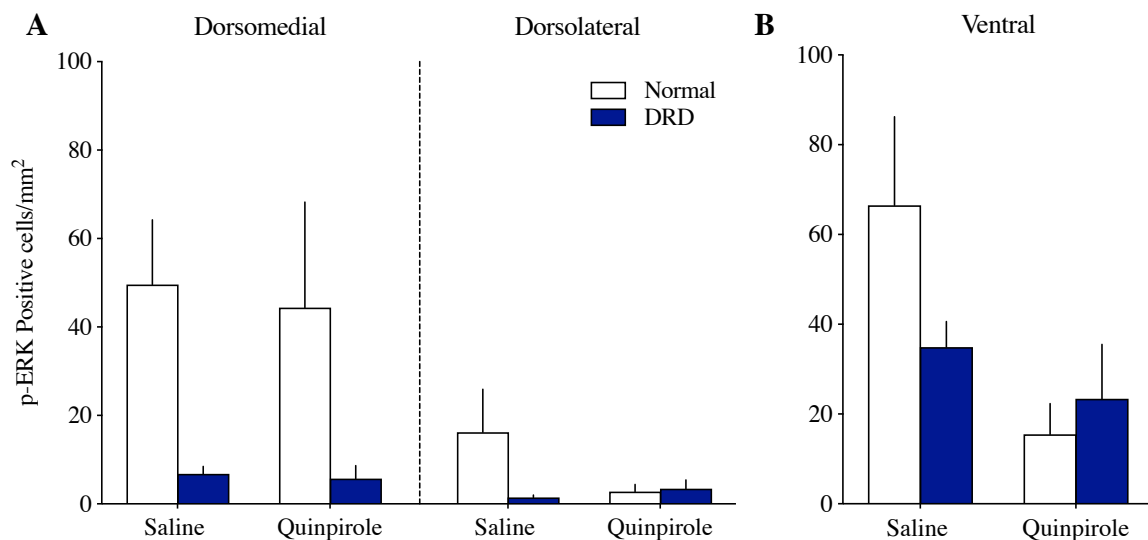


Figure 3.10. Effects of quinpirole treatment on striatal p-ERK immunoreactivity in normal and DRD mice. (A) p-ERK immunoreactivity in quinpirole- and saline-treated normal and DRD mice in dorsomedial and dorsolateral striatum was tested a genotype x treatment x region ANOVA. Quinpirole treatment had no effect of p-ERK immunoreactivity [treatment x region x genotype interaction effect, $F(1, 46) = 0.14$, $p > 0.1$]. Greater p-ERK immunoreactivity was observed in the dorsomedial striatum compared to the dorsolateral striatum of normal mice and there were very low baseline levels of p-ERK immunoreactivity in both regions in DRD mice [region x genotype interaction effect, $F(1, 46) = 4.97$, $p <$

0.05]. (B) In ventral striatum, p-ERK immunoreactivity in quinpirole- and saline-treated normal and DRD mice was tested with a two-way ANOVA. p-ERK immunoreactivity was decreased in response to quinpirole treatment compared to saline treatment [main effect of treatment, $F(1, 23) = 5.17$, $p < 0.05$]. Values represent mean + SEM; $n = 6-8$ /group.

D2R agonist-mediated c-Fos immunoreactivity

To determine whether D2R-mediated regulation of c-Fos is dysregulated in DRD mice, the effects of quinpirole treatment on c-Fos immunoreactivity in dorsomedial and dorsolateral striatum of normal and DRD mice were assessed. The effects of quinpirole treatment on c-Fos immunoreactivity in the ventral striatum of normal and DRD mice were also assessed.

In normal and DRD mice, quinpirole treatment reduced c-Fos immunoreactivity compared to saline (main effect of treatment, $p < 0.01$) in dorsomedial and to a lesser extent, dorsolateral, striatum (trend for main effect of region, $p = 0.06$; Figure 3.11A). Similarly, in ventral striatum, quinpirole treatment resulted in a modest decrease in c-Fos immunoreactivity in normal and DRD mice compared to saline (trend for a main effect of treatment, $p = 0.06$; Figure 3.11B). Overall, these results suggest that D2R-activation inhibits c-Fos induction in normal and DRD mice.

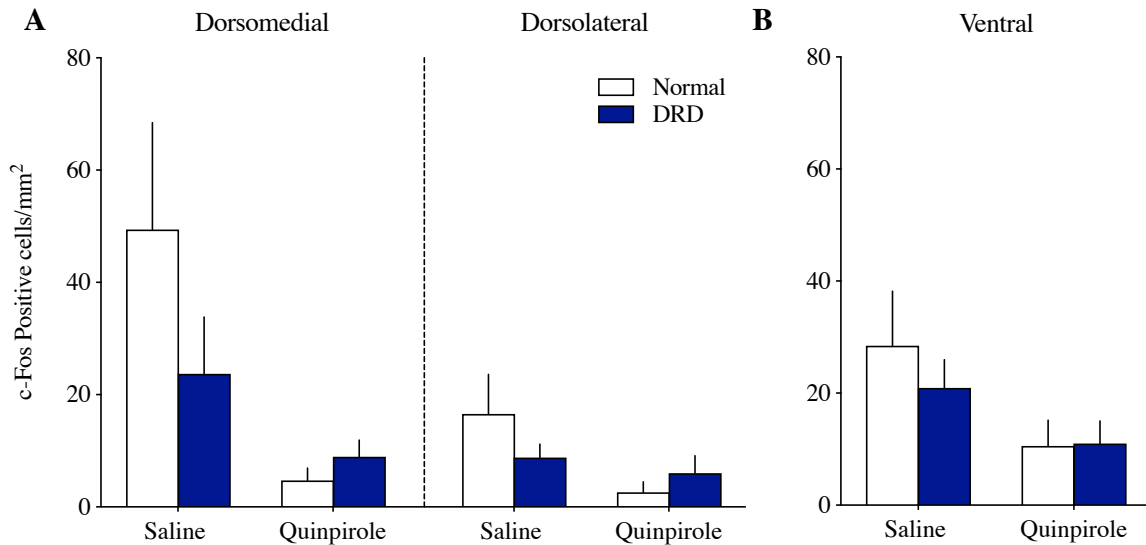


Figure 3.11. Effects of quinpirole treatment on striatal c-Fos immunoreactivity in normal and DRD mice. (A) c-Fos immunoreactivity in quinpirole- and saline-treated normal and DRD mice in dorsomedial and dorsolateral striatum was tested using a genotype x treatment x region ANOVA. In normal and DRD mice, quinpirole treatment reduced c-Fos immunoreactivity compared to saline [main effect of treatment, $F(1, 46) = 7.83, p < 0.01$] in dorsomedial and to a lesser extent, dorsolateral, striatum [trend for a main effect of region, $F(1, 46) = 3.78, p = 0.06$]. (B) In ventral striatum, c-Fos immunoreactivity in quinpirole- and saline-treated normal and DRD mice was tested with a two-way ANOVA. Quinpirole treatment resulted in a modest decrease in c-Fos immunoreactivity in normal and DRD mice compared to saline [trend for a main effect of treatment, $F(1, 23) = 3.94, p = 0.06$]. Values represent mean + SEM; $n = 6-8$ /group.

3.4.5. D2R antagonist-mediated signaling

Previous work has demonstrated that blocking the inhibitory effects of D2Rs with an antagonist is an effective approach for unmasking abnormal signaling pathways in the striatum (Gerfen, Miyachi et al. 2002). Therefore, normal and DRD mice were treated with the D2R antagonist, raclopride, and p-PKA-sub, p-ERK, and c-Fos immunoreactivity were assessed.

D2R antagonist-mediated p-PKA-sub immunoreactivity

I determined whether treatment with raclopride would reveal abnormal D2R-mediated PKA signaling in DRD mice. Specifically, the effects of raclopride treatment on p-PKA-sub immunoreactivity were assessed in the striatum of normal and DRD mice. Raclopride treatment did not significantly affect p-PKA-sub immunoreactivity in either normal or DRD mice in any striatal region (Figures 3.12A,B); however, there was a trend for reduced p-PKA-sub immunoreactivity in ventral striatum following raclopride treatment in DRD, but not normal, mice (trend for treatment x genotype interaction effect, $p = 0.09$; Figure 3.12B).

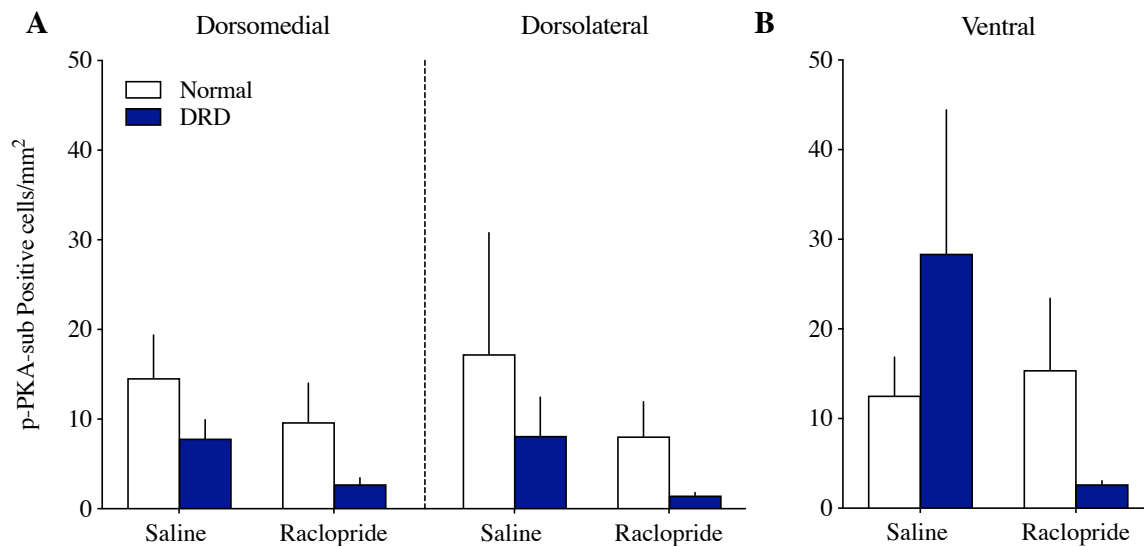


Figure 3.12. Effects of raclopride treatment on striatal p-PKA-sub immunoreactivity in normal and DRD mice. (A) p-PKA-sub immunoreactivity in raclopride- and saline-treated normal and DRD mice in dorsomedial and dorsolateral striatum was tested using a genotype x treatment x region ANOVA. Raclopride treatment did not significantly affect p-PKA-sub immunoreactivity in either normal or DRD mice in dorsomedial or dorsolateral striatum [treatment x region x genotype interaction effect, $F(1, 36) =$

0.01, $p > 0.1$]. (B) In ventral striatum, p-PKA-sub immunoreactivity in raclopride- and saline-treated normal and DRD mice was tested with a two-way ANOVA. Raclopride treatment did not significantly affect p-PKA-sub immunoreactivity in either normal or DRD mice. There was a trend for reduced p-PKA-sub immunoreactivity following raclopride treatment in DRD, but not normal, mice [treatment x genotype interaction effect, $F(1, 17) = 1.86$, $p = 0.09$]. Values represent mean + SEM; $n = 4-8$ /group.

D2R antagonist-mediated p-ERK immunoreactivity

Previous work suggests D2Rs function to inhibit c-Fos expression and that D2R antagonism blocks the inhibitory effects of D2R-activation, which results in ERK phosphorylation in the striatum (Gerfen, Miyachi et al. 2002). To determine whether D2R antagonism would reveal abnormal p-ERK signaling in DRD mice, the effects of raclopride treatment on p-ERK immunoreactivity were assessed in the striatum of normal and DRD mice.

Raclopride treatment had no effect on p-ERK immunoreactivity. Greater p-ERK immunoreactivity was observed in the dorsomedial striatum compared to the dorsolateral striatum of normal mice, whereas there were very low baseline levels of p-ERK immunoreactivity in both regions in DRD mice (region x genotype interaction, $p < 0.05$; Figure 13.3A). These results suggest there may be regional differences in the baseline regulation of ERK phosphorylation. Further, baseline regulation of ERK phosphorylation may be abnormal in DRD mice. In ventral striatum, raclopride treatment increased p-ERK immunoreactivity in normal, but not DRD mice (treatment x genotype interaction effect, $p < 0.001$; Figure 3.13B), suggesting that, overall, p-ERK responses to D2R antagonism are blunted in the ventral striatum of DRD mice.

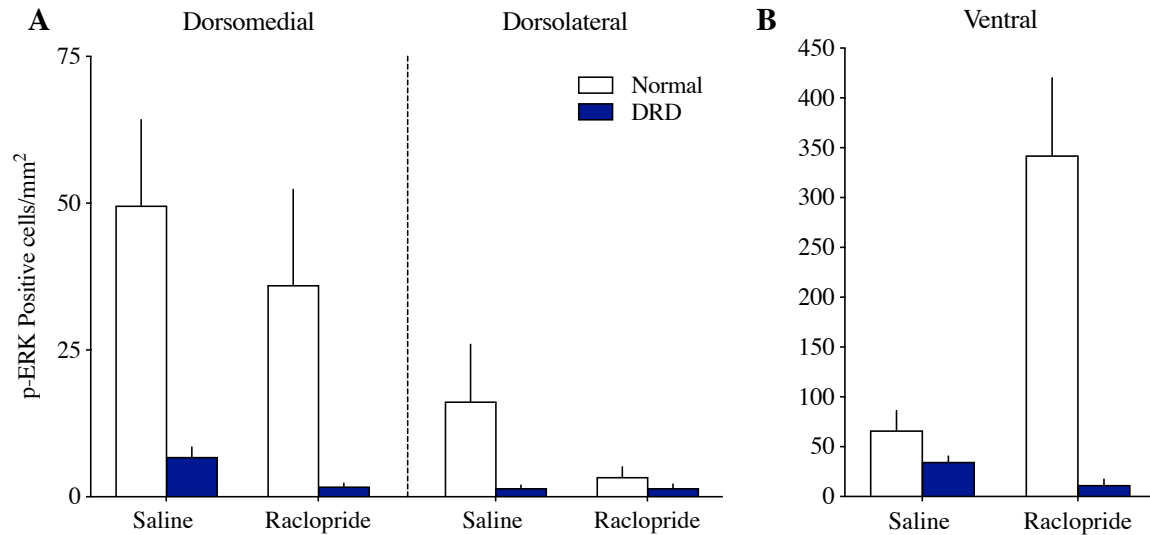


Figure 3.13. Effects of raclopride treatment on striatal p-ERK immunoreactivity in normal and DRD mice. (A) p-ERK immunoreactivity in raclopride- and saline-treated normal and DRD mice in dorsomedial and dorsolateral striatum was tested using a genotype x treatment x region ANOVA. Raclopride treatment had no effect on p-ERK immunoreactivity [treatment x region x genotype interaction effect, $F(1, 38) = 0.02$, $p > 0.1$]. Greater p-ERK immunoreactivity was observed in the dorsomedial striatum compared to the dorsolateral striatum of normal mice, whereas there were very low baseline levels of p-ERK immunoreactivity in both regions in DRD mice [region x genotype interaction effect, $F(1, 38) = 4.40$, $p < 0.05$]. (B) In ventral striatum, p-ERK immunoreactivity in raclopride- and saline-treated normal and DRD mice was tested with a two-way ANOVA. Raclopride treatment increased p-ERK immunoreactivity in normal, but not DRD mice [treatment x genotype interaction effect [$F(1, 19) = 23.11$, $p < 0.001$]. Values represent mean + SEM; $n = 4-8$ /group; y-axes differ.

D2R antagonist-mediated c-Fos immunoreactivity

To determine whether blocking inhibitory D2Rs would reveal abnormal signaling associated with c-Fos induction, the effects of raclopride treatment on c-Fos immunoreactivity in dorsomedial and dorsolateral striatum of normal and DRD mice were assessed. The effects of

raclopride treatment on c-Fos immunoreactivity in the ventral striatum of normal and DRD mice were also assessed.

Raclopride, compared to saline, treatment increased c-Fos immunoreactivity in normal, but not DRD mice (treatment x genotype interaction effect, $p < 0.0001$; Figure 3.14A) in the dorsomedial, and to a slightly greater extent, dorsolateral, striatum (trend for a significant treatment x region x genotype interaction effect, $p = 0.07$; Figure 3.14A). Dual immunofluorescence in a normal mouse revealed raclopride-induced c-Fos immunoreactivity was expressed in ~65% of D2R-MSNs in the dorsomedial striatum (Figure 3.14C), and in ~79% of D2R-MSNs in dorsolateral striatum (Figure 3.14D) suggesting that the effect was occurring in both D1R- and D2R-positive MSNs. Similarly, in ventral striatum, raclopride, compared to saline, treatment increased c-Fos immunoreactivity in normal, but not DRD mice (treatment x genotype interaction effect, $p < 0.0001$; Figure 3.14B). These results further suggest that, in contrast to normal mice, D2Rs do not significantly contribute to the regulation of intracellular c-Fos signaling pathways in DRD mice.

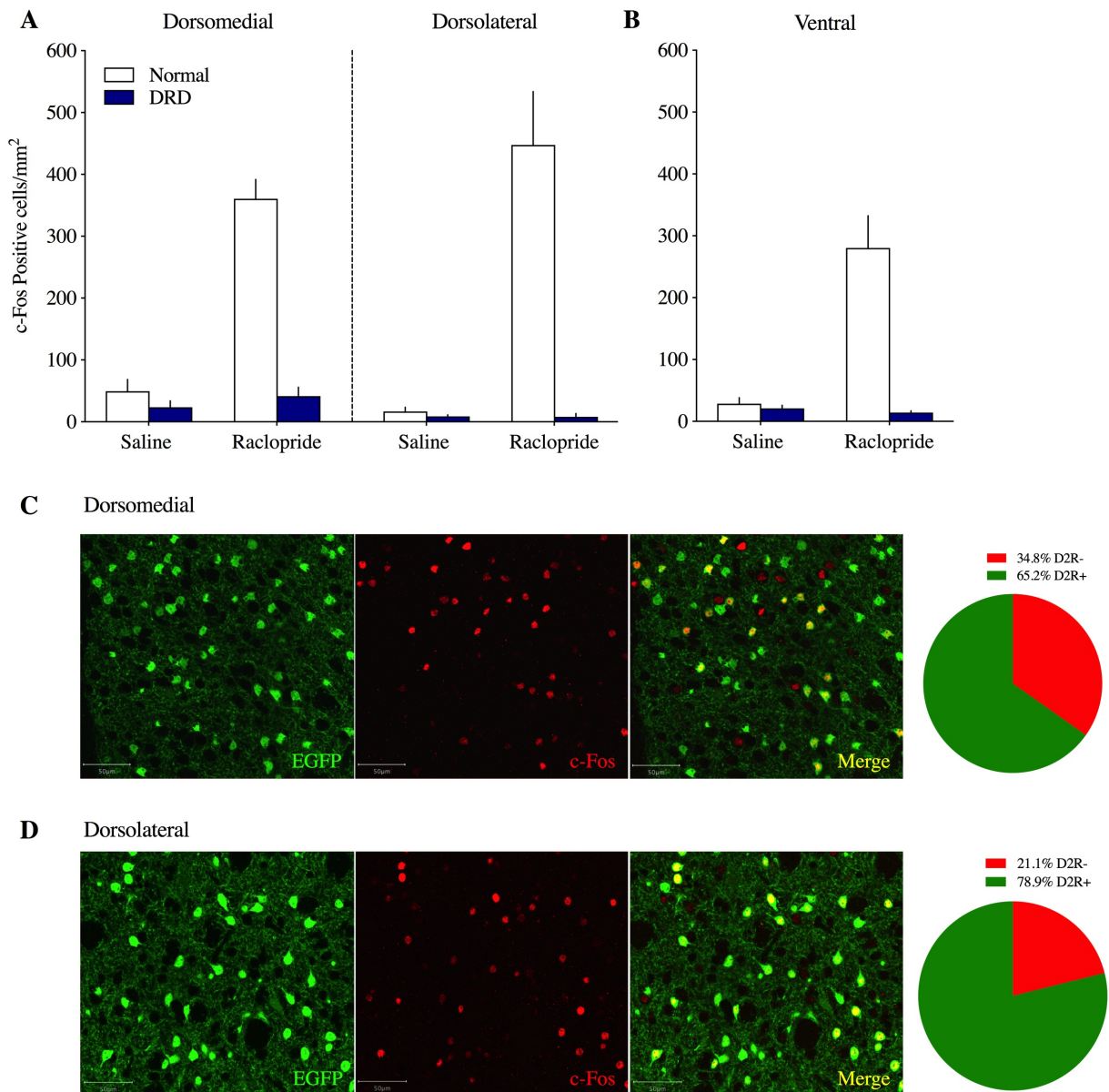


Figure 3.14. Effects of raclopride treatment on striatal c-Fos immunoreactivity in normal and DRD mice. (A) c-Fos immunoreactivity in raclopride- and saline-treated normal and DRD mice in dorsomedial and dorsolateral striatum was tested using a genotype x treatment x region ANOVA. Raclopride, compared to saline, treatment increased c-Fos immunoreactivity in normal, but not DRD mice [treatment x genotype interaction effect, $F(1, 38) = 99.08$, $p < 0.0001$] in the dorsomedial and to a slightly greater extent, dorsolateral striatum (trend for a significant treatment x region x genotype interaction effect [$F(1, 38) = 3.61$, $p = 0.07$]). (B) In ventral striatum, c-Fos immunoreactivity in raclopride- and saline-treated

normal and DRD mice was tested with a two-way ANOVA. Raclopride, compared to saline, treatment increased c-Fos immunoreactivity in normal, but not DRD mice [treatment x genotype interaction effect, $F(1, 19) = 42.57, p < 0.0001$]. Values represent mean + SEM; $n = 4-8/\text{group}$. Dual immunofluorescence from a normal mouse revealed c-Fos immunoreactivity was expressed in (C) ~65% of D2R-MSNs in the dorsomedial striatum (D) and in ~79% of D2R-MSNs in the dorsolateral striatum.

3.5. Discussion

Here I identified abnormal downstream D1R- and D2R-mediated signaling responses in the DRD mouse striatum that may underlie dystonia. First, I demonstrated that abnormalities in dopamine-mediated signaling pathways did not arise from changes in the number of D1R- or D2R-MSNs. In DRD mice, supersensitive D1R-mediated signaling was observed throughout the striatum as evidenced by increased PKA activity and ERK phosphorylation. The response to D2R-antagonism was abolished in DRD mice, as evidenced by changes in ERK phosphorylation and c-Fos expression. D2R-antagonism caused a robust increase in c-Fos expression throughout the striatum of normal mice but failed to induce striatal c-Fos expression in DRD mice. These results are summarized in Table 3.1 and provide evidence that in DRD mice, D1R-mediated signaling is supersensitive and D2R-mediated signaling is blunted or abolished.

Table 3.1. Summary of immunohistochemistry results

		Dorsomedial		Dorsolateral		Ventral	
		Normal	DRD	Normal	DRD	Normal	DRD
SKF 81297	p-PKA-sub	-	↑	-	↑	-	↑*
	p-ERK	↓	↑	↓	↑	↓	↑
	c-Fos	-	-	-	-	-	-
Quinpirole	p-PKA-sub	-	-	-	-	↑*	↓*
	p-ERK	-	-	-	-	↓	↓
	c-Fos	↓	↓	↓	↓	↓*	↓*
Raclopride	p-PKA-sub	-	-	-	-	-	↓*
	p-ERK	-	-	-	-	↑	-
	c-Fos	↑	-	↑	-	↑	-

* indicates trend in data

arrows indicate significant effects

3.5.1. Distribution of D1R- and D2R-MSNs

That abnormalities in dopamine-mediated signaling pathways did not arise from changes in the number of D1R-MSNs and D2R-MSNs is consistent with previous data showing that in DRD mice there was no change in the abundance of striatal mRNA encoding D1Rs or D2Rs compared to normal mice. Similarly, DD mice do not exhibit changes in dopamine receptor expression (Kim, Szczycka et al. 2000). Previous data in DRD mice also showed there were no differences in the affinity of D1Rs or D2Rs (Rose, Yu et al. 2015). Thus changes in D1R- and D2R-mediated signaling are likely attributable to changes in signaling pathways and not alterations in receptor affinity or distribution.

3.5.2. Regional differences in dopamine signaling in the dorsal striatum

Regional differences in baseline ERK phosphorylation were observed in normal and DRD mice. Greater p-ERK was observed in the dorsomedial compared to the dorsolateral striatum in normal and DRD mice. Overall, slightly lower levels of p-ERK were observed throughout the dorsal striatum in DRD mice compared to normal mice. This difference may be due to loss of baseline dopamine signaling in DRD mice. Further, D1R-activation induced greater levels of p-ERK in the dorsomedial compared to the dorsolateral striatum, which may be due to the increased baseline levels in this region. D1R-mediated PKA activity was positively correlated with D1R-mediated ERK phosphorylation in the dorsomedial striatum. This suggests supersensitive postsynaptic signaling in the dorsomedial striatum may be differentially regulated compared to dorsolateral or ventral striatum. However, the mechanism underlying the regional differences is not known, but could arise from both presynaptic and postsynaptic regulation of ERK phosphorylation.

3.5.3. D1R-mediated signaling

D1R-stimulated PKA activity was potentiated in D1R-MSNs throughout the striatum of DRD, but not normal mice. Given adenylate cyclase is necessary for the synthesis of cAMP and subsequent PKA-mediated signaling, this is consistent with previous data showing D1R-stimulated adenylate cyclase activity is potentiated in striatal homogenates of DRD mice compared to normal mice (Rose, Yu et al. 2015).

In DRD mice, there was a small increase in p-ERK within D1R-MSNs throughout the striatum in response to D1R-activation. This is similar to other models of dopamine depletion, in which ERK is phosphorylated in the dorsal striatum via D1R-activation (Kim, Szczyepka et al. 2000, Gerfen, Miyachi et al. 2002, Kim, Palmiter et al. 2006). D1R-mediated PKA activity in

DRD mice was positively correlated with ERK phosphorylation in the dorsomedial striatum, where the increase in ERK phosphorylation was greatest. PKA does not directly phosphorylate ERK; however, there are number of proposed pathways that indirectly link PKA activity and p-ERK. For example, ERK phosphorylation may occur via integration of D1Rs, NMDARs, and DARPP-32 signaling (Valjent, Pascoli et al. 2005). In normal mice, D1R-activation resulted in a small decrease of ERK phosphorylation throughout the striatum; however, D1R-activation has been shown to induce p-ERK in the ventral striatum (Gerfen, Miyachi et al. 2002). Nonetheless, these results support supersensitive D1R-mediated cAMP signaling in DRD mice.

D1R-activation did not affect c-Fos expression in the striatum of normal or DRD mice. This is somewhat surprising given expression of c-Fos can be induced downstream of PKA activation (Andersson, Konradi et al. 2001). While p-ERK was increased in DRD mice, there was not a parallel increase in c-Fos expression. However, in both the 6-OHDA-lesioned rodent model (Gerfen, Keefe et al. 1995, Berke, Paletzki et al. 1998, Gerfen, Miyachi et al. 2002) and the DD mouse model (Kim, Szczycka et al. 2000), D1R-mediated expression of c-Fos is abnormally elevated and is associated with ERK phosphorylation (Kim, Szczycka et al. 2000, Gerfen, Miyachi et al. 2002, Kim, Palmiter et al. 2006). These differences suggest dopamine-mediated c-Fos expression may reflect abnormal signaling pathways that may distinguish dystonia from other dopamine deficient models in which dystonia is not observed.

One limitation is that I used a low dose of SKF 81297 for these experiments. This dose was used because it has been previously shown to alleviate abnormal movements in DRD mice (Rose, Yu et al. 2015). The absence of p-ERK in the ventral striatum of normal mice may also be attributable to the use of a low dose of SKF 81297. Further, higher doses of SKF 81297 may

reveal greater supersensitivity in D1R-mediated signaling and ultimately induce c-Fos expression in the dorsal striatum of DRD mice.

3.5.4. D2R-mediated signaling

D2R-antagonism increased striatal c-Fos expression in predominately D2R-MSNs in normal mice, but not in DRD mice. This is consistent with previous results showing an increase in c-Fos expression following treatment with the D2R antagonist, haloperidol, in normal mice (Dragunow, Robertson et al. 1990, Robertson and Fibiger 1992).

D2R-antagonism may induce c-Fos in D2R-MSNs by allowing unopposed adenosine A2A receptor (A2AR)-mediated signaling (Agnati, Ferre et al. 2003). A2ARs are expressed on D2R-MSNs and may induce c-Fos via activation of the cAMP-PKA signaling, which under normal conditions is restrained by the tonic inhibitory effect of D2Rs (Schiffmann, Fisone et al. 2007). Therefore, in DRD mice, the reciprocal relationship between D2Rs and A2ARs may be dysregulated. Specifically, the failure of D2R-antagonism to induce c-Fos expression may be due to insufficient postsynaptic inhibitory D2R-mediated tone in DRD mice. This hypothesis is supported by previous work that showed D2R-stimulated adenylate cyclase activity is blunted in striatal homogenates of DRD mice compared to normal mice (Rose, Yu et al. 2015).

While expression of c-Fos in response to raclopride treatment predominately occurred in D2R-MSNs of normal mice, expression of c-Fos also occurred in D1R-MSNs. D2R-antagonism may also affect D2 autoreceptors on nigrostriatal terminals and/or through blockade of D2Rs on corticostriatal terminals (Dragunow, Robertson et al. 1990). Disinhibition of both corticostriatal and nigrostriatal inputs may account for the increase in c-Fos in D1R-MSNs. The exact

mechanism by which D2R-antagonism increases c-Fos in normal mice is not known; however, these results suggest that D2R signaling is blunted in DRD mice.

D2R-antagonism induced ERK phosphorylation in the ventral striatum of normal, but not DRD, mice. This finding is consistent with previous work that has shown D2R-antagonism induces p-ERK in the dopamine-intact, but not depleted, striatum of 6-OHDA-lesioned rodents (Gerfen, Miyachi et al. 2002). However, it is somewhat surprising that D2R-antagonism did not affect ERK phosphorylation in the dorsal striatum in normal mice, as has been previously shown (Gerfen, Miyachi et al. 2002). Examining ERK phosphorylation 15 min following D2R antagonism, as occurred in the aforementioned study, may reveal similar effects and allow for further determination regarding dysregulated D2R-mediated signaling in DRD mice.

3.5.5. Implications of blunted D2R inhibition in DRD mice

D2R-mediated signaling has been relatively unexplored in animal models of dopamine depletion, so it is difficult to discern how blunted D2R inhibition in DRD mice may distinguish dystonia from other dopamine deficiencies that do not lead to dystonia. However, previous work has shown that antagonism of D2Rs fails to induce p-ERK in the dopamine-depleted striatum of 6-OHDA-lesioned rats (Gerfen, Miyachi et al. 2002), which suggests D2R-mediated signaling is sensitive to deficiencies in dopamine signaling.

Dysregulations in D2R-mediated signaling in DRD mice may underlie the expression of dystonia. Specifically, D2R antagonism worsens dystonia, and dysregulations in reciprocal D2R- and A2AR- mediated signaling may inform our understanding of this effect (Rose, Yu et al. 2015). Under normal conditions, D2Rs exert a tonic inhibitory effect, which restrains the ability of G α olf-coupled A2ARs to activate the cAMP-PKA signaling (Schiffmann, Fisone et

al. 2007). If D2Rs are blunted, then there are likely compensatory mechanisms in A2AR-mediated signaling to account for the lack of aberrant cAMP-PKA signaling, as evidenced by the low baseline levels of PKA activity, ERK phosphorylation, and c-Fos expression observed in the striatum of DRD mice. In order to determine whether the balance of D2R- and A2AR-mediated intracellular signaling affects dystonia, future studies can test if activation of A2ARs worsens dystonia, or conversely whether antagonism of A2ARs alleviates dystonia.

3.5.6. Conclusions

The development of dystonia is likely the result of dopamine depletion along with very specific abnormalities in dopamine-mediated signaling pathways. DRD mice showed supersensitive D1R-mediated signaling, similar to what is observed in other animal models of dopamine depletion. However, further assessments regarding D1R-mediated expression of c-Fos may ultimately reveal alterations in D1R-mediated signaling pathways that are unique to dystonia.

D2R-mediated signaling is blunted or abolished in DRD mice. As discussed, D2R-antagonism may alter multiple D2R-mediated signaling pathways including blockade of D2 autoreceptors on nigrostriatal terminals and/or through blockade of D2Rs on corticostriatal terminals (Dragunow, Robertson et al. 1990). Future experiments aimed at determining which D2R-mediated mechanisms underlie D2R-antagonism induced c-Fos are necessary.

Understanding the precise nature of D2R-mediated signaling, and reciprocal regulation via A2AR-mediated signaling, may inform our understanding of dystonia.

Chapter 4: Determining the therapeutic mechanism of L-DOPA in a mouse model of DOPA-responsive dystonia

4.1. Abstract

The work in this chapter identifies L-DOPA-induced postsynaptic intracellular signaling cascades in the DRD mouse striatum. Immunohistochemistry was used to examine changes in L-DOPA-mediated regulation of PKA activity, ERK phosphorylation, and c-Fos expression in the striatum of normal and DRD mice. Here I demonstrated that L-DOPA treatment induced striatal PKA activity, ERK phosphorylation, and c-Fos expression in D1R-MSNs throughout the striatum of DRD mice compared to normal mice. Further, L-DOPA-induced ERK phosphorylation was elevated in the dorsomedial striatum compared to the dorsolateral striatum of DRD mice. L-DOPA-induced signaling alterations, specifically the regional differences in ERK phosphorylation, may reflect an anti-dystonic mechanism. Understanding the mechanism by which L-DOPA induces alterations in signaling pathways may allow for the identification of novel drug targets for dystonias that arise from other etiologies for which there are no effective treatments.

4.2. Introduction

L-DOPA is highly effective at alleviating dystonia in patients with DOPA-responsive dystonia. An abnormal reduction in dopamine neurotransmission is implicated in many forms of dystonia. Therefore, understanding the therapeutic mechanism of L-DOPA may uncover anti-dystonic mechanisms that could serve as drug targets for dystonias that arise from other etiologies for which there are no effective treatments. Because DRD mice have face, etiologic, and predictive validity, this model may be useful to uncover the mechanism(s) underlying the therapeutic efficacy of L-DOPA (Rose, Yu et al. 2015). Identification of a therapeutic mechanism of L-DOPA would also support the development of more selective small molecules to treat dystonia.

Evidence from DRD mice suggests changes in postsynaptic striatal intracellular signaling cascades may underlie the therapeutic mechanism of L-DOPA. Indeed, microinjection of L-DOPA directly into the striatum ameliorates dystonia in DRD mice, but cerebellar microinjections had no effect (Rose, Yu et al. 2015). To examine the postsynaptic intracellular signaling cascades that may underlie the therapeutic mechanism of L-DOPA, I utilized immunohistochemistry to assess L-DOPA-mediated changes in 1) PKA activity using an indirect assessment of PKA substrate phosphorylation, 2) ERK phosphorylation, and 3) c-Fos expression in the striatum of normal and DRD mice.

4.3. Methods

Mice. Male and female adult (3-6 month) mice homozygous for the c.1160C>A *Th* mutation (DRD; drd/drd) and littermates carrying two wild-type alleles (normal; +/+) were used for all experiments and were previously described (Chapter 3). Christine Donsante, MS, generated all mice used in all experiments described. Housing conditions were in accordance with Emory

University's Institutional Animal Care and Use Committee (IACUC). The light period was 7am to 7pm. All procedures were conducted in accordance with Emory's IACUC and Division of Animal Resources guidelines and were approved by IACUC. Mice were maintained as previously described (Rose, Yu et al. 2015).

Drug challenges. Drugs were injected s.c. in saline (0.9% NaCl) in a volume of 10 ml/kg unless otherwise noted. L-DOPA was obtained from Sigma-Aldrich (St. Louis, MO). L-DOPA (10 mg/kg) at the dose selected was chosen because it has previously been shown to alleviate dystonia in DRD mice (Rose, Yu et al. 2015). Mice were treated with drug between 12-4 pm and were sacrificed 45 min later.

Immunohistochemistry. Immunohistochemistry (bright-field and immunofluorescence) was performed as previously described (Chapter 2 and 3).

Image analysis and cell counts. Bright-field immunohistochemistry and immunofluorescence was analyzed as previously described (Chapter 2 and 3).

Statistics. Prism 8 was used for all analyses. Detailed statistical results are presented in the figure legends. Counts of p-PKA-sub, p-ERK and c-Fos positive cells per square mm in dorsomedial and dorsolateral striatum were analyzed using a treatment x region x genotype ANOVA, whereas results in ventral striatum were analyzed using a two-way treatment x genotype ANOVA.

4.4. Results

4.4.1. L-DOPA-induced p-PKA-sub immunoreactivity

To examine postsynaptic intracellular signaling cascades that may underlie the therapeutic mechanism of L-DOPA, the effects of L-DOPA treatment on p-PKA-sub immunoreactivity in dorsomedial and dorsolateral striatum of normal and DRD mice were assessed. The effects of L-DOPA treatment on p-PKA-sub immunoreactivity in the ventral striatum of normal and DRD mice were also assessed.

Compared to saline treatment, L-DOPA treatment increased p-PKA-sub immunoreactivity in the dorsomedial and dorsolateral striatum of DRD but not normal mice (treatment x genotype interaction effect, $p < 0.05$; Figure 4.1A). Dual immunofluorescence in the dorsomedial (Figure 4.1C) and dorsolateral (data not shown) striatum of a DRD mouse revealed L-DOPA-induced p-PKA-sub immunoreactivity was not expressed in D2R-MSNs. In ventral striatum, there was a trend for a main effect of genotype ($p = 0.09$; Figure 4.1B) with increased p-PKA-sub immunoreactivity observed in DRD mice. These results suggest that in DRD mice, PKA-mediated signal transduction pathways in D1R-MSNs are supersensitive.

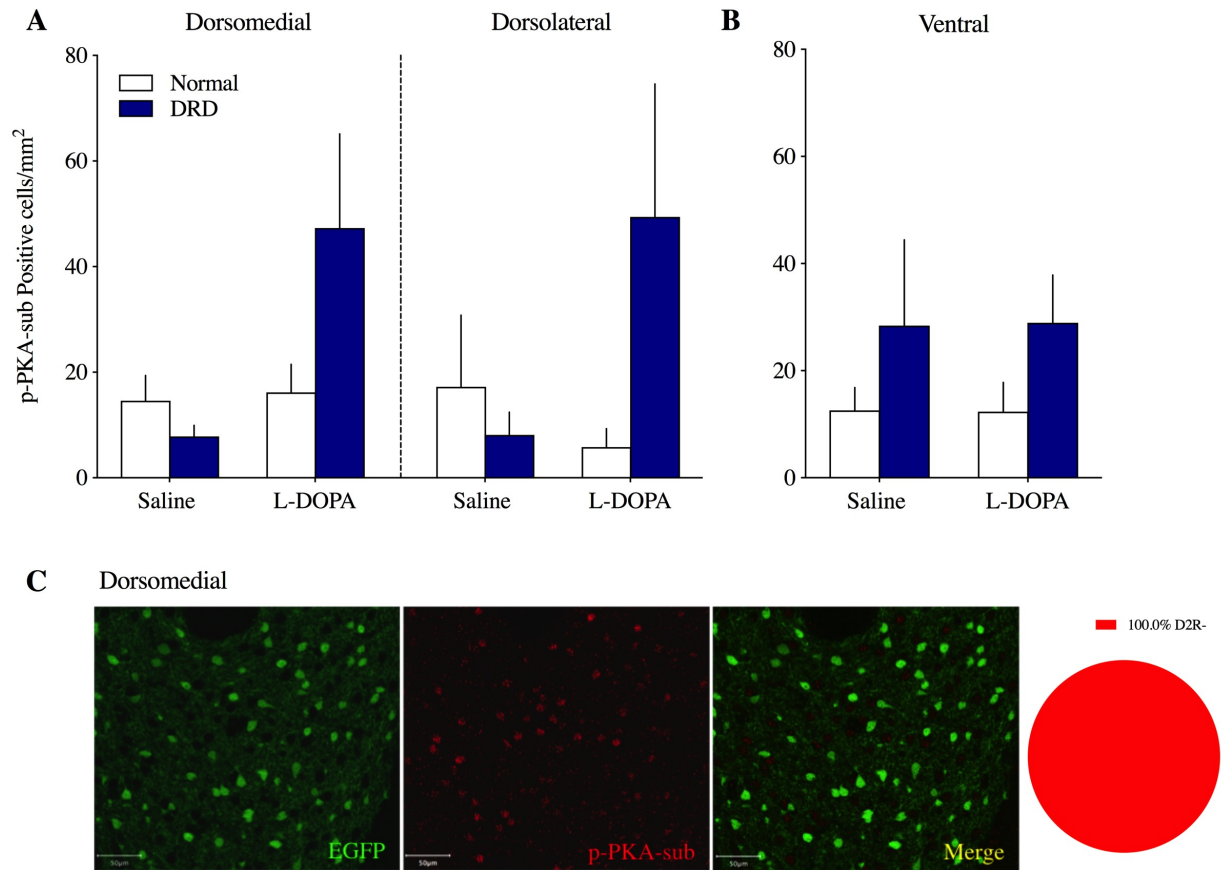


Figure 4.1. Effects of L-DOPA treatment on striatal p-PKA-sub immunoreactivity in normal and DRD mice. (A) p-PKA-sub immunoreactivity in L-DOPA- and saline-treated normal and DRD mice in dorsomedial and dorsolateral striatum was tested using a three-way genotype x treatment x region ANOVA. Compared to saline treatment, L-DOPA treatment increased p-PKA-sub immunoreactivity in the dorsomedial and dorsolateral striatum of DRD but not normal mice [treatment x genotype interaction effect, $F(1, 48) = 6.33$, $p < 0.05$]. (B) In ventral striatum, p-PKA-sub immunoreactivity in L-DOPA- and saline-treated normal and DRD mice was tested with a two-way ANOVA. There was a trend for increased p-PKA-sub immunoreactivity observed in DRD mice [trend for a main effect of genotype, $F(1, 23) = 3.10$, $p = 0.09$]. Values represent mean + SEM; $n = 6-8$ /group. (C) Dual immunofluorescence from the dorsomedial striatum of a DRD mouse revealed L-DOPA-induced p-PKA-sub immunoreactivity was not expressed in D2R-MSNs.

4.4.2. L-DOPA-induced p-ERK immunoreactivity

The effects of L-DOPA treatment on p-ERK immunoreactivity in dorsomedial, dorsolateral, and ventral striatum of normal and DRD mice were assessed. Compared to saline treatment, L-DOPA treatment induced greater p-ERK immunoreactivity in the dorsolateral, and to a greater extent, the dorsomedial, striatum in DRD but not normal mice (treatment x region x genotype interaction effect, $p < 0.0001$; Figure 4.2A). Dual immunofluorescence from the dorsomedial (Figure 4.2C) and dorsolateral (data not shown) striatum of a DRD mouse revealed L-DOPA-induced p-ERK immunoreactivity was not expressed in D2R-MSNs. Similarly in ventral striatum, L-DOPA induced greater p-ERK immunoreactivity in DRD but not normal mice (treatment x genotype interaction effect, $p < 0.0001$; Figure 4.2B). These results suggest that in DRD mice, L-DOPA induces p-ERK throughout the striatum but preferentially in the dorsomedial striatum within D1R-MSNs.

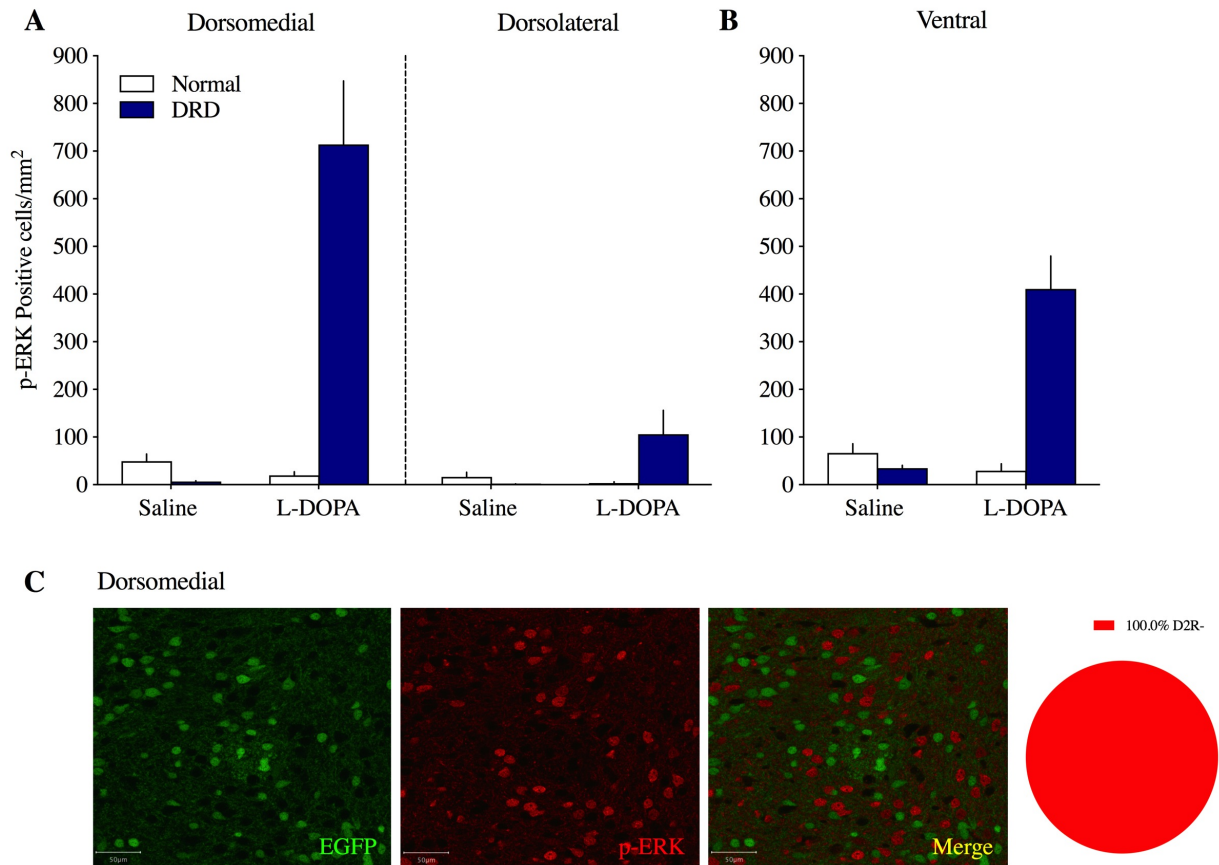


Figure 4.2. Effects of L-DOPA treatment on striatal p-ERK immunoreactivity in normal and DRD mice. (A) p-ERK immunoreactivity in L-DOPA- and saline-treated normal and DRD mice in dorsomedial and dorsolateral striatum was tested using a three-way genotype x treatment x region ANOVA. Compared to saline treatment, L-DOPA treatment induced p-ERK immunoreactivity in the dorsolateral, and to a greater extent, the dorsomedial, striatum in DRD but not normal mice [treatment x region x genotype interaction effect, $F(1, 50) = 19.90$, $p < 0.0001$]. (B) In ventral striatum, p-ERK immunoreactivity in L-DOPA- and saline-treated normal and DRD mice was tested with a two-way ANOVA. L-DOPA induced p-ERK immunoreactivity in DRD but not normal mice [treatment x genotype interaction effect, $F(1, 25) = 33.03$, $p < 0.0001$]. Values represent mean + SEM; $n = 7-8$ /group. (C) Dual immunofluorescence from the dorsomedial striatum of a DRD mouse revealed L-DOPA-induced p-ERK immunoreactivity was not expressed in D2R-MSNs.

4.4.3. L-DOPA-induced c-Fos immunoreactivity

The effects of L-DOPA treatment on c-Fos immunoreactivity in dorsomedial, dorsolateral, and ventral striatum of normal and DRD mice were assessed. Compared to saline treatment, L-DOPA treatment increased c-Fos immunoreactivity in the dorsomedial and dorsolateral striatum of DRD but not normal mice (treatment x genotype interaction effect, $p < 0.01$; Figure 4.3A). There were no regional differences in c-Fos expression. Dual immunofluorescence from the dorsomedial (Figure 4.3C) and dorsolateral (Figure 4.3D) striatum of a DRD mouse revealed L-DOPA-induced c-Fos immunoreactivity was not expressed in D2R-MSNs. Similarly in ventral striatum, L-DOPA treatment compared to saline treatment increased c-Fos immunoreactivity in DRD but not normal mice (treatment x genotype interaction effect, $p < 0.01$; Figure 4.3B). The results suggest that in DRD mice, L-DOPA induces c-Fos expression throughout the striatum in D1R-MSNs.

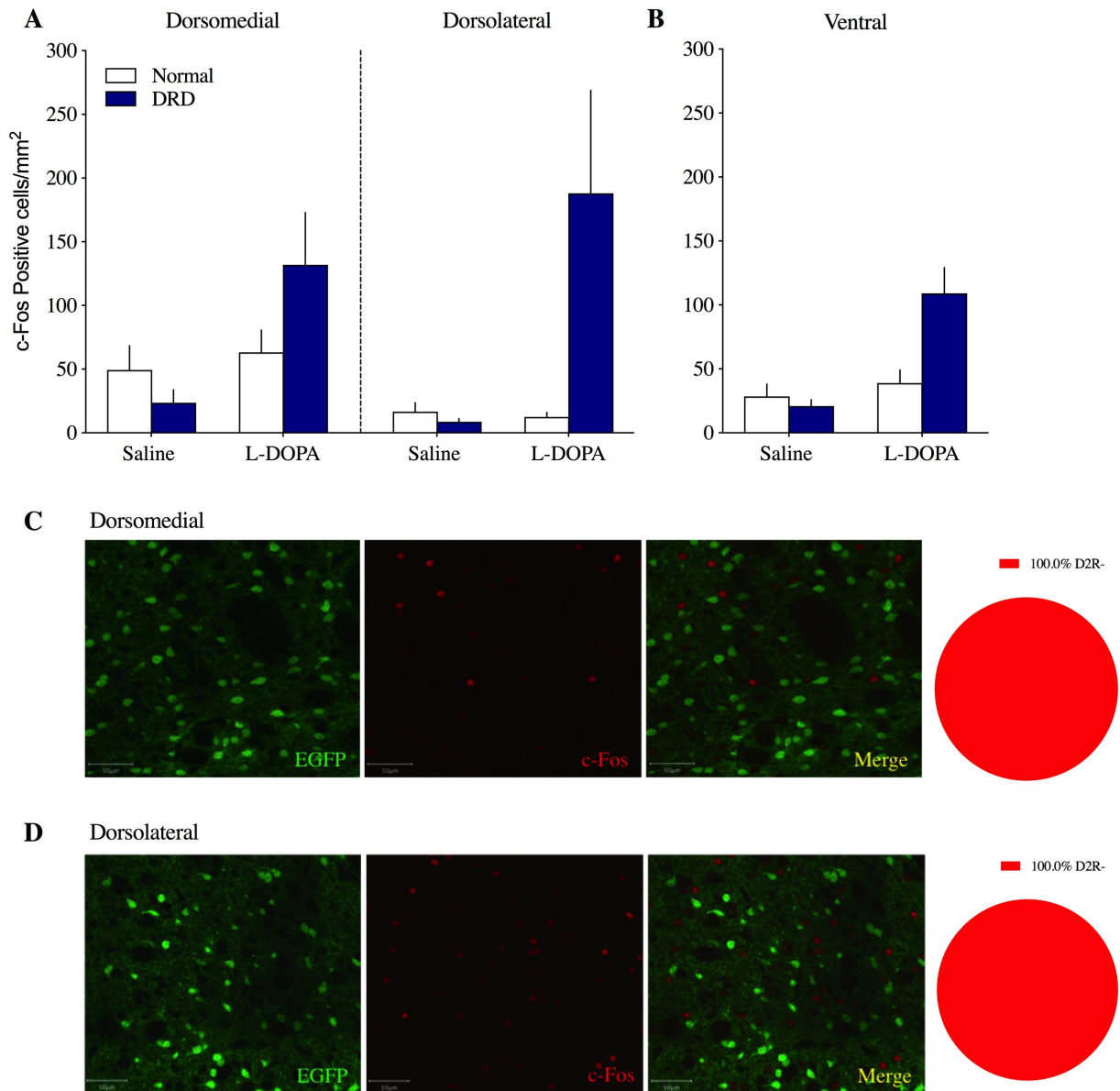


Figure 4.3. Effects of L-DOPA treatment on striatal c-Fos immunoreactivity in normal and DRD mice. (A) c-Fos immunoreactivity in L-DOPA- and saline-treated normal and DRD mice in dorsomedial and dorsolateral striatum was tested using a three-way genotype x treatment x region ANOVA. Compared to saline treatment, L-DOPA treatment increased c-Fos immunoreactivity in the dorsomedial and dorsolateral striatum of DRD but not normal mice [treatment x genotype interaction effect, $F(1, 50) = 9.01$, $p < 0.01$]. (B) In ventral striatum, c-Fos immunoreactivity in L-DOPA- and saline-treated normal and DRD mice was tested with a two-way ANOVA. L-DOPA treatment compared to saline treatment

increased c-Fos immunoreactivity in DRD but not normal mice [treatment x genotype interaction effect, $F(1, 25) = 9.76, p < 0.01$]. Values represent mean + SEM; $n = 7-8/\text{group}$. Dual immunofluorescence from the dorsomedial (C) and dorsolateral (D) striatum of a DRD mouse revealed L-DOPA-induced c-Fos immunoreactivity was not expressed in D2R-MSNs.

4.4.3. Correlation of L-DOPA-induced p-PKA-sub, p-ERK, and c-Fos immunoreactivity

L-DOPA treatment increased immunoreactivity of p-PKA-sub, p-ERK, and c-Fos immunoreactivity in DRD mice only. To examine whether increases in p-PKA-sub, p-ERK, and c-Fos immunoreactivity were related, I determined whether L-DOPA-induced p-PKA-sub, p-ERK and, and c-Fos immunoreactivity were correlated in the dorsomedial and dorsolateral striatum of DRD mice. No significant correlations were observed (Figure 4.4A-E) except for L-DOPA-induced p-ERK and c-Fos immunoreactivity in the dorsolateral striatum ($p < 0.05$; Figure 4.4F). Overall, L-DOPA-induced PKA activity, ERK phosphorylation, and c-Fos expression may be independently or differentially regulated in the dorsal striatum of DRD mice.

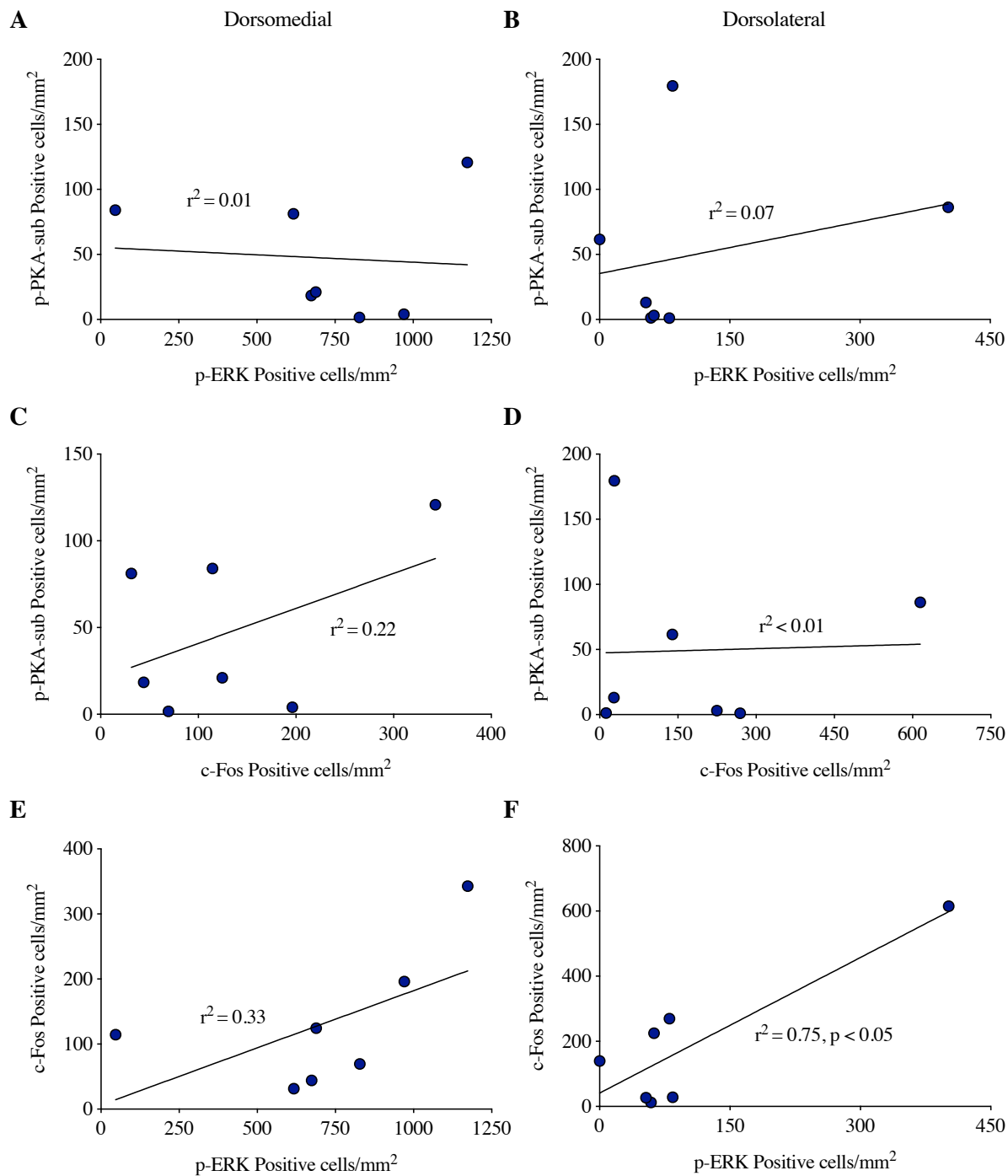


Figure 4.4. Correlation of p-PKA-sub, p-ERK and, and c-Fos immunoreactivity following L-DOPA treatment in DRD mice. L-DOPA-induced p-PKA-sub and p-ERK immunoreactivity in the (A) dorsolateral striatum [$r(7) = -0.08, p > 0.1$] and (B) dorsolateral striatum [$r(7) = 0.27, p > 0.1$] were not correlated. L-DOPA-induced p-PKA-sub and c-Fos immunoreactivity in the (C) dorsomedial striatum

[$r(7) = 0.46$, $p > 0.1$] and the (D) dorsolateral striatum [$r(7) = 0.04$, $p > 0.1$] were not correlated. L-DOPA-induced p-ERK and c-Fos immunoreactivity in the (E) dorsomedial striatum [$r(7) = 0.57$, $p > 0.1$] were not correlated, but L-DOPA-induced p-ERK and c-Fos immunoreactivity in the (F) dorsolateral striatum [$r(7) = 0.86$, $p < 0.05$] were correlated.

4.5. Discussion

I identified L-DOPA-induced postsynaptic intracellular signaling cascades in the DRD mouse striatum. Here I demonstrated that L-DOPA treatment induced striatal PKA activity, ERK phosphorylation, and c-Fos expression in D1R-MSNs throughout the striatum of DRD mice. L-DOPA-induced ERK phosphorylation was elevated in the dorsomedial striatum compared to the dorsolateral striatum of DRD mice.

L-DOPA treatment had no effect on the assessed postsynaptic intracellular signaling cascades in the normal mouse striatum. This is not surprising given previous studies have shown that L-DOPA treatment does not induce ERK phosphorylation or c-Fos expression in normal animals (Kim, Szczypka et al. 2000, Westin, Vercaemmen et al. 2007). This is likely due to the fact the L-DOPA treatment does not increase striatal dopamine release in normal mice (Downs, Fan et al. 2019).

4.5.1 L-DOPA-induced postsynaptic intracellular signaling cascades

In DRD mice, L-DOPA induced PKA activity in the dorsal striatum in D1R-MSNs, and there was a trend for increased PKA activity in the ventral striatum. Adenylate cyclase is necessary for the synthesis of cAMP and subsequent PKA-mediated signaling, so these results are consistent with previous findings that show D1R-stimulated adenylate cyclase activity is potentiated in striatal homogenates of DRD mice compared to normal mice (Rose, Yu et al. 2015) and

consistent with my findings in Chapter 3 (Figure 3.5) that D1R-activation stimulates PKA activity in D1R-MSNs throughout the striatum of DRD mice. These results further support that D1R-mediated cAMP signaling is supersensitive in DRD mice.

In DRD mice, ERK phosphorylation was increased in D1R-MSNs predominately in the dorsomedial striatum following L-DOPA treatment. This is consistent with that fact that in DRD mice, there was a moderate increase in p-ERK in response to D1R-activation that was greatest in dorsomedial striatum (Chapter 3, Figure 3.6). Increased ERK phosphorylation in response to L-DOPA has also been shown to develop after prolonged absence of dopaminergic input, as observed in the 6-OHDA-lesioned (Westin, Vercammen et al. 2007, Darmopil, Martin et al. 2009, Santini, Alcacer et al. 2009) and DD (Kim, Szczyпка et al. 2000) models. In the 6-OHDA-lesioned model, ERK phosphorylation is also restricted to D1R-MSNS (Darmopil, Martin et al. 2009, Santini, Alcacer et al. 2009).

Expression of c-Fos was increased following L-DOPA treatment selectively in D1R-MSNs throughout the striatum of DRD mice. D1R-activation did not induce c-Fos expression in the striatum of DRD mice (Chapter 3, Figure 3.8); however, these seemingly discrepant finding may be due to the enhanced ERK phosphorylation following L-DOPA treatment that was not observed after D1R-activation alone. L-DOPA-induced p-ERK and c-Fos immunoreactivity in the dorsolateral striatum were positively correlated, which is consistent with studies showing D1R-mediated expression of c-Fos is associated with ERK phosphorylation in the dopamine-depleted striatum (Gerfen, Keefe et al. 1995, Berke, Paletzki et al. 1998, Kim, Szczyпка et al. 2000, Gerfen, Miyachi et al. 2002, Kim, Palmiter et al. 2006). However, ERK phosphorylation was not correlated with c-Fos expression in the dorsomedial striatum where L-DOPA-induced p-ERK was the greatest. Alterations in nondopaminergic striatal inputs including corticostriatal

glutamatergic signaling may also directly regulate c-Fos expression (Schwarzschild, Cole et al. 1997).

4.5.2. Regional differences in L-DOPA-induced ERK phosphorylation

L-DOPA induced greater ERK phosphorylation in the dorsomedial striatum compared to the dorsolateral striatum of DRD mice. This is consistent with the baseline regional differences in p-ERK observed in normal and DRD mice (Chapter 3). Greater p-ERK was observed in the dorsomedial compared to the dorsolateral striatum in normal and DRD mice. Additionally, D1R-activation induced greater levels of p-ERK in the dorsomedial compared to the dorsolateral striatum (Chapter 3). Previous work has shown amphetamine-induced c-Fos expression in D1R- and D2R-MSNs was greatest in the dorsomedial striatum (Ren, Guo et al. 2017). This suggests that the dorsomedial striatum may be sensitive to differential dopamine regulation.

As discussed (Chapter 2), it is, perhaps, not surprising that the distribution of ERK phosphorylation is not uniform across the striatum. Glutamatergic inputs to the striatum project in a somatotopic manner forming segregated loops and distinct functional territories within the striatum (Redgrave, Rodriguez et al. 2010, Hintiryan, Foster et al. 2016, Anderson, Krienen et al. 2018). The dorsomedial striatum, which is responsible for cognitive function and goal-directed behavior, receives input from cortical regions responsible for associative functions (Redgrave, Rodriguez et al. 2010, Graybiel and Grafton 2015). In fact, ERK phosphorylation in the rat posterior dorsomedial striatum was shown to be necessary for the encoding and performance of goal-directed actions (Shiflett, Brown et al. 2010). This suggests that abnormalities in goal-directed behavior may underlie dystonia. Interestingly, motor symptoms in Parkinson's disease have been associated with the reliance on a goal-directed mode of action due to progressive

degeneration of lateral sections of the caudate putamen, which are associated with habitual behavior (Redgrave, Rodriguez et al. 2010). This not only supports that the differences in ERK phosphorylation have functional correlates, but that the abnormalities in striatal subdivisions may be specific to dystonia

In contrast to DRD mice, in the 6-OHDA-lesioned model, L-DOPA-induced p-ERK was uniform throughout the striatum; however, only subregions of the dorsomedial and dorsolateral striatum were assessed (Westin, Vercammen et al. 2007). This suggests that while D1R sensitivity may occur in response to dopamine depletion, the regional differences in D1R sensitivity are specific to dystonia. Both L-DOPA treatment and D1R-activation induced greater ERK phosphorylation in the dorsomedial striatum, which suggests postsynaptic supersensitive D1Rs may mediate this effect. However, the regional differences in ERK phosphorylation may be due to a variety of striatal abnormalities. In DRD mice, L-DOPA-induced PKA activity was not correlated with L-DOPA-induced ERK phosphorylation, whereas PKA activity and ERK phosphorylation induced by D1R-activation were positively in the dorsomedial striatum (Chapter 3, Figure 3.7). This finding may be due to that fact that PKA activity does not directly phosphorylate ERK, and may reflect the contribution of other neurotransmitter systems. Additional experiments assessing the contribution of pre- and post-synaptic effects of L-DOPA-mediated signaling are needed to determine the underlying mechanism and significance of regional differences in ERK phosphorylation.

4.5.3. Conclusions

L-DOPA-induced striatal PKA activity, ERK phosphorylation, and c-Fos expression may reflect an anti-dystonic mechanism. Understanding the mechanism of L-DOPA-induced postsynaptic

intracellular signaling cascades in DRD mice, specifically the regional differences in ERK phosphorylation may reveal striatal subdivisions that play an important role in the expression of dystonia.

Chapter 5: Determining the role of D1Rs and D2Rs in the therapeutic mechanism of L-DOPA in a mouse model of DOPA-responsive dystonia

5.1. Abstract

Here I examined the role of D1Rs and D2Rs in L-DOPA-mediated signaling in the dorsal striatum. Specifically, to determine the role of D1R and D2R signaling in L-DOPA-mediated signaling, D1Rs or D2Rs were blocked in the presence of L-DOPA, and immunohistochemistry was used to examine changes in PKA activity, ERK phosphorylation, and c-Fos expression in the dorsal striatum of normal and DRD mice. To determine the role of D1R and D2R signaling in the therapeutic efficacy of L-DOPA, D1Rs and/or D2Rs were blocked in the presence of L-DOPA and abnormal movements and locomotor activity were assessed. I demonstrated that in DRD mice, L-DOPA-induced supersensitivity in D1R-MSNs is mediated by D1Rs and PKA activity was also regulated by D2Rs. Further, D1R antagonism and D2R antagonism separately did not abolish L-DOPA-induced alleviation of abnormal movements; however, combined D1R and D2R antagonism blocked, in part, L-DOPA-induced alleviation of abnormal movements. Future studies assessing abnormal D1R and D2R signaling may ultimately uncover the mechanism underlying dystonia in DRD mice.

5.2. Introduction

Understanding the therapeutic mechanism of L-DOPA may uncover anti-dystonic mechanisms for the treatment of many forms of dystonia that arise from other etiologies for which there are no effective treatments. L-DOPA functions as an indirect D1R and D2R agonist, so while the precise dystonic, and thus anti-dystonic, mechanisms are unknown, D1R- and D2R-mediated signaling pathways likely contribute to the therapeutic mechanism of L-DOPA.

In DRD mice, L-DOPA treatment induced striatal PKA activity, ERK phosphorylation, and c-Fos expression in D1R-MSNs in the dorsal and ventral striatum. Given the dorsal striatum is predominantly involved in motor control, and L-DOPA-mediated supersensitivity in D1R-MSNs did not differ in dorsal and ventral striatum, the role of D1Rs and D2Rs in L-DOPA-mediated signaling in the dorsal striatum were assessed. Specifically, I utilized immunohistochemistry to examine the role D1R and D2R signaling in L-DOPA-mediated changes in 1) PKA activity using an indirect assessment of PKA substrate phosphorylation, 2) ERK phosphorylation, and 3) c-Fos expression in the dorsal striatum of normal and DRD mice. To determine the role of D1R and D2R signaling in the therapeutic efficacy of L-DOPA, D1Rs and/or D2Rs were blocked in the presence of L-DOPA and abnormal movements and locomotor activity were assessed.

5.3. Methods

Mice. Male and female adult (2-6 month) mice homozygous for the c.1160C>A *Th* mutation (DRD; drd/drd) and littermates carrying two wild-type alleles (normal; +/+) were used for all experiments and were previously described (Chapter 3). Kaitlyn Roman, a Neuroscience PhD candidate, and Christine Donsante, MS, generated all mice used in the experiments

described. Housing conditions were in accordance with Emory University's Institutional Animal Care and Use Committee (IACUC). The light period was 7am to 7pm. All procedures were conducted in accordance with Emory's IACUC and Division of Animal Resources guidelines and were approved by IACUC. Mice were maintained as previously described (Rose, Yu et al. 2015).

Locomotor and behavioral assessment. Mice were tested in a behavioral suite separate from the location of home cages. Prior to all testing periods, mice were habituated to the behavior suite for > 3 hrs. Locomotor activity was tested in automated photocell activity cages (29 x 50 cm), each equipped with 12 infrared beams arranged in a 4 x 8 grid (San Diego Instruments; San Diego, CA) and a computer recorded beam breaks per 5 min time bins for the duration of the test period. For drug challenges, testing began at 2 pm, and locomotor activity was recorded immediately after injection for 70 min. Abnormal movements were assessed in parallel to the recording of locomotor activity. Abnormal movement assessment began 10 min after injection and was assessed as previously described (Chapter 3). Behavioral scorers were blinded to treatment.

Drug challenges. To determine the role of D1R and D2R signaling in L-DOPA-mediated signaling in the dorsal striatum, D1Rs or D2Rs were blocked by pretreatment with the D1-like receptor antagonist, SCH 23390 hydrochloride (SCH 23390) or the D2R antagonist, raclopride (both obtained from Tocris Biosciences; Minneapolis, MN) in the presence of L-DOPA treatment and immunohistochemistry was used to examine changes in PKA activity, ERK phosphorylation, and c-Fos expression in the dorsal striatum of normal and DRD mice. To determine the role of

D1R and D2R signaling in the therapeutic efficacy of L-DOPA, D1Rs and/or D2Rs were blocked by pretreatment with SCH 23390 and/or raclopride in presence of L-DOPA treatment and abnormal movements and locomotor activity were assessed. Drug doses were chosen based on previous reports demonstrating they are behaviorally active in DRD mice. L-DOPA (10 mg/kg) at the dose selected was chosen because it has previously been shown to alleviate dystonia in DRD mice (Rose, Yu et al. 2015). SCH 23390 (1 mg/kg) and raclopride (1 mg/kg) at the doses selected worsen dystonia in DRD mice (Rose, Yu et al. 2015). Drugs were injected s.c. in saline (0.9% NaCl) in a volume of 10 ml/kg unless otherwise noted. L-DOPA was obtained from Sigma-Aldrich (St. Louis, MO). In experiments where mice were administered a pretreatment and treatment drug, the pretreatment drug was administered 10 min prior to treatment drug. For locomotor and behavioral assessments, mice were given at least a 4-day drug washout between drug challenges. For terminal experiments, mice were treated with drug between 12-4 pm and were sacrificed 45 min later.

Immunohistochemistry. Bright-field immunohistochemistry was performed as previously described (Chapter 2 and 3).

Image analysis and cell counts. Bright-field immunohistochemistry was analyzed as previously described (Chapter 2 and 3).

Statistics. Prism 8 was used for all analyses. Detailed statistical results are presented in the figure legends. The effects of pretreatment condition (SCH 23390 or raclopride) on L-DOPA-mediated p-PKA-sub, p-ERK and c-Fos positive cells counts per square mm for each striatal

region were determined using a treatment x region ANOVA with Holm-Sidak *post hoc* analyses where appropriate. The effects of pretreatment condition (SCH 23390, raclopride, or SCH 23390 plus raclopride) on L-DOPA-mediated abnormal movements and locomotor activity were analyzed using a one-way ANOVA with Holm-Sidak *post hoc* analyses where appropriate

5.4. Results

5.4.1. Role of D1Rs in L-DOPA-induced abnormal striatal signaling in DRD mice

To determine whether D1R signaling mediates L-DOPA-induced PKA activity, the effects of SCH 23390 pretreatment on L-DOPA-induced p-PKA-sub immunoreactivity in dorsomedial and dorsolateral striatum were assessed. There were no differences in p-PKA-sub immunoreactivity between DRD mice treated with saline or SCH 23390 (data not shown). As described in Chapter 4 (Figure 4.1), in DRD mice, L-DOPA treatment alone, compared to saline treatment, increased p-PKA-sub immunoreactivity [main effect of treatment, $F(2, 28) = 5.15$, $p < 0.05$; $p < 0.05$ Holm-Sidak *post hoc* analysis L-DOPA vs saline; Figure 5.1A]. Pretreatment with SCH 23390 blocked the effects of L-DOPA ($p < 0.05$ Holm-Sidak *post hoc* analysis L-DOPA vs SCH 23390 plus L-DOPA; Figure 5.1A).

Similarly, to determine whether D1R signaling mediates L-DOPA-induced ERK phosphorylation, the effects of SCH 23390 pretreatment on L-DOPA-induced p-ERK immunoreactivity in dorsomedial and dorsolateral striatum were assessed. There were no differences in p-ERK immunoreactivity between DRD mice treated with saline or SCH 23390 (data not shown). As previously shown in Chapter 4 (Figure 4.2), L-DOPA induced greater p-ERK immunoreactivity in the dorsomedial compared to the dorsolateral striatum of DRD mice [treatment x region interaction effect, $F(2, 30) = 13.70$, $p < 0.0001$; Figure 5.1B]. In DRD mice

treated with L-DOPA alone, p-ERK immunoreactivity was increased compared to DRD mice treated with saline ($p < 0.0001$ Holm-Sidak *post hoc* analysis L-DOPA vs saline; Figure 5.1B). SCH 23390 treatment blocked L-DOPA-induced p-ERK immunoreactivity in dorsomedial and dorsolateral striatum ($p < 0.0001$ Holm-Sidak *post hoc* analysis L-DOPA vs SCH 23390 plus L-DOPA; Figure 5.1B).

The effects of SCH 23390 pretreatment on L-DOPA-induced c-Fos immunoreactivity in dorsomedial and dorsolateral striatum were assessed in order to determine whether D1R signaling mediates L-DOPA-induced c-Fos expression. There were no differences in c-Fos immunoreactivity between DRD mice treated with saline or SCH 23390 (data not shown). In DRD mice treated with L-DOPA alone, c-Fos immunoreactivity was increased compared to DRD mice treated with saline [main effect of treatment, $F(2, 30) = 6.88$, $p < 0.01$; $p < 0.01$ Holm-Sidak *post hoc* analysis L-DOPA vs saline; Figure 5.1C]. This effect was previously shown in Chapter 4 (Figure 4.3). SCH 23390 treatment blocked the effects of L-DOPA ($p < 0.05$ Holm-Sidak *post hoc* analysis L-DOPA vs SCH 23390 plus L-DOPA; Figure 5.1C). Overall, these results demonstrate that in the dorsal striatum, D1Rs mediate L-DOPA-induced increases in p-pKA-sub, p-ERK, and c-Fos immunoreactivity.

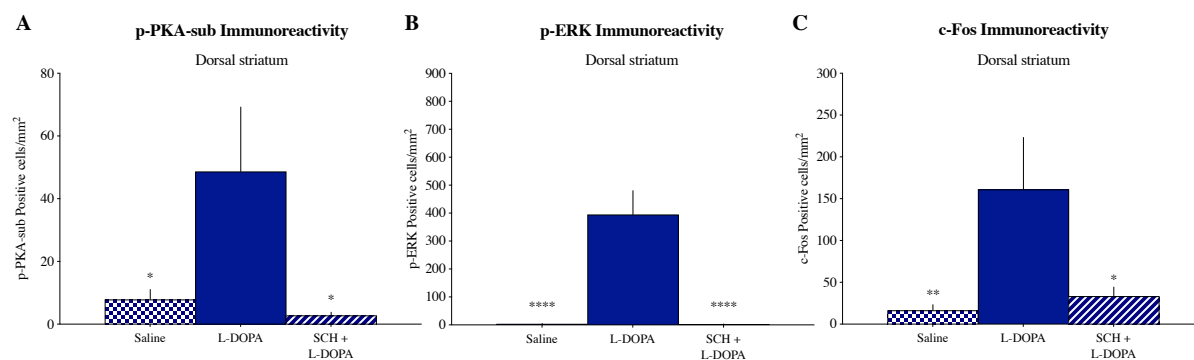


Figure 5.1. Effects of SCH 23390 pretreatment on L-DOPA-induced abnormal striatal signaling in

DRD mice. p-PKA-sub (A), p-ERK (B), and c-Fos (C) immunoreactivity in DRD mice treated with saline, L-DOPA, or SCH 23390 + L-DOPA (SCH + L-DOPA) in dorsomedial and dorsolateral striatum was tested with a treatment x region ANOVA with Holm-Sidak *post hoc* analyses where appropriate. Results for dorsomedial and dorsolateral striatum are shown combined (dorsal striatum). (A) L-DOPA treatment increased p-PKA-sub immunoreactivity [main effect of treatment, $F(2, 28) = 5.15$, $p < 0.05$; $p < 0.05$ *post hoc* analysis L-DOPA vs saline]. Pretreatment with SCH 23390 blocked the effects of L-DOPA ($p < 0.05$ *post hoc* analysis L-DOPA vs SCH + L-DOPA). (B) L-DOPA treatment induced greater p-ERK immunoreactivity in the dorsomedial compared to the dorsolateral striatum of DRD mice [treatment x region interaction effect, $F(2, 30) = 13.70$, $p < 0.0001$]. p-ERK immunoreactivity was increased following L-DOPA treatment ($p < 0.0001$ *post hoc* analysis L-DOPA vs saline). SCH 23390 treatment blocked L-DOPA-induced striatal p-ERK immunoreactivity ($p < 0.0001$ *post hoc* analysis L-DOPA vs SCH + L-DOPA). (C) L-DOPA treatment increased c-Fos immunoreactivity [main effect of treatment, $F(2, 30) = 6.88$, $p < 0.01$; $p < 0.01$ *post hoc* analysis L-DOPA vs saline]. SCH 23390 treatment blocked the effects of L-DOPA ($p < 0.05$ *post hoc* analysis L-DOPA vs SCH + L-DOPA). Values represent mean + SEM; * $p < 0.05$, **** $p < 0.0001$; $n = 4-7$ /group.

5.4.2. Role of D2Rs in L-DOPA-induced abnormal striatal signaling in DRD mice

To determine whether D2R signaling mediates L-DOPA-induced PKA activity, the effects of raclopride pretreatment on L-DOPA-induced p-PKA-sub immunoreactivity in dorsomedial and dorsolateral striatum were assessed. There were no differences in p-PKA-sub immunoreactivity between DRD mice treated with saline or raclopride (data not shown). As shown previously, in DRD mice treated with L-DOPA alone, p-PKA-sub immunoreactivity was increased compared to DRD mice treated with saline [main effect of treatment, $F(2, 28) = 4.56$, $p < 0.05$; $p < 0.05$ Holm-Sidak *post hoc* analysis L-DOPA vs saline; Figure 5.2A]. Pretreatment with raclopride

blocked the effects of L-DOPA ($p < 0.05$ Holm-Sidak *post hoc* analysis L-DOPA vs raclopride plus L-DOPA; Figure 5.2A).

The effects of raclopride pretreatment on L-DOPA-induced p-ERK immunoreactivity in dorsomedial and dorsolateral striatum were assessed in order to determine whether D2R signaling mediates L-DOPA-induced ERK phosphorylation. There were no differences in p-ERK immunoreactivity between DRD mice treated with saline or raclopride (data not shown). As shown previously, in DRD mice, L-DOPA induced greater p-ERK immunoreactivity in the dorsomedial striatum compared to the dorsolateral striatum [treatment x region interaction effect, $F(2, 30) = 7.047$, $p < 0.01$; $p < 0.0001$ Holm-Sidak *post hoc* analysis L-DOPA vs saline; Figure 5.2B]. There was a trend for raclopride treatment to reduce L-DOPA-induced p-ERK immunoreactivity in the dorsal striatum ($p = 0.06$ Holm-Sidak *post hoc* analysis L-DOPA vs raclopride plus L-DOPA; Figure 5.2B).

Finally, the effects of raclopride pretreatment on L-DOPA-induced c-Fos immunoreactivity in dorsomedial and dorsolateral striatum were assessed in order to determine whether D2R signaling mediates L-DOPA-induced c-Fos expression. There were no differences in c-Fos immunoreactivity between DRD mice treated with saline or raclopride (data not shown). In DRD mice treated with L-DOPA alone, c-Fos immunoreactivity was increased compared to DRD mice treated with saline [main effect of treatment, $F(2, 30) = 5.905$, $p < 0.01$; $p < 0.01$ Holm-Sidak *post hoc* analysis L-DOPA vs saline; Figure 5.2C], as previously shown. Raclopride pretreatment did not significantly affect the L-DOPA-induced increase in c-Fos expression ($p > 0.1$ Holm-Sidak *post hoc* analysis; Figure 5.2C). These results suggest that in the dorsal striatum, D2Rs mediate L-DOPA-induced PKA and to a lesser extent, p-ERK signaling, but not L-DOPA-induced c-Fos expression.

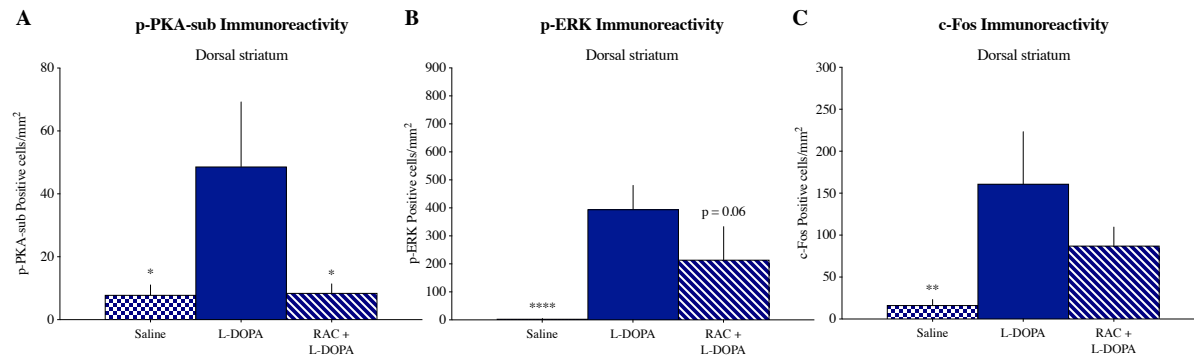


Figure 5.2. Effects of raclopride pretreatment on L-DOPA-induced abnormal striatal signaling in DRD mice. p-PKA-sub (A), p-ERK (B), and c-Fos (C) immunoreactivity in DRD mice treated with saline, L-DOPA, or raclopride + L-DOPA (RAC + L-DOPA) in dorsomedial and dorsolateral striatum was tested with a treatment x region ANOVA with Holm-Sidak *post hoc* analyses where appropriate. Results for dorsomedial and dorsolateral striatum are shown combined (dorsal striatum). (A) L-DOPA treatment increased p-PKA-sub immunoreactivity [$F(2, 28) = 4.56, p < 0.05$; $p < 0.05$ *post hoc* analysis L-DOPA vs saline]. Pretreatment with raclopride blocked the effects of L-DOPA ($p < 0.05$ *post hoc* analysis L-DOPA vs RAC + L-DOPA). (B) L-DOPA treatment induced greater p-ERK immunoreactivity in the dorsomedial striatum compared to the dorsolateral striatum [treatment x region interaction effect, $F(2, 30) = 7.047, p < 0.01$; $p < 0.0001$ *post hoc* analysis L-DOPA vs saline]. There was a trend for raclopride treatment to reduce L-DOPA-induced p-ERK immunoreactivity in the dorsal striatum ($p = 0.06$ *post hoc* analysis L-DOPA vs RAC + L-DOPA). (C) L-DOPA treatment increased c-Fos immunoreactivity [main effect of treatment, $F(2, 30) = 5.905, p < 0.01$; $p < 0.01$ *post hoc* analysis L-DOPA vs saline]. Raclopride pretreatment did not significantly affect the L-DOPA-induced increase in c-Fos expression ($p > 0.1$ *post hoc* analysis L-DOPA vs RAC + L-DOPA). Values represent mean + SEM; * $p < 0.01$, ** $p < 0.01$, **** $p < 0.0001$; $n = 4-7$ /group.

5.4.3. Effects of dopamine receptor antagonist treatment on baseline behaviors

Because SCH 23390 and raclopride are known to produce akinesia in mice, which is a potential confound for these experiments, locomotor activity was assessed in normal and DRD mice and abnormal movements were assessed in DRD mice treated with SCH 23390 and/or raclopride to determine whether antagonist treatment alone affected baseline behaviors. Compared to saline treatment, SCH 23390 treatment reduced locomotor activity in normal mice (Student's *t* tests, $p < 0.0001$; data not shown); however, SCH 23390 treatment did not affect locomotor activity in DRD mice (Student's *t* tests, $p > 0.1$; Figure 5.3A). Compared to saline treatment, SCH 23390 treatment also had no effect on abnormal movements in DRD mice (Student's *t* tests, $p > 0.1$; Figure 5.3B). Compared to saline treatment, raclopride treatment reduced locomotor activity in normal mice (Student's *t* tests, $p < 0.001$; data not shown); however, raclopride treatment did not affect locomotor activity in DRD mice (Student's *t* tests, $p > 0.1$; Figure 5.3A). Raclopride treatment also had no effect on abnormal movements in DRD mice (Student's *t* tests, $p > 0.1$; Figure 5.3B). Compared to saline treatment, SCH 23390 plus raclopride (SCH 23390 + raclopride) treatment reduced locomotor activity in normal mice (Student's *t* tests, $p < 0.0001$; data not shown); however, SCH 23390 + raclopride treatment did not affect locomotor activity in DRD mice (Student's *t* tests, $p > 0.1$; Figure 5.3A). SCH 23390 + raclopride treatment also had no effect on abnormal movements in DRD mice (Student's *t* tests, $p > 0.1$; Figure 5.3B).

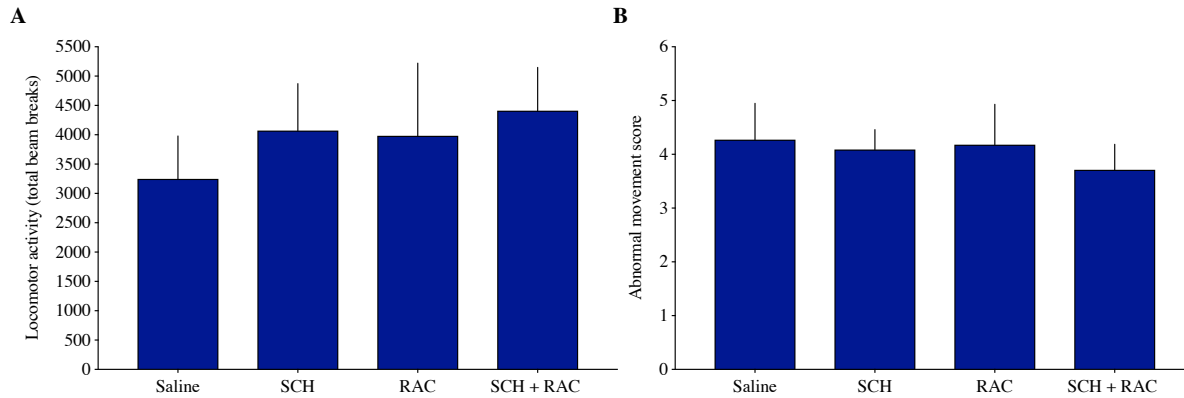


Figure 5.3. Effects of dopamine receptor antagonists on baseline behaviors. (A) Student's *t* tests revealed locomotor activity in DRD mice treated with SCH 23390, raclopride, or SCH 23390 + raclopride did not differ from mice treated with saline (all *p*'s > 0.1). (B) Student's *t* tests revealed abnormal movements in DRD mice treated with SCH 23390, raclopride, or SCH 23390 + raclopride did not differ from mice treated with saline (all *p*'s > 0.1). Values represent mean + SEM; *n* = 7-11/group.

5.4.4. Role of D1Rs in L-DOPA-induced behavioral effects

To determine the role of D1R signaling in L-DOPA-induced alleviation of abnormal movements, the effects of SCH 23390 pretreatment on the ability of L-DOPA to alleviate abnormal movements was assessed. As previously demonstrated (Rose, Yu et al. 2015), L-DOPA alleviated abnormal movements [main effect of treatment, $F(1.335, 13.35) = 20.57, p < 0.001$; $p < 0.01$ Holm-Sidak *post hoc* analysis L-DOPA vs saline; Figure 5.4A), and increased locomotor activity in DRD mice compared to saline treatment [main effect of treatment, $F(1.304, 13.04) = 38.56, p < 0.0001$; $p < 0.0001$ Holm-Sidak *post hoc* analysis L-DOPA vs saline; Figure 5.4B]. Abnormal movements in DRD mice treated with SCH 23390 plus L-DOPA did not differ from mice treated with L-DOPA alone ($p > 0.1$ Holm-Sidak *post hoc* analysis L-DOPA vs SCH 23390 plus L-DOPA; Figure 5.4A). This suggests D1Rs do not mediate the ability of L-DOPA to reduce abnormal movements. However, SCH 23390 pretreatment blocked the L-DOPA-induced

increase in locomotor activity ($p < 0.0001$ Holm-Sidak *post hoc* analysis L-DOPA vs SCH 23390 plus L-DOPA; Figure 5.4B), demonstrating that this dose of SCH 23390 was behaviorally active.

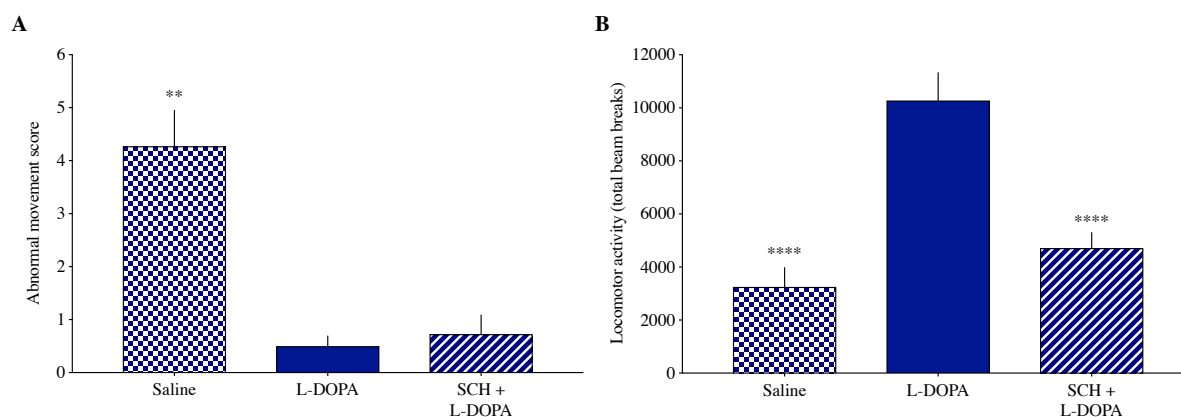


Figure 5.4. Effects of SCH 23390 pretreatment on L-DOPA-mediated abnormal movements and locomotor activity in DRD mice. (A) Abnormal movements and (B) locomotor activity in DRD mice

treated with saline, L-DOPA alone, or SCH 23390 plus L-DOPA (SCH + L-DOPA) were tested with a repeated measures one-way ANOVA with Holm-Sidak *post hoc* analyses where appropriate. (A) In mice treated with L-DOPA alone, abnormal movements were decreased compared to mice treated with saline [main effect of treatment, $F(1.335, 13.35) = 20.57$, $p < 0.001$; $p < 0.01$ *post hoc* analysis L-DOPA vs saline] and did not differ from mice treated with SCH + L-DOPA ($p > 0.1$ *post hoc* analysis L-DOPA vs SCH + L-DOPA). (B) In mice treated with L-DOPA alone, locomotor activity was increased compared to mice treated with saline [main effect of treatment, $F(1.304, 13.04) = 38.56$, $p < 0.0001$; $p < 0.0001$ *post hoc* analysis L-DOPA vs saline] and SCH + L-DOPA ($p < 0.0001$ *post hoc* analysis L-DOPA vs SCH + L-DOPA). Values represent mean + SEM; ** $p < 0.01$, **** $p < 0.0001$ indicates significantly different than L-DOPA treated group; $n = 11$ /group.

5.4.5. Role of D2Rs in L-DOPA-induced behavioral effects

To determine the role of D2R signaling in L-DOPA-induced alleviation of abnormal movements,

the effect of raclopride pretreatment on the ability of L-DOPA to alleviate abnormal movements was assessed. L-DOPA, compared to saline treatment, alleviated abnormal movements [main effect of treatment, $F(1.128, 11.28) = 29.15, p < 0.001$; $p < 0.01$ Holm-Sidak *post hoc* analysis L-DOPA vs saline; Figure 5.5A), and increased locomotor activity in DRD mice [main effect of treatment, $F(1.660, 16.60) = 29.81, p < 0.0001$; $p < 0.001$ Holm-Sidak *post hoc* analysis L-DOPA vs saline; Figure 5.5B]. Abnormal movements in DRD mice treated with raclopride plus L-DOPA did not differ from mice treated with L-DOPA alone ($p > 0.1$ Holm-Sidak *post hoc* analysis L-DOPA vs raclopride plus L-DOPA; Figure 5.5A). In mice treated with L-DOPA alone, there was a trend for increased locomotor activity compared to mice treated with raclopride plus L-DOPA ($p = 0.09$ Holm-Sidak *post hoc* analysis L-DOPA vs raclopride plus L-DOPA; Figure 5.5B). This suggests D2Rs do not mediate the ability of L-DOPA to reduce abnormal movements or L-DOPA-induced hyperactivity.

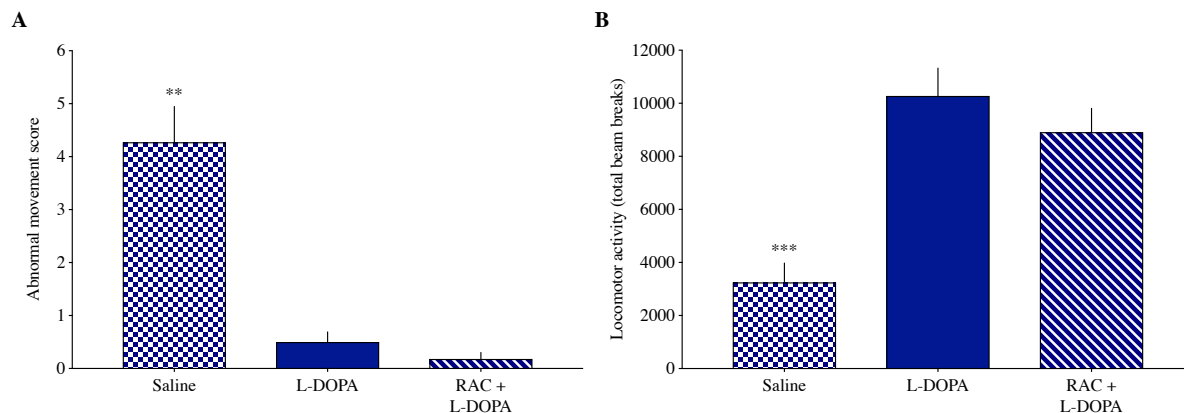


Figure 5.5. Effects of raclopride pretreatment on L-DOPA-mediated abnormal movements and locomotor activity in DRD mice. (A) Abnormal movements and (B) locomotor activity in DRD mice treated with saline, L-DOPA alone, or raclopride plus L-DOPA (RAC + L-DOPA) were tested with a repeated measures one-way ANOVA with Holm-Sidak *post hoc* analyses where appropriate. (A) In mice

treated with L-DOPA alone, abnormal movements were decreased compared to mice treated with saline [main effect of treatment, $F(1.128, 11.28) = 29.15$, $p < 0.001$; $p < 0.01$ *post hoc* analysis L-DOPA vs saline] and did not differ from mice treated with RAC + L-DOPA ($p > 0.1$ *post hoc* analysis L-DOPA vs RAC + L-DOPA). (B) In mice treated with L-DOPA alone, locomotor activity was increased compared to mice treated with saline [main effect of treatment, $F(1.660, 16.60) = 29.81$, $p < 0.0001$; $p < 0.001$ *post hoc* analysis L-DOPA vs saline]. In mice treated with L-DOPA alone, there was a trend for increased locomotor activity compared to mice treated with RAC + L-DOPA ($p = 0.09$ *post hoc* analysis L-DOPA vs RAC + L-DOPA). Values represent mean + SEM; ** $p < 0.01$, *** $p < 0.001$ indicates significantly different than L-DOPA treated group; $n = 11$ /group.

5.4.6. Role of D1R plus D2R-activation in L-DOPA-induced behavioral effects

To determine if co-activation of D1Rs and D2s is required for L-DOPA to alleviate abnormal movements, the effects of SCH 23390 + raclopride pretreatment on the ability of L-DOPA to alleviate abnormal movements were assessed. L-DOPA, compared to saline treatment, alleviated abnormal movements [main effect of treatment, $F(2, 30) = 21.93$, $p < 0.0001$; $p < 0.0001$ Holm-Sidak *post hoc* analysis L-DOPA vs saline; Figure 5.6A], and increased locomotor activity in DRD mice [main effect of treatment, $F(2, 30) = 4.602$, $p < 0.05$; $p < 0.05$ Holm-Sidak *post hoc* analysis L-DOPA vs saline; Figure 5.6B]. Abnormal movements were significantly increased in DRD mice treated with SCH 23390 + raclopride plus L-DOPA compared to mice treated with L-DOPA alone ($p < 0.05$ Holm-Sidak *post hoc* analysis L-DOPA vs SCH 23390 + raclopride plus L-DOPA; Figure 5.6A). Locomotor activity was increased in DRD mice treated with L-DOPA alone compared to mice treated with SCH 23390 + raclopride plus L-DOPA ($p < 0.05$ Holm-Sidak *post hoc* analysis L-DOPA vs SCH 23390 + raclopride plus L-DOPA; Figure 5.6B). These results suggest a synergistic effect of D1Rs plus D2Rs in the effect of L-DOPA.

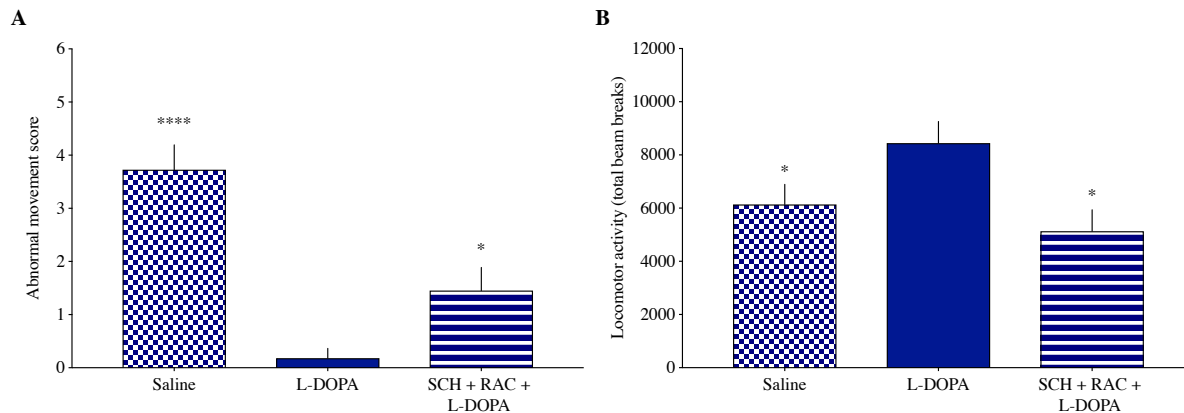


Figure 5.6. Effects of combined SCH 23390 and raclopride pretreatment on L-DOPA-mediated abnormal movements and locomotor activity in DRD mice. (A) Abnormal movements and (B) locomotor activity in DRD mice treated with saline, L-DOPA alone, or SCH 23390 + raclopride plus L-DOPA (SCH + RAC + L-DOPA) were tested with a repeated measures one-way ANOVA with Holm-Sidak *post hoc* analyses where appropriate. (A) In mice treated with L-DOPA alone, abnormal movements were decreased compared to mice treated with saline [main effect of treatment, $F(2, 30) = 21.93$, $p < 0.0001$; $p < 0.0001$ *post hoc* analysis L-DOPA vs saline]. Abnormal movements were increased in mice treated with SCH 23390 + raclopride plus L-DOPA compared to mice treated with L-DOPA alone ($p < 0.05$ *post hoc* analysis L-DOPA vs SCH 23390 + RAC + L-DOPA). (B) In mice treated with L-DOPA alone, locomotor activity was increased compared to mice treated with saline [main effect of treatment, $F(2, 30) = 4.602$, $p < 0.05$; $p < 0.05$ *post hoc* analysis L-DOPA vs saline] and mice treated with SCH + RAC + L-DOPA ($p < 0.05$ *post hoc* analysis L-DOPA vs SCH + RAC + L-DOPA). Values represent mean + SEM; * $p < 0.05$, ** $p < 0.01$, **** $p < 0.0001$ indicates significantly different than L-DOPA treated group; $n = 11$ /group.

5.5. Discussion

L-DOPA-induced PKA activity, ERK phosphorylation, and c-Fos expression in the dorsal striatum was dependent on D1Rs and PKA activity was also dependent on D2Rs. I demonstrated that L-DOPA treatment can alleviate dystonia via D1R- and D2R-signaling. L-DOPA-induced hyperactivity was shown to be dependent predominately on D1R-activation.

5.5.1. Role of D1Rs and D2Rs in the therapeutic effect of L-DOPA

In DRD mice, L-DOPA alleviates abnormal movements (Rose, Yu et al. 2015). Here I showed that L-DOPA treatment alleviates dystonia through D1R and D2R signaling. D1R antagonism alone did not abolish L-DOPA-induced alleviation of abnormal movements. Similarly, D2R antagonism alone did not abolish L-DOPA-induced alleviation of abnormal movements. Rather, combined D1R and D2R antagonism blocked L-DOPA-induced alleviation of abnormal movements. This is consistent with previous data in DRD mice that shows D1R- or D2R-activation alleviated abnormal movements in DRD mice (Rose, Yu et al. 2015). Conversely, this data supports that a reduction in dopamine signaling at both D1Rs and D2Rs is necessary for the expression of dystonia. Antagonism of either D1Rs or D2Rs worsens the dystonia (Rose, Yu et al. 2015), which is consistent with the aforementioned findings, and determining the associated signaling pathways may reveal the mechanism underlying dystonia.

Further, in contrast to normal mice, D1R- and D2R-antagonism does not induce akinesia in DRD mice. Akinesia can result from the use of antipsychotics, which antagonize D2Rs, and can limit the overall therapeutic window (Sanberg 1980, Li, Snyder et al. 2016). Understanding this difference may inform our understanding of how dopamine depletion at both D1Rs and DRs results in dystonia.

5.5.2. Significance of D1R-antagonism in dystonia

In this chapter, I demonstrated that D1R-antagonism abolished L-DOPA-induced PKA activity, ERK phosphorylation, and c-Fos expression in the dorsal striatum. This is consistent with my findings from Chapter 3 that show D1R-mediated signaling is supersensitive. However, D1R-antagonism did not block L-DOPA-induced alleviation of abnormal movement, which suggests supersensitive D1R-mediated signaling by itself does not mediate the therapeutic actions of L-DOPA. D1R-antagonism did block L-DOPA-induced hyperactivity. This is consistent with previous work showing D1R-activation induces locomotor hyperactivity in DRD mice (Rose, Yu et al. 2015) and suggests D1R-mediated supersensitivity is related to locomotor hyperactivity and perhaps not the expression dystonia.

Findings in the DD model support the conclusion that D1R supersensitivity mediates locomotor hyperactivity but not dystonia. In DD mice, chronic L-DOPA treatment attenuated L-DOPA-induced hyperactivity, and this attenuation of hyperactivity was correlated with a reduction of L-DOPA-induced striatal c-Fos expression (Kim, Szczypka et al. 2000). Since DD mice do not exhibit dystonia, this suggests the hyperactivity and the associated supersensitive D1R-mediated signaling may be due to chronic dopamine depletion and may not be specific to the development of dystonia. D1R-activation and L-DOPA administration may therefore be revealing a supersensitive system that develops after prolonged absence of dopaminergic input.

5.5.3. Significance of D2R-antagonism in dystonia

D2R-antagonism blocked L-DOPA-induced PKA activity throughout the dorsal striatum and there was a trend for D2R antagonism to block L-DOPA-induced ERK phosphorylation. This is surprising given L-DOPA-induced PKA activity and p-ERK was limited to D1R-MSNs. This

finding is in contrast to what is observed in the 6-OHDA-lesioned model in which D2R-antagonism (Westin, Vercammen et al. 2007) and genetic inactivation of D2Rs (Darmopil, Martin et al. 2009) did not block L-DOPA-induced ERK phosphorylation. In DRD mice, alterations in pre- or postsynaptic D2R signaling, such as reciprocal A2AR-mediated signaling, D2 autoreceptors on nigrostriatal terminals, and/or D2Rs on corticostriatal terminals, may mediate L-DOPA-induced PKA activation and ERK phosphorylation. In DRD mice, D2R-antagonism did not block L-DOPA-induced c-Fos expression. L-DOPA-induced alterations in nondopaminergic striatal inputs including excitatory glutamatergic signaling may also induce c-Fos expression (Schwarzschild, Cole et al. 1997).

5.5.4. Conclusions

These results show that D1R-signaling pathways contribute to the therapeutic mechanism of L-DOPA and to L-DOPA-induced abnormal striatal signaling and locomotor hyperactivity that are observed in other models of dopamine depletion. D2R-mediated signaling pathways contribute to the therapeutic mechanism of L-DOPA and alterations in D2R signaling may be specific to the expression of dystonia. Future studies aimed at assessing the relationship between D1R- and D2R-mediated abnormal striatal signaling, locomotor hyperactivity, and the development of dystonia are necessary.

Chapter 6: General discussion

Dopamine neurotransmission in the basal ganglia is abnormal in many different forms of dystonia; however, the precise nature of abnormal dopamine-mediated signaling pathways is unknown. A chronic dopamine deficit per se is not sufficient to cause dystonia as neither 6-OHDA-lesioned mice nor DD mice exhibit dystonia, despite profound long-term reductions in dopamine neurotransmission (Gerfen, Keefe et al. 1995, Zhou and Palmiter 1995, Berke, Paletzki et al. 1998, Kim, Szczyпка et al. 2000, Gerfen, Miyachi et al. 2002). It is likely that the timing and extent of striatal dopaminergic loss are likely relevant factors for the development of dystonia and that these factors ultimately contribute to specific abnormalities in postsynaptic dopamine-mediated signaling pathways that may lead to the development of dystonia. I utilized the DRD mouse model to determine the precise nature of striatal dysfunction that may distinguish dystonia from other abnormal motor phenotypes.

I determined that abnormalities in both D1Rs and D2Rs in combination are necessary for the expression of dystonia. I determined that DRD mice exhibit blunted D2R-mediated signaling; specifically, the failure of D2R-antagonism to elicit c-Fos expression in the DRD mouse striatum may be a defining feature of dystonia. I determined that DRD mice exhibit supersensitive striatal D1R-mediated signaling. My results suggest that abnormal D1R-mediated PKA activity, ERK phosphorylation, and c-Fos expression may be necessary, but not sufficient, for the expression of dystonia. Determining the relationship between D1R- and D2R-mediation of abnormal striatal signaling may ultimately reveal the precise nature of dopamine-mediated signaling that results in dystonia.

6.1. Blunted D2R-mediated signaling in DRD mouse striatum

In DRD mice, inhibitory D2R-signaling was blunted, and understanding the precise nature of abnormal D2R-mediated signaling may inform our understanding of dystonia. Specifically, D2R-antagonism increased striatal c-Fos expression in predominately D2R-MSNs in normal mice, but not in DRD mice. Increased c-Fos following D2R-antagonism in normal mice has been previously reported (Dragunow, Robertson et al. 1990, Robertson and Fibiger 1992), suggesting that this observation was not an artifact of our specific mouse strain or methods. However, dopamine receptor antagonists, including raclopride, can also affect D3Rs and using selective D2R and D3R antagonists (Manvich, Petko et al. 2019) may help determine the precise nature of abnormal D2R-mediated signaling.

The failure of D2R-antagonism to induce c-Fos expression may be due to insufficient postsynaptic inhibitory D2R-mediated tone in DRD mice. Previous work in DRD mice showed D2R-mediated adenylate cyclase activity is blunted in striatal homogenates of DRD mice compared to normal mice (Rose, Yu et al. 2015). As discussed, D2R-MSNs also express A2ARs, which are G α olf-coupled and stimulate cAMP (Schiffmann, Jacobs et al. 1991, Schiffmann, Fisone et al. 2007). Therefore, A2ARs on D2R-MSNs reciprocally regulate cAMP, and under normal conditions, tonic activation of D2Rs results in inhibition of cAMP (Schiffmann, Fisone et al. 2007). D2R-antagonism may induce c-Fos in D2R-MSNs by allowing unopposed A2AR-mediated signaling (Agnati, Ferre et al. 2003). Dysregulations in reciprocal D2R- and A2AR-mediated signaling may underlie the expression of dystonia given D2R antagonism worsens dystonia in DRD mice (Rose, Yu et al. 2015). A recent study suggests caffeine, an A2AR antagonist, is not effective at improving motor symptoms in patients with Parkinson's disease (Postuma, Anang et al. 2017); however, studies in DRD mice may identify an antidystonic effect

of A2AR-antagonism that is specific to dystonia. To determine whether the balance of D2R- and A2AR-mediated intracellular signaling affects dystonia, future studies can test if activation of A2ARs worsens dystonia, or conversely whether antagonism of A2ARs alleviates dystonia. D2R-antagonism may also affect D2Rs on cholinergic interneurons or corticostriatal terminals (Dragunow, Robertson et al. 1990).

It is also possible that alterations in molecular mechanisms that function to decrease G protein-mediated signaling may also be abnormal in D2R-MSNs of DRD mice. This may include compensatory changes involving G protein-coupled receptor kinases (GRKs), β -arrestins, and Regulator of G-protein Signaling (RGS) proteins.

In general, GRK-mediated phosphorylation of GPCRs promotes translocation of β -arrestins to the receptor, which results in desensitization and internalization of GPCRs and subsequent decreased G protein-mediated signaling. However, GRKs also play a role in β -arrestin-mediated signaling (Watari, Nakaya et al. 2014). In D2R-MSNs, G protein- and β -arrestin-mediated signaling are important for D2R-mediated inhibition of D2R-MSNs (Rose, Pack et al. 2018), and in the DRD mouse striatum, this balance may be disrupted. Biased agonists that selectively activate GRK/ β -arrestin-dependent signaling can be used to determine whether this signaling pathway is differentially regulated in the DRD mouse striatum. For example, β -arrestin-biased signaling may predominate over $G_{\alpha i}$ -mediated signaling (Gorvin, Babinsky et al. 2018) due to compensatory mechanisms related to chronic dopamine depletion in DRD mice. As discussed, the free $\beta\gamma$ complex can also modulate G protein signaling and activate unique signal transduction pathways (Smrcka 2008), and biased agonists may also be used to determine the contribution of $\beta\gamma$ -mediated signaling (Brust, Hayes et al. 2015).

RGS proteins function as the predominant family of GTPase-activating proteins (GAPs)

for heterotrimeric G proteins. GAPs stimulate the intrinsic GTPase activity to negatively regulate GPCRs (Xie and Martemyanov 2011). Changes in the relative amount or function of RGS9, which is enriched in the basal ganglia and has been shown to mediate dopamine signaling, may result in blunted D2R inhibition. Aberrant D2R-mediated responses have been observed in other models of dystonia. In a mouse model of *TOR1A* dystonia, dopamine activation of $G\alpha_{i/o}$ in D2R-MSNs was impaired, and A2AR antagonism rescues some of these deficits (Napolitano, Pasqualetti et al. 2010). Interestingly, striatal levels of RGS9 were downregulated in this model and may compensate for the decreased D2R availability (Napolitano, Pasqualetti et al. 2010).

D2R-MSN

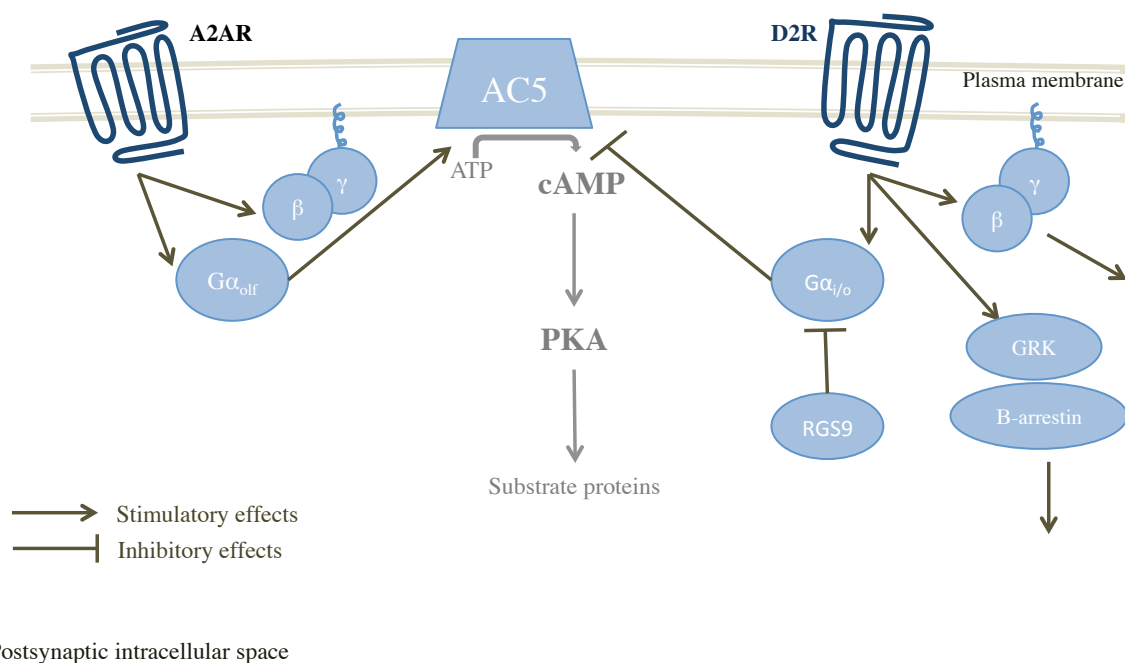


Figure 6.1. Potential mediators of blunted D2R-mediated signaling in D2R-MSNs. In the DRD mouse striatum, blunted D2R-mediated signaling in D2R-MSNs may reflect abnormalities in multiple D2R-mediated signaling pathways. Future experiments assessing A2AR-mediated signaling, GRK/ β -arrestin-dependent signaling, $\beta\gamma$ -mediated signaling, and alterations in the relative amount or function of

RGS9 may uncover the precise nature of abnormal D2R-mediated signaling in D2R-MSNs.

6.2. Supersensitive D1R-mediated signaling in DRD mouse striatum

In DRD mice, D1R-mediated signaling is sensitized. This is similar to what is observed in other animal models of dopamine depletion and suggests sensitized D1R-mediated signaling in the DRD mouse striatum may be due to chronic depletion of dopamine and may not be specific to the development of dystonia. However, the mechanisms underlying D1R-supersensitivity may differ between other dopamine-depleted animals and DRD mice, thus delineating these differences may ultimately inform our understanding of dystonia.

In the dorsal striatum of DRD mice, D1R-activation induced PKA activity and ERK phosphorylation predominately in D1R-MSNs. Adenylate cyclase is necessary for the synthesis of cAMP and subsequent PKA-mediated signaling, so these results are consistent with previous findings that show D1R-stimulated adenylate cyclase activity is sensitized in striatal homogenates of DRD mice compared to normal mice (Rose, Yu et al. 2015). In other models of dopamine depletion abnormal ERK phosphorylation following D1R-activation is similarly observed (Gerfen, Keefe et al. 1995, Berke, Paletzki et al. 1998, Kim, Szczypka et al. 2000, Gerfen, Miyachi et al. 2002, Kim, Palmiter et al. 2006). However, in adult 6-OHDA-lesioned animals, chronic L-DOPA-induced ERK phosphorylation via D1R-MSNs is associated with the development of a non-dystonic form of dyskinesia (Westin, Vercammen et al. 2007, Darmopil, Martin et al. 2009), whereas L-DOPA-induced ERK phosphorylation via D1R-MSNs is associated with the amelioration of abnormal movements in DRD mice. Thus, mechanisms downstream of ERK phosphorylation and/or other signaling defects may distinguish 6-OHDA-lesioned parkinsonian animals from DRD mice.

For example, the balance of D1R- and M4 mAChR-mediated intracellular signaling in D1R-MSNs may underlie the expression of dystonia. In D1R-MSNs, dopamine signaling is reciprocally regulated by M4 mAChRs, which couple to G α i/o proteins to inhibit cAMP. D1R-activation in DRD mice may, in addition to activating sensitized signaling pathways, oppose M4 mAChRs-mediated signaling. In DRD mice, D1R-antagonism worsens the dystonia (Rose, Yu et al. 2015). D1R antagonism may therefore increase dystonia via unmasking of M4 mAChR-mediated signaling. Compounds targeting M4 mAChRs (i.e. xanomeline or M4 positive allosteric modulators) can be tested in the DRD mouse model to determine whether M4 mAChR activation, and associated signaling pathways, increases dystonia. Conversely, M4 antagonists may be potential therapeutic options for dystonia.

Future studies aimed at determining the mechanisms underlying D1R-supersensitivity and the mechanisms downstream of ERK phosphorylation and/or other signaling defects may inform our understanding of abnormal intracellular postsynaptic signaling mechanisms that underlie dystonia. For example, in addition to PKA, the exchange protein directly activated by cAMP (Epac) can also transduce cAMP-mediated signaling (Cheng, Ji et al. 2008) and these signal transduction pathways may be differentially affected by dopamine depletion.

Understanding reciprocal D1R- and M4 mAChR-mediated intracellular signaling in D1R-MSNs may also reveal novel mechanisms that underlie the expression of dystonia.

6.3. Significance of L-DOPA-induced abnormal signaling in dystonia

L-DOPA treatment alleviated abnormal movements and induced abnormal signaling and locomotor hyperactivity in DRD mice. Therefore, it is necessary to determine whether L-DOPA-induced abnormal signaling and locomotor hyperactivity is necessary for the alleviation of

dystonia or reflects a disparate mechanism related to dopamine depletion, but not dystonia.

D1R-antagonism blocked L-DOPA-induced PKA activity, ERK phosphorylation, and c-Fos expression in the dorsal striatum of DRD mice. D2R-antagonism blocked L-DOPA-induced PKA activity in dorsal striatum and there was a trend for D2R-antagonism to block L-DOPA-induced ERK phosphorylation in dorsal striatum of DRD mice. This is surprising given L-DOPA-induced PKA and p-ERK was limited to D1R-MSNs. D2R antagonism may indirectly alter L-DOPA-induced PKA activity and ERK phosphorylation in D1R-MSNs via presynaptic D2Rs on corticostriatal terminals or nigrostriatal terminals. Similarly, cocaine-induced locomotor activity and ERK phosphorylation, in the dorsolateral striatum, was partially blocked by D2R-antagonism (Valjent, Corvol et al. 2000); however, the mechanism underlying this effect is not known. This finding is in contrast to what is observed in the 6-OHDA-lesioned model. D2R-antagonism (Westin, Vercaemmen et al. 2007) and genetic inactivation of D2Rs (Darmopil, Martin et al. 2009) did not block L-DOPA-induced ERK phosphorylation in 6-OHDA-lesioned animals. Nonetheless, these results suggest supersensitive PKA/p-ERK/c-Fos signaling may underlie the abnormal hyperactivity in DRD mice, and that this effect is mediated via D1R- and D2R-signaling.

Notably, D1R-antagonism did not abolish L-DOPA-induced alleviation of abnormal movement, which suggests L-DOPA-induced PKA activity, ERK phosphorylation, and c-Fos expression via supersensitive D1R-mediated signaling by itself is not sufficient to alleviate abnormal movements in DRD mice. However, L-DOPA-induced hyperactivity was shown to be dependent on D1R-signaling, which is consistent with the hyperactivity observed in DRD mice in response to D1R-activation (Rose, Yu et al. 2015). Therefore, L-DOPA-induced abnormal signaling and locomotor hyperactivity may be necessary, but not sufficient, to alleviate abnormal

movements (Figure 6.2). In DD adult mice, D1R-antagonism also blocked L-DOPA-induced locomotor activity (Kim, Szczypka et al. 2000). However, adult DD mice do not exhibit dystonia, which suggests the hyperactivity observed in both DD and DRD mice may be due to chronic depletion of dopamine but may not be specific to the development of dystonia. In fact, behavioral and neuronal sensitization as a consequence of neurotransmitter depletion is a known phenomenon, and behavioral and neuronal sensitivity to L-DOPA has been shown to develop after prolonged absence of dopaminergic input (Gerfen, Keefe et al. 1995, Kostrzewa 1995, Berke, Paletzki et al. 1998, Kim, Szczypka et al. 2000, Gerfen, Miyachi et al. 2002).

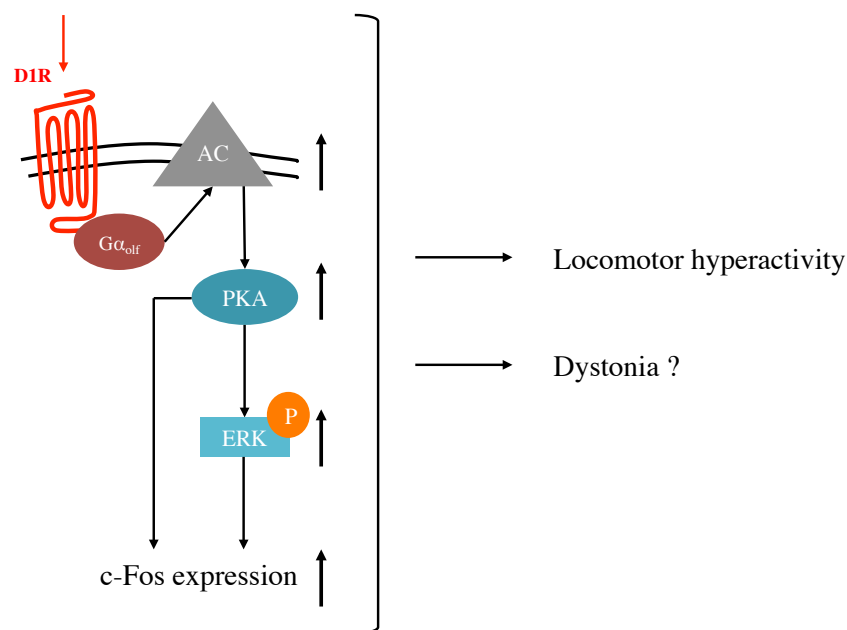


Figure 6.2. Schematic of D1R supersensitivity in the DRD mouse striatum and its relationship to locomotor hyperactivity and dystonia. In the dorsal striatum of DRD mice, D1R-stimulation induces increased adenylyl cyclase (AC), PKA activity, ERK phosphorylation, and c-Fos expression in D1R-MSNs. Supersensitive D1R-mediated signaling by itself is not sufficient to alleviate abnormal movements in DRD mice; however, L-DOPA-induced hyperactivity was shown to be dependent on D1R-signaling.

Previous work in the DD mouse model supports that L-DOPA-induced abnormal striatal signaling is associated with locomotor hyperactivity and demonstrates a potential paradigm to delineate L-DOPA-mediated locomotor hyperactivity and alleviation of dystonia in DRD mice. In the DD mouse model, it was shown that the chronic presence of dopamine signaling, that is, chronic L-DOPA administration, reversed sensitized locomotor activity and striatal intracellular signaling (Kim, Szczypka et al. 2000, Kim, Palmiter et al. 2006). Specifically DD mice were treated with L-DOPA every 4 hrs, and L-DOPA-induced c-Fos immunoreactivity was decreased beginning 14 hrs after chronic treatment began and was almost completely abolished 38 hrs after chronic treatment began. L-DOPA-induced locomotor hyperactivity was abolished by the seventh day of chronic treatment. L-DOPA restriction for 24 hr did not reinstate the L-DOPA-induced locomotor hyperactivity, which suggests that locomotor hyperactivity is maintained by changes in transcriptional regulation, or other alterations including circuit level changes, which take days to reverse (Kim, Szczypka et al. 2000). It is not known whether the locomotor hyperactivity observed in the DRD mouse model is similarly maintained by changes that occur acutely or over the course of days and how these changes may mediate the effects of acute L-DOPA treatment.

L-DOPA treatment alleviates dystonia through a mechanism that can signal through either D1Rs or D2Rs. This is consistent with previous data in DRD mice that shows D1R- or D2R-activation alleviated abnormal movements in DRD mice (Rose, Yu et al. 2015). Future studies aimed at differentiating the mechanism underlying D1R- and D2R-mediated locomotor hyperactivity and D1R- and D2R-mediated alleviation of abnormal movements may ultimately identify the mechanism underlying dystonia. Specifically, future studies testing whether chronic L-DOPA treatment affects the ability of acute L-DOPA treatment to induce locomotor

hyperactivity, elicit abnormal striatal intracellular signaling, and ultimately alleviate abnormal movements may determine the role of L-DOPA-induced activation of PKA, ERK phosphorylation, and c-Fos expression in dystonia.

6.4. Mechanism of L-DOPA-induced abnormal signaling in dystonia

L-DOPA treatment induced PKA activity, robust ERK phosphorylation, and c-Fos expression selectively in D1R-MSNs in the dorsal striatum of DRD mice. L-DOPA-induced ERK phosphorylation was increased in the dorsomedial compared to dorsolateral striatum and this regional difference in ERK phosphorylation may reveal striatal subdivisions, and associated mechanisms, that are necessary for the expression of dystonia. While ERK phosphorylation may be necessary, but not sufficient, for alleviation of dystonia, understanding how ERK is phosphorylated in the dorsal striatum of DRD mice may ultimately reveal the nature of abnormalities in D1R- and D2R-signaling in dystonia.

PKA does not directly phosphorylate ERK; however, there are number of proposed pathways that indirectly link PKA activity and ERK (Figure 6.3). PKA signaling through DARPP-32 has been shown to be permissive of ERK phosphorylation. PKA-mediated phosphorylation of DARPP-32 at Thr34 converts DARPP-32 into a potent inhibitor of protein phosphatase 1 (PP1). PP1 has been shown to be permissive of p-ERK by regulating phosphorylation of the striatal enriched tyrosine phosphatase (STEP). De-phosphorylation of STEP de-phosphorylates the tyrosine residue of the ERK (Valjent, Pascoli et al. 2005). Thus, inhibition of PPI prevents de-phosphorylation of STEP, which prevents STEP from dephosphorylating ERK. Glutamatergic signaling has been shown to directly phosphorylate ERK via an NMDAR-dependent mechanism that requires calcium influx (Thomas and Huganir 2004).

Previous evidence from work examining cocaine or amphetamine administration suggests activation of ERK is dependent on concurrent dopaminergic and NMDAR activation (Valjent, Corvol et al. 2000). This model proposes that ERK phosphorylation may therefore serve as a coincidence detector of concurrent dopaminergic and glutamatergic signaling in MSNs.

Treatment with L-DOPA and psychostimulants, but not a D1R-selective agonist, may result in concurrent dopaminergic and glutamatergic signaling via presynaptic regulation of dopamine signaling. L-DOPA may activate concurrent dopaminergic and glutamatergic signaling via dopamine enhancement of glutamatergic signaling (Girault, Valjent et al. 2007) or potentially co-release of glutamate (Dani and Zhou 2004). This may result in enhanced ERK phosphorylation via NMDAR-mediated ERK phosphorylation and coincident amplification via PKA-mediated inhibition of ERK de-phosphorylation. This may in part explain the robust increase in ERK phosphorylation following L-DOPA treatment compared to the mild increase in ERK phosphorylation following treatment with a D1R-selective agonist. Further, excitatory glutamatergic signaling may also elicit c-Fos expression via p-ERK (Broussard 2012) or via calcium signaling.

Pretreatment with the NMDAR antagonist, MK801, does not affect D1R-activation-induced expression of p-ERK (Vanhoutte, Barnier et al. 1999) or c-Fos (Gerfen, Miyachi et al. 2002) in the dopamine-depleted striatum of 6-OHDA-lesioned animals, which suggests D1R supersensitivity observed in the dopamine-depleted striatum is not mediated by NMDARs. However, corticostriatal stimulation was shown to potentiate D1R-induced p-ERK (Keefe and Gerfen 1996). Determining whether abnormal ERK phosphorylation is induced via NMDAR-signaling may reveal novel alterations in presynaptic glutamatergic signaling that underlie dystonia.

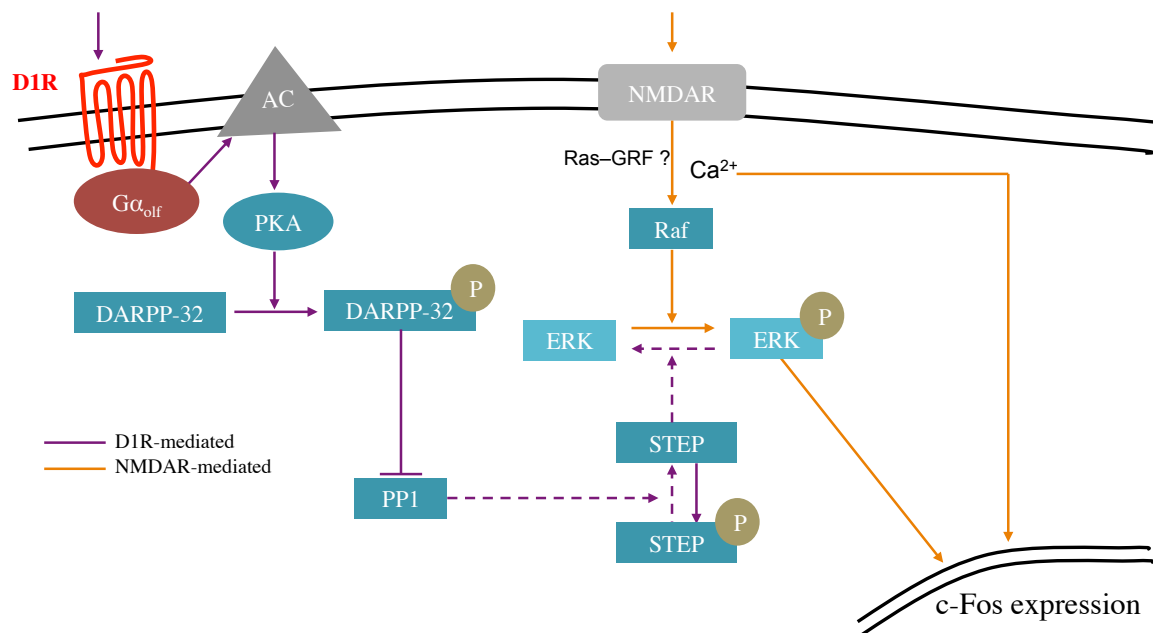


Figure 6.3. Proposed mechanism of sensitized PKA/p-ERK/c-Fos signaling in D1R-MSNs in the dorsal striatum of DRD mice. D1R-activation induces sensitized PKA activity. PKA phosphorylates DARPP-32 on the Thr34 residue, which enables its activity as a potent inhibitor of PP1. Inhibition of PP1 prevents de-phosphorylation of STEP, which prevents STEP from dephosphorylating ERK. Overall D1R-activation is permissive of ERK phosphorylation. Dashed lines indicate reduced signaling and solid lines indicate increased signaling. Glutamatergic signaling via NMDARs activates Raf through a mechanism that has not been fully elucidated, but may involve calcium-dependent mechanisms and require calcium/calmodulin-dependent protein kinase II (CaMKII). It may also involve Ras-GRF, a guanine-nucleotide exchange factor activated by calcium/calmodulin binding. ERK is ultimately phosphorylated and may activate c-Fos expression via calcium-dependent signaling. Phosphorylated ERK can translocate to the nucleus and induce c-Fos expression. This figure has been adapted from Girault, Valjent et al. (2007).

6.5. Regional differences in postsynaptic intracellular signaling cascades in dystonia

The regional differences in ERK phosphorylation may indicate specific striatal subdivisions that

are uniquely abnormal in DRD mice and therefore associated with dystonia. While L-DOPA-induced ERK phosphorylation may contribute to sensitized D1R-mediated signaling and associated locomotor, and not to dystonia per se, the regional differences in ERK phosphorylation may reveal striatal abnormalities that are associated with dystonia. In fact, ERK phosphorylation in the rat dorsomedial striatum was shown to be necessary for encoding and performance of goal-directed actions (Girault, Valjent et al. 2007). As discussed, aberrant control of goal-directed and habitual control in the caudate putamen is associated with motor symptoms in Parkinson's disease (Redgrave, Rodriguez et al. 2010). Thus the regional differences in ERK phosphorylation likely have functional correlates that may be necessary for the alleviation of abnormal movements or may reveal abnormalities that underlie dystonia.

Treatment with L-DOPA or a D1R-selective agonist induced regional differences in p-ERK in D1R-MSNs, which suggests sensitivity in postsynaptic D1Rs may mediate this effect. In fact, co-release of dopamine and glutamate, which may underlie increase ERK expression, has been shown to occur in a region-specific manner (Shiflett, Brown et al. 2010). However, regulation from multiple pre- and postsynaptic mechanisms may be necessary for ERK phosphorylation. For example, in 6-OHDA-lesioned mice, increased G α olf protein has been observed in the dorsolateral striatum; however, this increase was not associated with L-DOPA-induced ERK phosphorylation (Cai and Ford 2018). Additional experiments assessing the contribution of pre- and postsynaptic regulation of L-DOPA-mediated signaling are needed to determine the underlying mechanism and significance of regional differences in ERK phosphorylation. GABAergic striatal interneuron composition also varies among striatal functional territories (Alcacer, Santini et al. 2012) and may contribute to differences in striatal subdivisions that play an important role in the expression of dystonia. These data do not preclude

the involvement of alterations in nondopaminergic striatal inputs and future studies examining the role of other striatal inputs, including NMDAR-mediated signaling, are necessary.

6.6. Conclusions and future directions

Until recently, it was not possible to identify the dysregulated striatal signaling pathways that underlie dystonia. Prior to the development of the DRD mouse model, animal models that exhibit dystonia caused by underlying defects in dopamine neurotransmission were not available. Studies using DRD mice allow for the identification of the precise nature of the striatal dysfunction that may distinguish dystonia from other abnormal motor phenotypes.

Here I have shown that abnormalities in both D1Rs and D2Rs in combination are necessary for the expression of dystonia. Examining reciprocal and unique signaling pathways in D1R- and D2R-MSNs may inform our understanding of how supersensitive D1R-mediated signaling and blunted D2R-mediated signaling contribute to the expression of dystonia. The present findings suggest differentiating striatal dysfunction that underlies locomotor hyperactivity versus dystonia is important for future studies.

Utilizing unbiased approaches to compare abnormal dopamine-mediated signaling in the dopamine-depleted striatum compared to the DRD mouse striatum may reveal differences that distinguish dystonia from other movement disorders in which dopamine is depleted, but dystonia is not observed. Given most of our understanding, and associated molecular tools, of how dopamine-mediated pathways can be dysregulated comes from models in which striatal dopamine is depleted but dystonia is not observed, this approach may also reveal novel mechanisms that underlie dystonia.

Appendix: Assessment of the striatal proteome in a mouse model of DOPA-responsive dystonia

A.1. Abstract

The striatal proteome of normal and DRD mice was examined to determine novel striatal abnormalities that may underlie dystonia. This unbiased examination identified 1,805 proteins in the striatum of DRD and normal mice, and 57 proteins were differentially regulated ($p < 0.05$). Twelve differentially regulated proteins were previously associated with dystonia and were related to mitochondrial functions and cell signaling pathways. Similarly, enrichment analysis supported a role for mitochondrial dysfunction and alterations cell signaling pathways in dystonia. Future studies will assess the mechanisms underlying mitochondrial dysfunction and dysregulated cell signaling in DRD mice.

A.2. Introduction

The development of dystonia likely results from dopamine depletion along with very specific abnormalities in postsynaptic dopamine-mediated signal transduction pathways. Dopamine depletion throughout development is associated with dystonia in humans and in the DRD mouse model; however, dysregulated postsynaptic dopamine-mediated signaling responses observed in other animal models of chronic dopamine deficiency are not associated with dystonia. The DRD mouse model therefore allows for an assessment of the precise nature of the striatal dysfunction that may distinguish dystonia from other abnormal motor phenotypes. We sought to determine novel striatal abnormalities that underlie dystonia by examining the striatal proteome.

A.3. Methods

Mice. Previous data (Chapter 3, Figure 3.2) showed abnormal movements in DRD mice carrying the RFPs (tdTom, EGFP, or both) did not differ from DRD mice without the RFPs which supports using DRD mice and normal mice with and without RFPs for analysis of the striatal proteome.

Tissue collection. Mice were sacrificed by cervical dislocation. Brains were rapidly removed and striata were rapidly dissected and frozen on dry ice by Anthony Downs, an MSP PhD candidate, together with MAB. Striata samples were stored at -80°C.

Tissue homogenization and digestion protocol. The protocol for tissue homogenization was adapted from a published method (Seyfried, Dammer et al. 2017) and was provided and

completed by the Integrated Proteomics Core, an Emory Neuroscience NINDS Core Facilities (ENNCF): www.cores.emory.edu/eipc/resources/index.html.

Samples were vortexed in 500 microL of urea lysis buffer (8M urea, 100 mM NaH₂PO₄, pH 8.5), including 3 uL (100x stock) Halt protease and phosphatase inhibitor cocktail (Pierce). All homogenization was performed using a Bullet Blender (Next Advance) according to manufacturer protocols. Protein supernatants were transferred to 1.5 mL Eppendorf tubes and sonicated (Sonic Dismembrator, Fisher Scientific) 3 times for 5 sec with 15 sec intervals of rest at 30% amplitude to disrupt nucleic acids and subsequently vortexed. Protein concentration was determined by the bicinchoninic acid (BCA) method, and samples were frozen in aliquots at -80°C. Protein homogenates (100 ug) were diluted with 50 mM NH₄HCO₃ to a final concentration of less than 2M urea and then treated with 1 mM dithiothreitol (DTT) at 25°C for 30 min followed by 5 mM iodoacetimide (IAA) at 25°C for 30 min in the dark. Protein was digested with 1:100 (w/w) lysyl endopeptidase (Wako) at 25°C for 2 hr and further digested overnight with 1:50 (w/w) trypsin (Promega) at 25°C. Resulting peptides were desalted with a Sep-Pak C18 column (Waters) and dried under vacuum.

LC-MS/MS data acquisition. The data acquisition by LC-MS/MS protocol was adapted from a published procedure (Seyfried, Dammer et al. 2017) and was provided and completed by the Integrated Proteomics Core, an Emory Neuroscience NINDS Core Facilities (ENNCF): www.cores.emory.edu/eipc/resources/index.html.

Derived peptides were resuspended in loading buffer (0.1% trifluoroacetic acid). Peptide mixtures (3 μL) were separated on a self-packed C18 (1.9 μm Dr. Maisch, Germany) fused silica column (25 cm x 75 μM internal diameter (ID); New Objective, Woburn, MA) by a Dionex

Ultimate 3000 RSLCNano and monitored on a Fusion mass spectrometer (ThermoFisher Scientific, San Jose, CA). Elution was performed over a 140 min gradient at a rate of 300nL/min with buffer B ranging from 3% to 99% (buffer A: 0.1% formic acid in water, buffer B: 0.1 % formic acid in acetonitrile). The mass spectrometer cycle was programmed to collect at the top speed for 3 sec cycles. The MS scans (300-1500 m/z range, 200,000 AGC, 50 ms maximum ion time) were collected at a resolution of 120,000 at m/z 200 in profile mode and the HCD MS/MS spectra (1.5 m/z isolation width, 30% collision energy, 10,000 AGC target, 35 ms maximum ion time) were detected in the ion trap. Dynamic exclusion was set to exclude previous sequenced precursor ions for 20 sec within a 10 ppm window. Precursor ions with +1, and +8 or higher charge states were excluded from sequencing.

Data analysis for label-free quantification. The label-free quantification analysis protocol was provided by, and completed under the guidance of the Emory Integrated Computational Core (EICC), one of the Emory Integrated Core Facilities (EICF), specifically, Ashok Dinasarapu, PhD, a bioinformatics scientist and was adapted from: http://www.cores.emory.edu/eicc/documents/2018_0904_EICC_Proteomics_Data_Analysis.pdf.

ThermoFisher generated RAW files, which contain MS/MS spectral counts, were used for label-free quantitation (LFQ) of proteins in eight biological samples. Base peak chromatograms were inspected visually using RawMeat software. All RAW files were processed together in a single run by MaxQuant version 1.6.0.16 with default parameters unless otherwise specified (<http://www.maxquant.org>). Database searches were performed using the Andromeda search engine (a peptide search engine based on probabilistic scoring) with the UniProt mouse sequence database (update date: 2017) and a contaminants database of common laboratory

contaminants. MaxQuant provides a contaminants.fasta database file within the software that is automatically added to the list of proteins for the in-silico digestion when this feature is enabled.

Precursor mass tolerance was set to 4.5 ppm in the main search, and fragment mass tolerance was set to 20 ppm. Digestion enzyme specificity was set to trypsin with a maximum of 2 missed cleavages. A minimum peptide length of 6 residues was required for identification. Up to 5 modifications per peptide were allowed; acetylation (protein N-terminal), oxidation (Met) and amidation (NQ) were set as variable modifications, and carbamidomethyl (Cys) was set as a fixed modification. No Andromeda score threshold was set for unmodified peptides. A minimum Andromeda score of 40 was required for modified peptides. Peptide and protein false discovery rates (FDR) were both set to 1% based off a target-decoy reverse database. Proteins that shared all identified peptides were combined into a single protein group. If all identified peptides from one protein were a subset of identified peptides from another protein, these proteins were also combined into that group. Peptides that matched multiple protein groups (“razor” peptides) were assigned to the protein group with the most unique peptides.

Peaks were detected in Full MS, and a three-dimensional peak was constructed as a function of peak centroid m/z (7.5 ppm threshold) and peak area over time. Following de-isotoping, peptide intensities were determined by extracted ion chromatograms based on the peak area at the retention time with the maximum peak height. Peptide intensities were normalized to minimize overall proteome difference based on the assumption that most peptides do not change in intensity between samples. Protein LFQ intensities were calculated from the median of pairwise intensity ratios of peptides identified in two or more samples and adjusted to the cumulative intensity across samples. Quantification was performed using razor and unique peptides, including those modified by acetylation (protein N-terminal), oxidation (Met) and

deamidation (NQ). A minimum peptide ratio of 1 was required for protein intensity normalization, and “Fast LFQ” was enabled.

Data processing and cluster analysis was performed using Perseus version 1.5.0.31 (<http://www.perseus-framework.org>). Contaminants and protein groups identified by a single peptide were filtered from the data set. FDR was calculated as the percentage of reverse database matches out of total forward and reverse matches. Protein group LFQ intensities were \log_2 transformed to reduce the effect of outliers. Data was filtered by valid values. A minimum of four valid values was required in at least one group (DRD or normal). For cluster analysis and statistical comparisons between proteomes, protein groups missing LFQ values were assigned values using imputation. Missing values were assumed to be biased toward low abundance proteins that were below the MS detection limit, referred to as “missing not at random”, an assumption that is frequently made in proteomics studies. The missing values were replaced with random values taken from a median downshifted Gaussian distribution to simulate low abundance LFQ values. Imputation was performed separately for each sample from a distribution with a width of 0.3 and downshift of 1.8. Hierarchical clustering was performed on Z-score normalized, \log_2 LFQ intensities using Euclidean distance and average linkage with k-means preprocessing (300 clusters). Log ratios were calculated as the difference in \log_2 LFQ intensity averages between experimental and control groups. Welsch’s t test calculations were used in statistical tests as histograms of LFQ intensities showed that all data sets approximated normal distributions. Base 10-fold-change values for ratios < 1 are represented as negative reciprocals of the ratios.

Assessment of proteins associated with dystonia. PubMed searches were performed to determine whether proteins differentially regulated in DRD mice compared to normal mice ($p < 0.05$) were previously associated with dystonia. Keywords included the differentially regulated protein (protein and gene name) and “dystonia”. Studies were reviewed and only those that demonstrated association between dystonia and the protein of interest were included. When differentially regulated proteins were components of a larger protein complex, the larger protein complex was also used as a keyword.

Bioinformatics analysis. Database Annotation, Visualization and Integrated Discovery (DAVID) Functional Annotation Tool (DAVID Bioinformatic Resources 6.8; NIAID/NIH, <https://david.ncifcrf.gov>; Huang et al., Sherman et al. 2009) was used to analyze the gene list associated with significant proteins ($p < 0.05$). Gene lists uploaded to DAVID to produce a functional annotation chart. Annotations were limited by species (*mus musculus*). Default databases and KEGG (Kyoto Encyclopedia of Genes and Genomes; KEGG_PATHWAY) database were used. Default options for medium stringency were used for functional annotation charts. Cytoscape with Enrichment Map plugin for visualizing DAVID output was used to depict integrations between annotations (pathways) and gene lists. Recommended overlap parameters were used (<http://apps.cytoscape.org/apps/enrichmentmap>). Pathways generated from DAVID in some cases have redundant or similar names (i.e. multiple ‘mitochondrion’ pathways) but differ on the individual genes that comprise each pathway.

A.4. Results

The unbiased examination of the striatal proteome identified 1,805 proteins in DRD (n = 4) and normal (n = 4) mouse striata. A volcano plot (Figure A.1) shows only one protein, TH, with FDR < 0.05. This finding is consistent with the reduced TH protein content and activity observed in DRD mice (Rose, Yu et al. 2015).

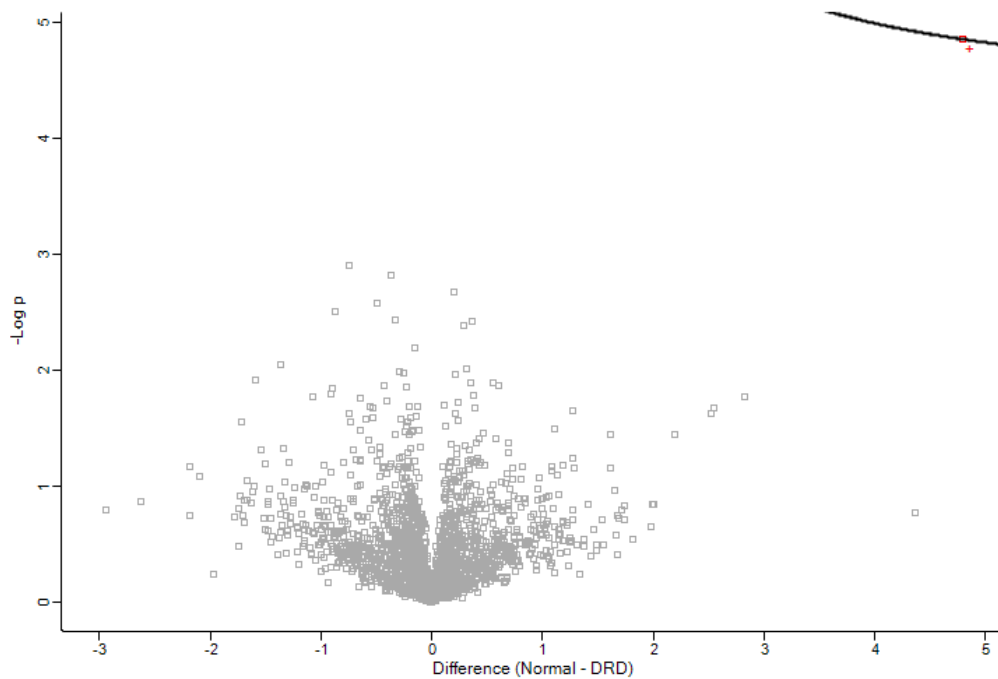


Figure A.1. Volcano plot of the significance levels of the expression difference between normal and DRD mice versus the mean difference in protein expression levels. Each dot represents one protein. The y-axis shows negative log₁₀ transformed P values obtained from protein by protein two-sided t-tests (e.g., 4 is equal to a P value of 10⁻⁴). Red (+) indicates the protein with enriched expression in normal mice (TH). A protein is called significantly enriched, if it shows a statistically significant expression difference between the DRD and normal (FDR ≤ 0.05).

Given this was an exploratory study, we identified proteins upregulated and downregulated in DRD compared to normal mice using the following nominal p-values cutoffs: $p < 0.001$, 0.01 , 0.05 , and 0.1 (Figure A.2). One protein, TH, was significantly downregulated in DRD mice when $p < 0.001$ was considered statistically significant (Figure A.2). Eight additional proteins were differentially regulated in the striatum of DRD compared to normal mice when $p < 0.01$ was considered statistically significant (Figure A.2). When $p < 0.05$ was considered statistically significant, 19 additional proteins were significantly downregulated in the striatum of DRD compared to normal mice, and 29 additional proteins were upregulated (Figure A.2). When $p < 0.1$ was considered statistically significant, an additional 44 additional proteins were significantly downregulated in the striatum of DRD compared to normal mice, and 35 additional proteins were upregulated (Figure A.2). The results of differentially regulated proteins, identified by the ProteinEN and GeneID, are represented in a heat map (Figure A.3). Manual assessment of differentially regulated proteins ($p < 0.05$) revealed 12 proteins in which pathogenic variants in associated genes, or mechanisms directly related to the proteins, were previously linked to the development of dystonia (Table A.1).

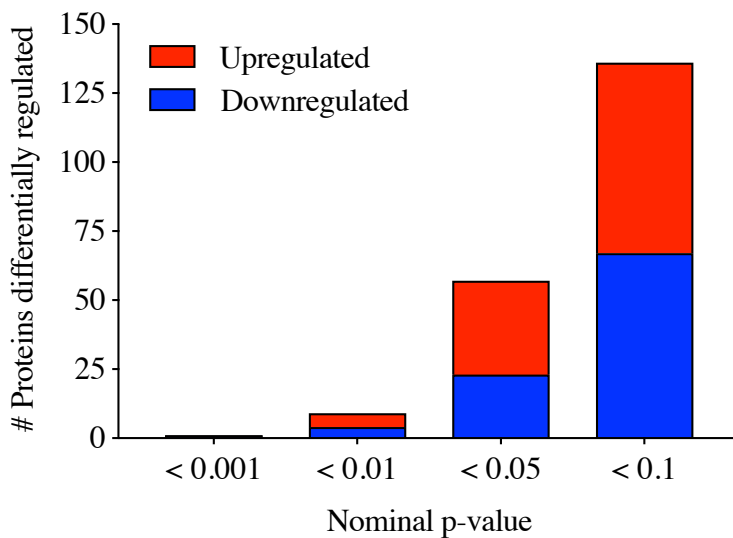


Figure A.2. Differentially regulated proteins in the striatum of DRD compared to normal mice.

Representation of the total number of proteins upregulated or downregulated in the striatum of DRD compared to normal mice at each nominal p-value. When $p < 0.001$ was considered statistically significant, one protein was significantly downregulated. When $p < 0.01$ was considered statistically significant, four total proteins were downregulated and five were upregulated. When $p < 0.05$ was considered statistically significant, 23 total proteins were downregulated and 34 were upregulated. When $p < 0.1$ was considered statistically significant, 67 total proteins were downregulated and 69 were upregulated.

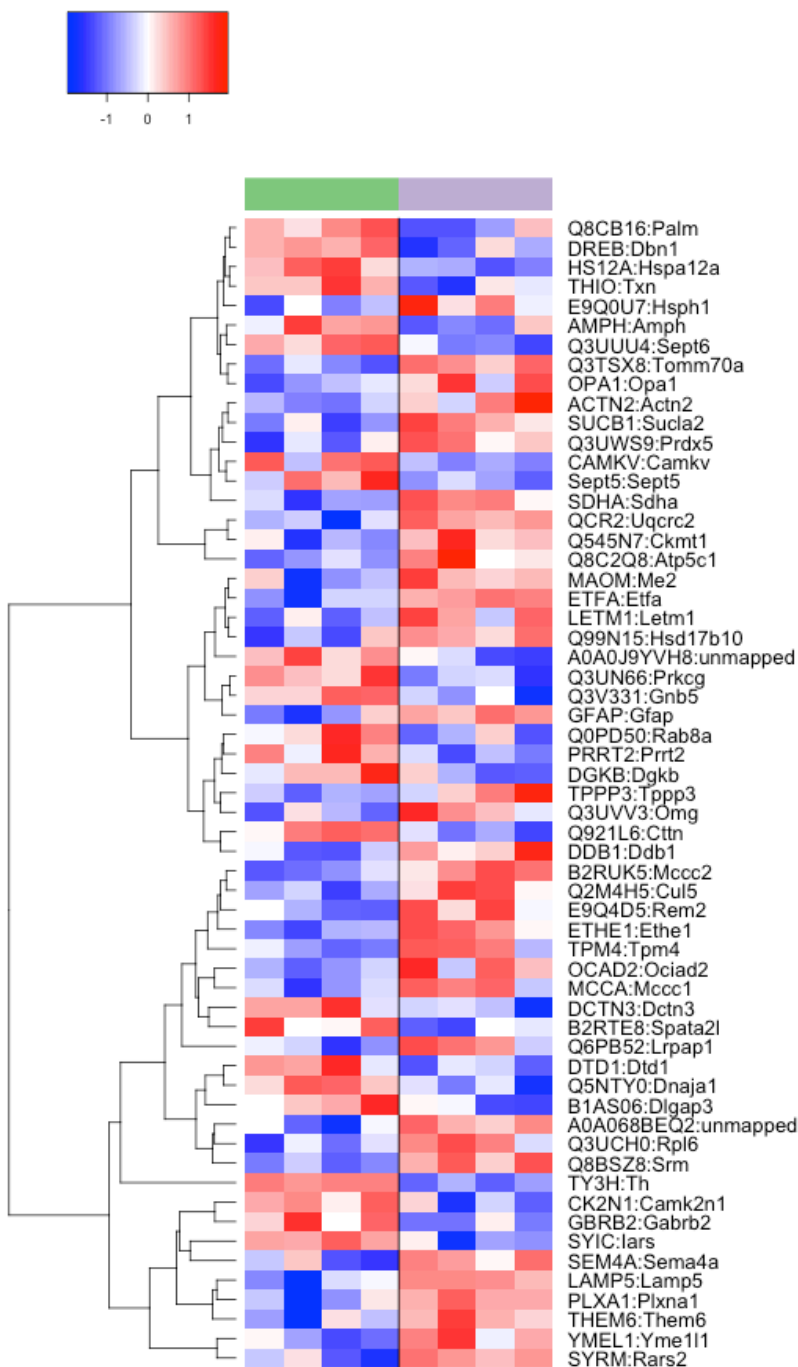


Figure A.3. Heat map of proteins upregulated and downregulated in the striatum of normal and DRD mice. Relative levels of differentially regulated proteins (p < 0.05) are presented. Protein ID and associated mapped gene names are clustered based on gene expression patterns. Red represents up-regulated proteins and blue represents down-regulated proteins (Z-scores). Green column represents

control samples ($n = 4$) and the purple column represents DRD samples ($n = 4$). Figure created by Ashok Dinasarapu, PhD.

Table A.1. Differentially regulated proteins ($p < 0.05$) previously associated with dystonia

p-value	Difference DRD-WT	Gene Name	Protein	Associated Dystonia/Disorder	References
0.0008	-3.72	<i>Th</i>	tyrosine hydroxylase	DOPA-responsive dystonia	(Knappskog, Flatmark et al. 1995, Rose, Yu et al. 2015)#
0.0041	0.87	<i>Ethe1</i>	sulfur dioxygenase	ethylmalonic encephalopathy	(Tiranti, Viscomi et al. 2009, Walsh, Sills et al. 2010)
0.0064	0.15	<i>Sdha</i>	flavoprotein subunit of succinate dehydrogenase	multisystem mitochondrial disease	(Renkema, Wortmann et al. 2015)
0.0101	-0.31	<i>Prkcg</i>	protein kinase C gamma	spinocerebellar ataxia type 14	(Miura, Nakagawara et al. 2009, Ganos, Zittel et al. 2014, Nibbeling, Delnooz et al. 2017)
0.0114	0.25	<i>Sucla2</i>	succinate-coenzyme A ligase, ADP-forming, beta subunit	dystonia deafness syndrome	(Maas, Marina et al. 2016, Garone, Gurgel-Giannetti et al. 2017)
0.0156	-0.56	<i>Prrt2</i>	proline-rich transmembrane protein 2	paroxysmal kinesigenic dyskinesias	(Zhang, Li et al. 2017, Marano, Motolese et al. 2018)
0.0185	-0.59	<i>Gabrb2</i>	GABA _A receptor, subunit beta 2	cervical dystonia	(Strzelczyk, Burk et al. 2011, Berman, Pollard et al. 2018)*
0.0229	-0.24	<i>Gnb5</i>	G protein subunit beta 5	<i>indirectly associated</i>	(Jenner 2008, Fuchs, Saunders-Pullman et al. 2013)*
0.0304	0.23	<i>Gfap</i>	glial fibrillary acidic protein	Alexander disease	(Jefferson, Absoud et al. 2010)
0.0320	0.74	<i>Rars2</i>	arginyl-tRNA synthetase 2, mitochondrial	pontocerebellar hypoplasia type 6	(Glamuzina, Brown et al. 2012)
0.0423	-0.94	<i>Camk2n1</i>	Ca ²⁺ /calmodulin dependent protein kinase II inhibitor 1	mouse model of GNAL haplodeficiency	(Pelosi, Menardy et al. 2017)*
0.0452	0.21	<i>Opa1</i>	OPA1, mitochondrial dynamin like GTPase	optic atrophy	(Liskova, Ulmanova et al. 2013)

* Indirectly associated with dystonia

Additional PubMed results not reviewed

DAVID was used to probe for novel cellular pathways that may be differentially regulated in DRD compared to normal mouse striatum. Cytoscape was used to depict integrations between these pathways and the associated gene list with p values < 0.05 (Figure A.4). Assessing differentially regulated proteins with p values < 0.05 revealed 14 enriched pathways (all p's < 0.001; Table A.2). Mitochondrial-related pathways were predominately enriched.

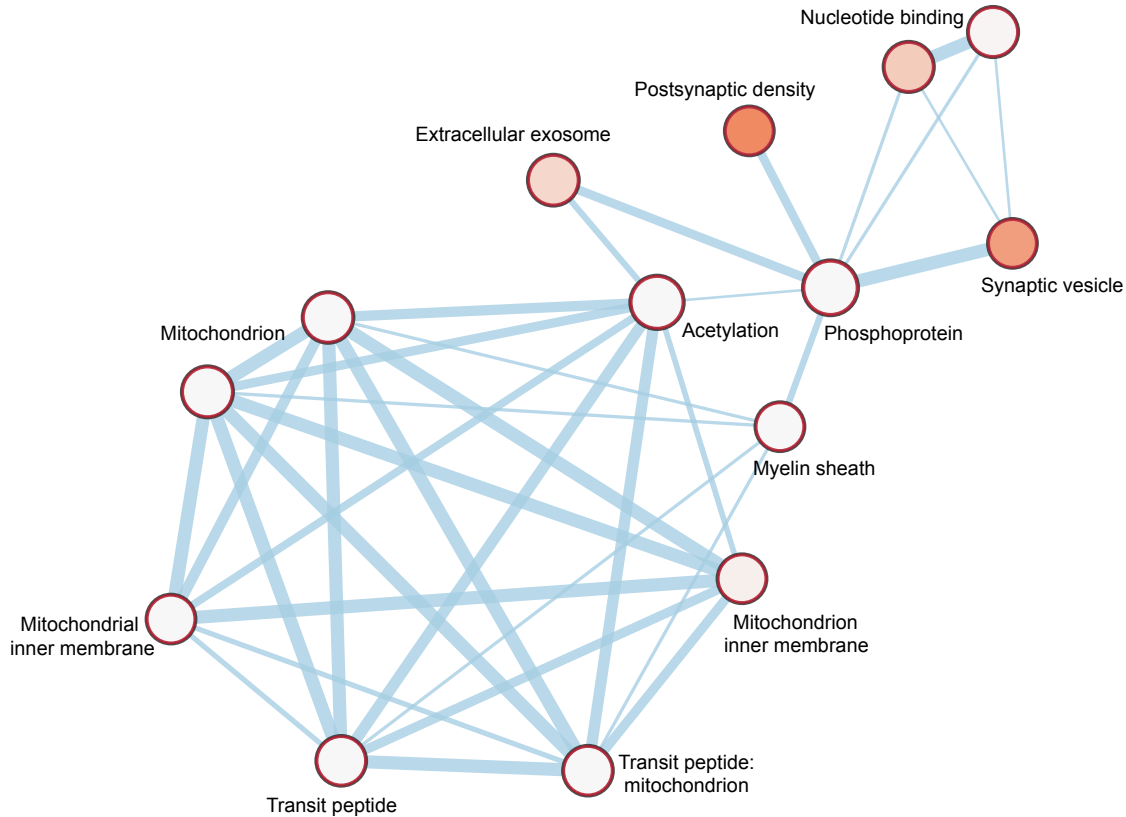


Figure A.4. Cytoscape enriched pathways of differentially expressed proteins ($p < 0.05$). Enriched pathways for proteins with p values < 0.05 are depicted using cytoscape. Outer circle color of node depicts associated p-value (all p's < 0.001) for enriched pathways. Lines and associated thickness depict pathways with the number of shared genes between the enriched pathways.

Table A.2. Cytoscape enriched pathways of differentially expressed proteins ($p < 0.05$)

Pathway Description	Genes	p value	FDR q-value
synaptic vesicle	TH SEPT5 AMPH RAB8A SEPT6	3.69E-04	0.011676451
transit peptide	UQCRC2 ME2 ETHE1 PRDX5 MCCC2 MCCC1 SUCLA2 ETFA OPA1 RARS2 SDHA LETM1 ATP5C1 CKMT1	1.98E-10	1.31E-08
myelin sheath	UQCRC2 SUCLA2 GFAP GNB5 OMG SDHA ATP5C1 CKMT1	8.00E-07	6.36E-05
phosphoprotein	UQCRC2 PALM ETHE1 PRDX5 TPM4 IARS HSPH1 CTTN RPL6 DNAJA1 SUCLA2 ETFA DDB1 SDHA TOMM70A ATP5C1 SEPT6 DBN1 CKMT1 TH GFAP SEPT5 GABRB2 DTD1 AMPH CAMKV CUL5 DGKB PRRT2 RAB8A DLGAP3 ACTN2 PRKCG LRPAP1 REM2 SPATA2L THEM6	1.34E-06	4.41E-05
mitochondrion	YME1L1 UQCRC2 TH HSD17B10 ME2 ETHE1 PRDX5 MCCC2 MCCC1 DNAJA1 SUCLA2 ETFA OPA1 RARS2 OCIAD2 SDHA LETM1 TOMM70A ATP5C1 CKMT1	4.71E-08	7.49E-06
mitochondrion	YME1L1 UQCRC2 HSD17B10 ME2 ETHE1 PRDX5 MCCC2 MCCC1 DNAJA1 SUCLA2 ETFA OPA1 RARS2 SDHA LETM1 TOMM70A ATP5C1 CKMT1	2.63E-10	1.16E-08
transit peptide: mitochondrion	UQCRC2 ME2 ETHE1 PRDX5 MCCC2 MCCC1 SUCLA2 ETFA OPA1 RARS2 SDHA LETM1 ATP5C1 CKMT1	1.77E-09	3.61E-07
postsynaptic density	PRKCG PALM CAMK2N1 RAB8A DLGAP3 DBN1	4.54E-04	0.011960936
nucleotide-binding	YME1L1 SEPT5 IARS HSPH1 DGKB MCCC2 RAB8A MCCC1 PRKCG SUCLA2 REM2 OPA1 RARS2 HSPA12A SEPT6 CKMT1	1.23E-05	3.23E-04
nucleotide binding	YME1L1 SEPT5 IARS HSPH1 DGKB MCCC2 RAB8A MCCC1 PRKCG SUCLA2 REM2 OPA1 RARS2 HSPA12A SEPT6 CKMT1	1.81E-04	0.029051447
acetylation	UQCRC2 TPPP3 HSD17B10 PALM ME2 SRM ETHE1 PRDX5 TPM4 IARS HSPH1 MCCC2 CTTN RPL6 MCCC1 DNAJA1 SUCLA2 ETFA OPA1 RARS2 DDB1 DCTN3 OCIAD2 SDHA HSPA12A LETM1 TOMM70A ATP5C1 SEPT6 DBN1	8.76E-12	1.16E-09
mitochondrial inner membrane	YME1L1 UQCRC2 HSD17B10 OPA1 OCIAD2 SDHA LETM1 ATP5C1 MCCC1 CKMT1	8.33E-07	4.42E-05
mitochondrion inner membrane	YME1L1 UQCRC2 OPA1 SDHA LETM1 ATP5C1 CKMT1	3.41E-05	7.49E-04
extracellular exosome	UQCRC2 TPPP3 GABRB2 PRDX5 TPM4 IARS HSPH1 RAB8A CTTN ACTN2 DNAJA1 SUCLA2 ETFA PLXNA1 DDB1 HSPA12A TOMM70A ATP5C1 CKMT1	1.33E-04	0.005289922

However, given dysregulated postsynaptic dopamine-mediated signaling pathways are observed in dystonia, we sought to identify potential molecular interactions that may identify specific abnormalities in postsynaptic dopamine-mediated signal transduction pathways that lead to the development of dystonia. DAVID was used to probe for novel signaling pathways within the KEGG pathway database that may be differentially regulated in DRD compared to normal mouse striatum. We identified enriched pathways for proteins with p values < 0.05 and cytoscape was used to depict integrations between KEGG pathways and the associated gene lists (Figure A.5). Assessing differentially regulated proteins with p values < 0.05 revealed eight enriched KEGG pathways (all p's < 0.09; Table A.3).

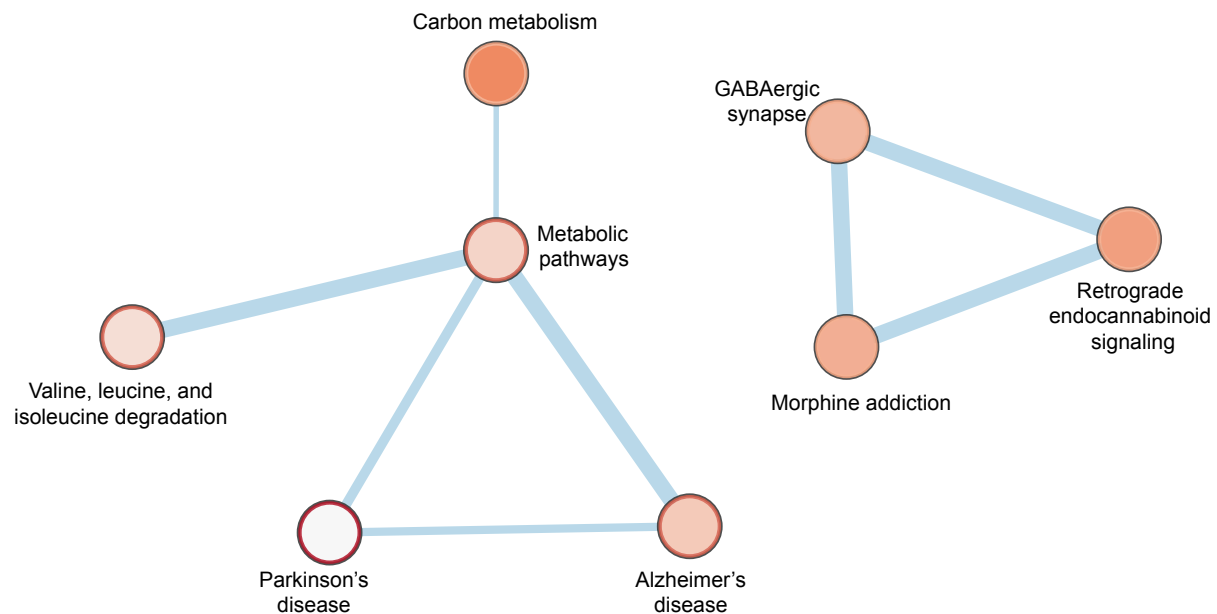


Figure A.5. Cytoscape enriched KEGG pathways of differentially expressed proteins ($p < 0.05$).

Enriched pathways for proteins with p values < 0.05 are depicted using cytoscape. Outer circle color of node depicts the associated p-value (all p's < 0.09) for enriched pathways. Lines and associated thickness depict pathways with the number of shared genes between enriched pathways.

Table A.3. Cytoscape enriched KEGG pathways of differentially expressed proteins ($p < 0.05$)

Pathway Description	Genes	p value	FDR q-value
morphine addiction	GABRB2 GNB5 PRKCG	0.056756114	0.599647403
metabolic pathways	UQCRC2 SDHA TH ATP5C1 MCCC2 HSD17B10 MCCC1 DGKB SRM CKMT1 SUCLA2	0.028718673	0.598691922
alzheimer's disease	UQCRC2 SDHA ATP5C1 HSD17B10	0.036469602	0.582326059
retrograde endocannabinoid signaling	GABRB2 GNB5 PRKCG	0.067940802	0.611250528
valine, leucine, and isoleucine degradation	MCCC2 HSD17B10 MCCC1	0.021714217	0.643639237
parkinson's disease	UQCRC2 SEPT5 SDHA TH ATP5C1	0.003190298	0.259453884
gabaergic synapse	GABRB2 GNB5 PRKCG	0.050396765	0.621737675
carbon metabolism	ME2 SDHA SUCLA2	0.083469874	0.640892686

A.5. Discussion

Our unbiased assessment of the DRD mouse proteome ($p < 0.05$) revealed 57 differentially regulated proteins when compared to the normal mouse striatum. Twelve differentially regulated proteins were previously linked to dystonia. A number of these proteins were related to mitochondrial functions and cell signaling pathways. Similarly, mitochondrial functions and cell signaling pathways were identified as enriched pathways.

Mitochondrial sulfur dioxygenase was increased in the DRD mouse striatum.

Mitochondrial sulfur dioxygenase is involved in the catabolism of sulfide, and pathogenic variants in the associated gene, *ETHE1*, lead to accumulation of toxic sulfide levels. Clinically this results in the development of ethylmalonic encephalopathy, a severe disorder that in some

cases is characterized by dystonia (Tiranti, Viscomi et al. 2009, Walsh, Sills et al. 2010). Further, increased levels of the flavoprotein subunit of succinate dehydrogenase (SDHA) were observed in the DRD mouse striatum. SDHA is largest catalytic subunit of the electron transport chain, and pathogenic variants in the SDHA gene lead to a multisystem mitochondrial disease, which may include Leigh syndrome, and is associated with dystonia (Renkema, Wortmann et al. 2015). OPA1, a mitochondrial, dynamin-related GTPase, was upregulated in DRD mouse striatum. A novel pathogenic variant in the OPA1 gene that results in optic atrophy and widespread neurological disease was recently associated with cervical dystonia; however, a clear relationship between the pathogenic variant and dystonia has not been determined (Liskova, Ulmanova et al. 2013). Mitochondrial dysfunction is a known cellular pathomechanism in both acquired and inherited dystonia (Thompson, Jinnah et al. 2011) and these results suggest it may be a relevant pathomechanism in the DRD mouse model or rather may result following the development of dystonia.

A number of these differentially regulated proteins are associated with both mitochondrial dysfunction and basal ganglia or neuronal pathology. This includes succinate-coenzyme A ligase, ADP-forming, beta subunit (SCS-A), which was upregulated in DRD mouse striatum. Pathogenic variants in the associated gene, *SUCLA2*, are associated with mitochondrial DNA depletion and subsequent lesions of the basal ganglia (Maas, Marina et al. 2016, Garone, Gurgel-Giannetti et al. 2017). Mitochondrial arginyl-transfer RNA synthetase, a protein essential for the translation of proteins, was upregulated in DRD mouse striatum. Pathogenic variants in the associated gene, *RARS2*, are associated with pontocerebellar hypoplasia type 6, a complex disorder that can be associated with dystonia and neurodegeneration (Glamuzina, Brown et al. 2012).

A number of differentially regulated proteins are also involved in cell signaling pathways, which is consistent with known pathomechanisms of dystonia. Decreased levels of protein kinase C (PKC) gamma were observed in DRD mice. PKC gamma is involved in neuronal signal transduction, and pathogenic variants in the associated gene, *PRKCG*, cause spinocerebellar ataxia type 14 (SCA14) in which dystonia is observed (Miura, Nakagawara et al. 2009, Ganos, Zittel et al. 2014, Nibbeling, Delnooz et al. 2017).

Decreased levels of proline-rich-transmembrane-protein-2 were observed in the DRD mouse striatum. This protein interacts with SNAP-25, a presynaptic membrane protein, to promote calcium-dependent vesicular exocytosis. Pathologic variants in the associated gene, *PRRT2*, disrupt synaptic function, specifically glutamate signaling and glutamate receptor activity (Li, Niu et al. 2015). *PRRT2* pathologic variants are frequently causative for a type of paroxysmal dyskinesia that is triggered by movements, termed paroxysmal kinesigenic dyskinesias (PKD; Zhang, Li et al. 2017, Marano, Motolese et al. 2018). PKD is a movement disorders in which the most common type of movement observed is dystonia (Bruno, Hallett et al. 2004).

Decreased levels of the GABA_A receptor beta2 subunit, which is involved in the trafficking and function of GABA_A receptors (Goetz, Arslan et al. 2007), were observed in DRD mouse striatum. Dysregulated GABA signaling was also identified in the Cytoscape enriched KEGG pathways. Alterations in GABA_A receptors have been observed in cervical dystonia (Berman, Pollard et al. 2018) and benzodiazepines, which function by enhancing inhibitory GABA activity, can be effective in treating dystonia (Strzelczyk, Burk et al. 2011). However, these effects are not specific to the striatum.

Levels of the G protein subunit beta 5 (G β 5) were decreased in the DRD mouse striatum. G proteins are heterotrimeric, consisting of α , β , and γ subunits. Loss of function pathogenic variants in the gene encoding the alpha subunit, *GNAL*, are associated with the development of dystonia (Fuchs, Saunders-Pullman et al. 2013). Further, GPCRs mediate dopamine intracellular signaling and are negatively regulated by RGS-proteins (Xie and Martemyanov 2011). Association with G β 5 is necessary for normal RGS9 function (Masuho, Wakasugi-Masuho et al. 2011), and alterations in RGS9 activity have been associated with other movement disorders (Jenner 2008).

Decreased levels of calcium/calmodulin dependent protein kinase II inhibitor 1 (CaMK2N1) were observed in the DRD mouse striatum. CaMK2N1 is an inhibitor of calcium/calmodulin-dependent protein kinase II (CaMKII), a key synaptic signaling protein that has also been shown to be dysregulated in a mouse model of *GNAL* haplodeficiency (Pelosi, Menardy et al. 2017).

Additionally, in the DRD mouse striatum, glial fibrillary acidic protein (GFAP) was upregulated, and pathogenic variants in the GFAP gene are associated with Alexander disease, a rare disorder of astrocytes, which has been associated with dystonia and basal ganglia abnormalities (Jefferson, Absoud et al. 2010).

These results suggest novel pathomechanisms in the DRD mouse model of dystonia. For example, abnormalities in mitochondrial function may contribute to the dystonia in DRD mice. However, the mechanism underlying mitochondrial dysfunction is not known. A previous study administered 3-NPA, a mitochondrial neurotoxin associated with increased striatal dopamine and basal ganglia lesions, to DYT1 knock-in mice to test whether mutant torsinA results in increased susceptibility to the effects of oxidative stress and ATP deficits (Bode, Massey et al. 2012).

While this study found no indications of sensitized responses, a similar methodology could be employed to assess mitochondrial dysfunction in DRD mice.

These results also support a relationship between abnormal cell signaling and dystonia in DRD mice. Future studies assessing the role of RGS-proteins in abnormal postsynaptic signaling in DRD mice may elucidate specific abnormal dopamine-mediated intracellular signaling mechanisms that underlie dystonia. To determine whether abnormal GABAergic signaling may also underlie dystonia in DRD mice, future studies can assess whether DRD mice display abnormal responses to benzodiazepines, including locomotor or sedative effects (Hsu, Chang et al. 2017). Determining the effectiveness of benzodiazepines at alleviating dystonia in DRD mice may also identify additional therapeutic mechanisms that can be studied in this model.

Results from these future studies may ultimately identify striatal abnormalities that underlie dystonia. Given a number of differentially regulated proteins in this study were previously associated with dystonia, the DRD mouse model may also identify pathomechanisms underlying DOPA-responsive dystonia that are common to many forms of dystonia.

References

- Ade, K. K., Y. Wan, M. Chen, B. Gloss and N. Calakos (2011). "An Improved BAC Transgenic Fluorescent Reporter Line for Sensitive and Specific Identification of Striatonigral Medium Spiny Neurons." Front Syst Neurosci **5**: 32.
- Agnati, L. F., S. Ferre, C. Lluís, R. Franco and K. Fuxe (2003). "Molecular mechanisms and therapeutical implications of intramembrane receptor/receptor interactions among heptahelical receptors with examples from the striatopallidal GABA neurons." Pharmacol Rev **55**(3): 509-550.
- Albanese, A., K. Bhatia, S. B. Bressman, M. R. Delong, S. Fahn, V. S. Fung, M. Hallett, J. Jankovic, H. A. Jinnah, C. Klein, A. E. Lang, J. W. Mink and J. K. Teller (2013). "Phenomenology and classification of dystonia: a consensus update." Mov Disord **28**(7): 863-873.
- Alcacer, C., L. Andreoli, I. Sebastianutto, J. Jakobsson, T. Fieblinger and M. A. Cenci (2017). "Chemogenetic stimulation of striatal projection neurons modulates responses to Parkinson's disease therapy." J Clin Invest **127**(2): 720-734.
- Alcacer, C., E. Santini, E. Valjent, F. Gaven, J. A. Girault and D. Herve (2012). "Galpha(olf) mutation allows parsing the role of cAMP-dependent and extracellular signal-regulated kinase-dependent signaling in L-3,4-dihydroxyphenylalanine-induced dyskinesia." J Neurosci **32**(17): 5900-5910.
- Anderson, K. M., F. M. Krienen, E. Y. Choi, J. M. Reinen, B. T. T. Yeo and A. J. Holmes (2018). "Gene expression links functional networks across cortex and striatum." Nat Commun **9**(1): 1428.

- Andersson, M., C. Konradi and M. A. Cenci (2001). "cAMP response element-binding protein is required for dopamine-dependent gene expression in the intact but not the dopamine-denervated striatum." J Neurosci **21**(24): 9930-9943.
- Araki, K. Y., J. R. Sims and P. G. Bhide (2007). "Dopamine receptor mRNA and protein expression in the mouse corpus striatum and cerebral cortex during pre- and postnatal development." Brain Res **1156**: 31-45.
- Asanuma, K., Y. Ma, J. Okulski, V. Dhawan, T. Chaly, M. Carbon, S. B. Bressman and D. Eidelberg (2005). "Decreased striatal D2 receptor binding in non-manifesting carriers of the DYT1 dystonia mutation." Neurology **64**(2): 347-349.
- Baizabal-Carvalho, J. F., J. Jankovic and J. Feld (2013). "Flu-like symptoms and associated immunological response following therapy with botulinum toxins." Neurotox Res **24**(2): 298-306.
- Balint, B. and K. P. Bhatia (2015). "Isolated and combined dystonia syndromes - an update on new genes and their phenotypes." Eur J Neurol **22**(4): 610-617.
- Bankhead, P., M. B. Loughrey, J. A. Fernandez, Y. Dombrowski, D. G. McArt, P. D. Dunne, S. McQuaid, R. T. Gray, L. J. Murray, H. G. Coleman, J. A. James, M. Salto-Tellez and P. W. Hamilton (2017). "QuPath: Open source software for digital pathology image analysis." Sci Rep **7**(1): 16878.
- Bastide, M. F., W. G. Meissner, B. Picconi, S. Fasano, P. O. Fernagut, M. Feyder, V. Francardo, C. Alcacer, Y. Ding, R. Brambilla, G. Fisone, A. Jon Stoessl, M. Bourdenx, M. Engeln, S. Navailles, P. De Deurwaerdere, W. K. Ko, N. Simola, M. Morelli, L. Groc, M. C. Rodriguez, E. V. Gurevich, M. Quik, M. Morari, M. Mellone, F. Gardoni, E. Tronci, D. Guehl, F. Tison, A. R. Crossman, U. J. Kang, K. Steece-Collier, S. Fox, M. Carta, M.

- Angela Cenci and E. Bezard (2015). "Pathophysiology of L-dopa-induced motor and non-motor complications in Parkinson's disease." Prog Neurobiol **132**: 96-168.
- Berke, J. D., R. F. Paletzki, G. J. Aronson, S. E. Hyman and C. R. Gerfen (1998). "A complex program of striatal gene expression induced by dopaminergic stimulation." J Neurosci **18**(14): 5301-5310.
- Berman, B. D., M. Hallett, P. Herscovitch and K. Simonyan (2013). "Striatal dopaminergic dysfunction at rest and during task performance in writer's cramp." Brain **136**(Pt 12): 3645-3658.
- Berman, B. D., R. T. Pollard, E. Shelton, R. Karki, P. M. Smith-Jones and Y. Miao (2018). "GABAA Receptor Availability Changes Underlie Symptoms in Isolated Cervical Dystonia." Front Neurol **9**: 188.
- Bertran-Gonzalez, J., C. Bosch, M. Maroteaux, M. Matamales, D. Herve, E. Valjent and J. A. Girault (2008). "Opposing patterns of signaling activation in dopamine D1 and D2 receptor-expressing striatal neurons in response to cocaine and haloperidol." J Neurosci **28**(22): 5671-5685.
- Bertran-Gonzalez, J., D. Herve, J. A. Girault and E. Valjent (2010). "What is the Degree of Segregation between Striatonigral and Striatopallidal Projections?" Front Neuroanat **4**.
- Bhatia, K. P. and C. D. Marsden (1994). "The behavioural and motor consequences of focal lesions of the basal ganglia in man." Brain **117** (Pt 4): 859-876.
- Blumenthal, S. A. (2012). "Earl Sutherland (1915-1974) [corrected] and the discovery of cyclic AMP." Perspect Biol Med **55**(2): 236-249.
- Bode, N., C. Massey and P. Gonzalez-Alegre (2012). "DYT1 knock-in mice are not sensitized against mitochondrial complex-II inhibition." PLoS One **7**(8): e42644.

- Bonci, A. and F. W. Hopf (2005). "The dopamine D2 receptor: new surprises from an old friend." Neuron **47**(3): 335-338.
- Bos, J. L., H. Rehmann and A. Wittinghofer (2007). "GEFs and GAPs: critical elements in the control of small G proteins." Cell **129**(5): 865-877.
- Boyson, S. J., P. McGonigle and P. B. Molinoff (1986). "Quantitative autoradiographic localization of the D1 and D2 subtypes of dopamine receptors in rat brain." J Neurosci **6**(11): 3177-3188.
- Breese, G. R., A. A. Baumeister, T. J. McCown, S. G. Emerick, G. D. Frye, K. Crotty and R. A. Mueller (1984). "Behavioral differences between neonatal and adult 6-hydroxydopamine-treated rats to dopamine agonists: relevance to neurological symptoms in clinical syndromes with reduced brain dopamine." J Pharmacol Exp Ther **231**(2): 343-354.
- Brennan, P. M. and I. R. Whittle (2008). "Intrathecal baclofen therapy for neurological disorders: a sound knowledge base but many challenges remain." Br J Neurosurg **22**(4): 508-519.
- Broussard, J. I. (2012). "Co-transmission of dopamine and glutamate." J Gen Physiol **139**(1): 93-96.
- Bruno, M. K., M. Hallett, K. Gwinn-Hardy, B. Sorensen, E. Considine, S. Tucker, D. R. Lynch, K. D. Mathews, K. J. Swoboda, J. Harris, B. W. Soong, T. Ashizawa, J. Jankovic, D. Renner, Y. H. Fu and L. J. Ptacek (2004). "Clinical evaluation of idiopathic paroxysmal kinesigenic dyskinesia: new diagnostic criteria." Neurology **63**(12): 2280-2287.
- Brust, T. F., M. P. Hayes, D. L. Roman, K. D. Burris and V. J. Watts (2015). "Bias analyses of preclinical and clinical D2 dopamine ligands: studies with immediate and complex signaling pathways." J Pharmacol Exp Ther **352**(3): 480-493.

- Burke, R. E., S. Fahn and C. D. Marsden (1986). "Torsion dystonia: a double-blind, prospective trial of high-dosage trihexyphenidyl." Neurology **36**(2): 160-164.
- Cahill, E., M. Salery, P. Vanhoutte and J. Caboche (2014). "Convergence of dopamine and glutamate signaling onto striatal ERK activation in response to drugs of abuse." Front Pharmacol **4**: 172.
- Cai, Y. and C. P. Ford (2018). "Dopamine Cells Differentially Regulate Striatal Cholinergic Transmission across Regions through Corelease of Dopamine and Glutamate." Cell Rep **25**(11): 3148-3157 e3143.
- Chan, C. S., J. D. Peterson, T. S. Gertler, K. E. Glajch, R. E. Quintana, Q. Cui, L. E. Sebel, J. L. Plotkin, W. Shen, M. Heiman, N. Heintz, P. Greengard and D. J. Surmeier (2012). "Strain-specific regulation of striatal phenotype in Drd2-eGFP BAC transgenic mice." J Neurosci **32**(27): 9124-9132.
- Cheng, X., Z. Ji, T. Tsalkova and F. Mei (2008). "Epac and PKA: a tale of two intracellular cAMP receptors." Acta Biochim Biophys Sin (Shanghai) **40**(7): 651-662.
- Cloud, L. J. and H. A. Jinnah (2010). "Treatment strategies for dystonia." Expert Opin Pharmacother **11**(1): 5-15.
- Cui, G., S. B. Jun, X. Jin, M. D. Pham, S. S. Vogel, D. M. Lovinger and R. M. Costa (2013). "Concurrent activation of striatal direct and indirect pathways during action initiation." Nature **494**(7436): 238-242.
- Damier, P., S. Thobois, T. Witjas, E. Cuny, P. Derost, S. Raoul, P. Mertens, J. C. Peragut, J. J. Lemaire, P. Burbaud, J. M. Nguyen, P. M. Llorca, O. Rascol and G. French Stimulation for Tardive Dyskinesia Study (2007). "Bilateral deep brain stimulation of the globus pallidus to treat tardive dyskinesia." Arch Gen Psychiatry **64**(2): 170-176.

Dani, J. A. and F. M. Zhou (2004). "Selective dopamine filter of glutamate striatal afferents."

Neuron **42**(4): 522-524.

Darmopil, S., A. B. Martin, I. R. De Diego, S. Ares and R. Moratalla (2009). "Genetic

inactivation of dopamine D1 but not D2 receptors inhibits L-DOPA-induced dyskinesia and histone activation." Biol Psychiatry **66**(6): 603-613.

Defazio, G., G. Abbruzzese, P. Livrea and A. Berardelli (2004). "Epidemiology of primary

dystonia." Lancet Neurol **3**(11): 673-678.

Defazio, G., M. Hallett, H. A. Jinnah, A. Conte and A. Berardelli (2017). "Blepharospasm 40

years later." Mov Disord **32**(4): 498-509.

DeLong, M. and T. Wichmann (2010). "Changing views of basal ganglia circuits and circuit

disorders." Clin EEG Neurosci **41**(2): 61-67.

Denny-Brown, D. (1965). "The Nature of Dystonia." Bull N Y Acad Med **41**: 858-869.

Dhanasekaran, N. and E. Premkumar Reddy (1998). "Signaling by dual specificity kinases."

Oncogene **17**(11 Reviews): 1447-1455.

Downs, A. M., X. Fan, C. Donsante, H. A. Jinnah and E. J. Hess (2019). "Trihexyphenidyl

rescues the deficit in dopamine neurotransmission in a mouse model of DYT1 dystonia."

Neurobiol Dis **125**: 115-122.

Dragunow, M., G. S. Robertson, R. L. Faull, H. A. Robertson and K. Jansen (1990). "D2

dopamine receptor antagonists induce fos and related proteins in rat striatal neurons."

Neuroscience **37**(2): 287-294.

Ernst, M., A. J. Zametkin, J. A. Matochik, D. Pascualvaca, P. H. Jons, K. Hardy, J. G.

Hankerson, D. J. Doudet and R. M. Cohen (1996). "Presynaptic dopaminergic deficits in

Lesch-Nyhan disease." N Engl J Med **334**(24): 1568-1572.

- Fan, X., Y. Donsante, H. A. Jinnah and E. J. Hess (2018). "Dopamine Receptor Agonist Treatment of Idiopathic Dystonia: A Reappraisal in Humans and Mice." J Pharmacol Exp Ther **365**(1): 20-26.
- Fienberg, A. A., N. Hiroi, P. G. Mermelstein, W. Song, G. L. Snyder, A. Nishi, A. Cheramy, J. P. O'Callaghan, D. B. Miller, D. G. Cole, R. Corbett, C. N. Haile, D. C. Cooper, S. P. Onn, A. A. Grace, C. C. Ouimet, F. J. White, S. E. Hyman, D. J. Surmeier, J. Girault, E. J. Nestler and P. Greengard (1998). "DARPP-32: regulator of the efficacy of dopaminergic neurotransmission." Science **281**(5378): 838-842.
- Ford, C. P. (2014). "The role of D2-autoreceptors in regulating dopamine neuron activity and transmission." Neuroscience **282**: 13-22.
- Fuchs, T., R. Saunders-Pullman, I. Masuho, M. S. Luciano, D. Raymond, S. Factor, A. E. Lang, T. W. Liang, R. M. Trosch, S. White, E. Ainehsazan, D. Herve, N. Sharma, M. E. Ehrlich, K. A. Martemyanov, S. B. Bressman and L. J. Ozelius (2013). "Mutations in GNAL cause primary torsion dystonia." Nat Genet **45**(1): 88-92.
- Gagnon, D., S. Petryszyn, M. G. Sanchez, C. Bories, J. M. Beaulieu, Y. De Koninck, A. Parent and M. Parent (2017). "Striatal Neurons Expressing D1 and D2 Receptors are Morphologically Distinct and Differently Affected by Dopamine Denervation in Mice." Sci Rep **7**: 41432.
- Gangarossa, G., J. Espallergues, A. de Kerchove d'Exaerde, S. El Mestikawy, C. R. Gerfen, D. Herve, J. A. Girault and E. Valjent (2013). "Distribution and compartmental organization of GABAergic medium-sized spiny neurons in the mouse nucleus accumbens." Front Neural Circuits **7**: 22.

- Ganos, C., S. Zittel, M. Minnerop, O. Schunke, C. Heinbokel, C. Gerloff, C. Zuhlke, P. Bauer, T. Klockgether, A. Munchau and T. Baumer (2014). "Clinical and neurophysiological profile of four German families with spinocerebellar ataxia type 14." Cerebellum **13**(1): 89-96.
- Garone, C., J. Gurgel-Giannetti, S. Sanna-Cherchi, S. Krishna, A. Naini, C. M. Quinzii and M. Hirano (2017). "A Novel SUCLA2 Mutation Presenting as a Complex Childhood Movement Disorder." J Child Neurol **32**(2): 246-250.
- Gerfen, C. R., T. M. Engber, L. C. Mahan, Z. Susel, T. N. Chase, F. J. Monsma, Jr. and D. R. Sibley (1990). "D1 and D2 dopamine receptor-regulated gene expression of striatonigral and striatopallidal neurons." Science **250**(4986): 1429-1432.
- Gerfen, C. R., K. A. Keefe and E. B. Gauda (1995). "D1 and D2 dopamine receptor function in the striatum: coactivation of D1- and D2-dopamine receptors on separate populations of neurons results in potentiated immediate early gene response in D1-containing neurons." J Neurosci **15**(12): 8167-8176.
- Gerfen, C. R., S. Miyachi, R. Paletzki and P. Brown (2002). "D1 dopamine receptor supersensitivity in the dopamine-depleted striatum results from a switch in the regulation of ERK1/2/MAP kinase." J Neurosci **22**(12): 5042-5054.
- Gerfen, C. R. and D. J. Surmeier (2011). "Modulation of striatal projection systems by dopamine." Annu Rev Neurosci **34**: 441-466.
- Geyer, M. and A. Markou (1995). Animal models for psychiatric disorders. Psychopharmacology: the fourth generation of progress. . New York, Raven Press: 787–798.

- Girault, J. A., E. Valjent, J. Caboche and D. Herve (2007). "ERK2: a logical AND gate critical for drug-induced plasticity?" Curr Opin Pharmacol **7**(1): 77-85.
- Glamuzina, E., R. Brown, K. Hogarth, D. Saunders, I. Russell-Eggitt, M. Pitt, C. de Sousa, S. Rahman, G. Brown and S. Grunewald (2012). "Further delineation of pontocerebellar hypoplasia type 6 due to mutations in the gene encoding mitochondrial arginyl-tRNA synthetase, RARS2." J Inherit Metab Dis **35**(3): 459-467.
- Goetz, T., A. Arslan, W. Wisden and P. Wulff (2007). "GABA(A) receptors: structure and function in the basal ganglia." Prog Brain Res **160**: 21-41.
- Gonzales, K. K. and Y. Smith (2015). "Striatal Cholinergic interneurons in the dorsal and ventral striatum: anatomical and functional considerations in normal and diseased conditions." Ann N Y Acad Sci **1349**: 1-45.
- Goodchild, R. E. and W. T. Dauer (2004). "Mislocalization to the nuclear envelope: an effect of the dystonia-causing torsinA mutation." Proc Natl Acad Sci U S A **101**(3): 847-852.
- Gorvin, C. M., V. N. Babinsky, T. Malinauskas, P. H. Nissen, A. J. Schou, A. C. Hanyaloglu, C. Siebold, E. Y. Jones, F. M. Hannan and R. V. Thakker (2018). "A calcium-sensing receptor mutation causing hypocalcemia disrupts a transmembrane salt bridge to activate beta-arrestin-biased signaling." Sci Signal **11**(518).
- Gottle, M., C. N. Prudente, R. Fu, D. Sutcliffe, H. Pang, D. Cooper, E. Veledar, J. D. Glass, M. Gearing, J. E. Visser and H. A. Jinnah (2014). "Loss of dopamine phenotype among midbrain neurons in Lesch-Nyhan disease." Ann Neurol **76**(1): 95-107.
- Graybiel, A. M. (2000). "The basal ganglia." Curr Biol **10**(14): R509-511.
- Graybiel, A. M. and S. T. Grafton (2015). "The striatum: where skills and habits meet." Cold Spring Harb Perspect Biol **7**(8): a021691.

Greene, P. E. and S. Fahn (1992). "Baclofen in the treatment of idiopathic dystonia in children."

Mov Disord **7**(1): 48-52.

Grillner, S. and B. Robertson (2016). "The Basal Ganglia Over 500 Million Years." Curr Biol

26(20): R1088-R1100.

Hammond, G. W. (1890). "Original case of athetosis." J. Nerv. Ment. Dis. **17**(555–556).

Hanson, P. I. and S. W. Whiteheart (2005). "AAA+ proteins: have engine, will work." Nat Rev

Mol Cell Biol **6**(7): 519-529.

He, F., S. Zhang, F. Qian and C. Zhang (1995). "Delayed dystonia with striatal CT lucencies

induced by a mycotoxin (3-nitropropionic acid)." Neurology **45**(12): 2178-2183.

Heiman, M., A. Heilbut, V. Francardo, R. Kulicke, R. J. Fenster, E. D. Kolaczyk, J. P. Mesirov,

D. J. Surmeier, M. A. Cenci and P. Greengard (2014). "Molecular adaptations of striatal

spiny projection neurons during levodopa-induced dyskinesia." Proc Natl Acad Sci U S A

111(12): 4578-4583.

Hemmings, H. C., Jr., P. Greengard, H. Y. Tung and P. Cohen (1984). "DARPP-32, a dopamine-

regulated neuronal phosphoprotein, is a potent inhibitor of protein phosphatase-1."

Nature **310**(5977): 503-505.

Hernandez-Lopez, S., T. Tkatch, E. Perez-Garci, E. Galarraga, J. Bargas, H. Hamm and D. J.

Surmeier (2000). "D2 dopamine receptors in striatal medium spiny neurons reduce L-

type Ca²⁺ currents and excitability via a novel PLC[β]₁-IP₃-calcineurin-signaling

cascade." J Neurosci **20**(24): 8987-8995.

Herve, D. (2011). "Identification of a specific assembly of the g protein golf as a critical and

regulated module of dopamine and adenosine-activated cAMP pathways in the striatum."

Front Neuroanat **5**: 48.

Herve, D., M. Levi-Strauss, I. Marey-Semper, C. Verney, J. P. Tassin, J. Glowinski and J. A.

Girault (1993). "G(olf) and Gs in rat basal ganglia: possible involvement of G(olf) in the coupling of dopamine D1 receptor with adenylyl cyclase." J Neurosci **13**(5): 2237-2248.

Herz, E. (1944). "b.Dystonia II Clinical classification." Archives of Neurology and Psychiatry **51**(4): 319-355.

Herz, E. (1944). "c.Dystonia III Pathology and conclusions." Archives of Neurology and Psychiatry **52**(1): 20-26.

Herz, E. (1944). "a.Dystonia I Historical review, analysis of dystonic symptoms and physiologic mechanisms involved." Archives of Neurology and Psychiatry **51**(4): 305-318.

Hintiryan, H., N. N. Foster, I. Bowman, M. Bay, M. Y. Song, L. Gou, S. Yamashita, M. S.

Bienkowski, B. Zingg, M. Zhu, X. W. Yang, J. C. Shih, A. W. Toga and H. W. Dong (2016). "The mouse cortico-striatal projectome." Nat Neurosci **19**(8): 1100-1114.

Horie, C., Y. Suzuki, M. Kiyosawa, M. Mochizuki, M. Wakakura, K. Oda, K. Ishiwata and K.

Ishii (2009). "Decreased dopamine D receptor binding in essential blepharospasm." Acta Neurol Scand **119**(1): 49-54.

Hsu, Y. T., Y. G. Chang, C. P. Chang, J. J. Siew, H. M. Chen, C. H. Tsai and Y. Chern (2017).

"Altered behavioral responses to gamma-aminobutyric acid pharmacological agents in a mouse model of Huntington's disease." Mov Disord **32**(11): 1600-1609.

Huang da, W., B. T. Sherman and R. A. Lempicki (2009). "Systematic and integrative analysis

of large gene lists using DAVID bioinformatics resources." Nat Protoc **4**(1): 44-57.

Hunnicut, B. J., B. C. Jongbloets, W. T. Birdsong, K. J. Gertz, H. Zhong and T. Mao (2016). "A

comprehensive excitatory input map of the striatum reveals novel functional organization." Elife **5**.

- Ichinose, H., T. Ohye, E. Takahashi, N. Seki, T. Hori, M. Segawa, Y. Nomura, K. Endo, H. Tanaka, S. Tsuji and et al. (1994). "Hereditary progressive dystonia with marked diurnal fluctuation caused by mutations in the GTP cyclohydrolase I gene." Nat Genet **8**(3): 236-242.
- Jankovic, J. and R. Tintner (2001). "Dystonia and parkinsonism." Parkinsonism Relat Disord **8**(2): 109-121.
- Jankovic, J., K. D. Vuong and J. Ahsan (2003). "Comparison of efficacy and immunogenicity of original versus current botulinum toxin in cervical dystonia." Neurology **60**(7): 1186-1188.
- Jefferson, R. J., M. Absoud, R. Jain, J. H. Livingston, V. D. K. MS and S. Jayawant (2010). "Alexander disease with periventricular calcification: a novel mutation of the GFAP gene." Dev Med Child Neurol **52**(12): 1160-1163.
- Jenner, P. (2008). "Molecular mechanisms of L-DOPA-induced dyskinesia." Nat Rev Neurosci **9**(9): 665-677.
- Jiang, M. and N. S. Bajpayee (2009). "Molecular mechanisms of go signaling." Neurosignals **17**(1): 23-41.
- Jin, L. Q., S. Goswami, G. Cai, X. Zhen and E. Friedman (2003). "SKF83959 selectively regulates phosphatidylinositol-linked D1 dopamine receptors in rat brain." J Neurochem **85**(2): 378-386.
- Jinnah, H. A., K. Egami, L. Rao, M. Shin, S. Kasim and E. J. Hess (2003). "Expression of c-FOS in the brain after activation of L-type calcium channels." Dev Neurosci **25**(6): 403-411.
- Jinnah, H. A. and S. A. Factor (2015). "Diagnosis and treatment of dystonia." Neurol Clin **33**(1): 77-100.

- Jinnah, H. A., E. Goodmann, A. R. Rosen, M. Evatt, A. Freeman and S. Factor (2016). "Botulinum toxin treatment failures in cervical dystonia: causes, management, and outcomes." J Neurol **263**(6): 1188-1194.
- Jinnah, H. A. and E. J. Hess (2018). "Evolving concepts in the pathogenesis of dystonia." Parkinsonism Relat Disord **46 Suppl 1**: S62-S65.
- Jinnah, H. A., E. J. Hess, M. S. Ledoux, N. Sharma, M. G. Baxter and M. R. DeLong (2005). "Rodent models for dystonia research: characteristics, evaluation, and utility." Mov Disord **20**(3): 283-292.
- Jinnah, H. A., V. Neychev and E. J. Hess (2017). "The Anatomical Basis for Dystonia: The Motor Network Model." Tremor Other Hyperkinet Mov (N Y) **7**: 506.
- Jinnah, H. A. and Y. V. Sun (2019). "Dystonia genes and their biological pathways." Neurobiol Dis **129**: 159-168.
- Karp, B. I., S. R. Goldstein, R. Chen, A. Samii, W. Bara-Jimenez and M. Hallett (1999). "An open trial of clozapine for dystonia." Mov Disord **14**(4): 652-657.
- Katada, T. and M. Ui (1982). "Direct modification of the membrane adenylate cyclase system by islet-activating protein due to ADP-ribosylation of a membrane protein." Proc Natl Acad Sci U S A **79**(10): 3129-3133.
- Keefe, K. A. and C. R. Gerfen (1995). "D1-D2 dopamine receptor synergy in striatum: effects of intrastriatal infusions of dopamine agonists and antagonists on immediate early gene expression." Neuroscience **66**(4): 903-913.
- Keefe, K. A. and C. R. Gerfen (1996). "D1 dopamine receptor-mediated induction of zif268 and c-fos in the dopamine-depleted striatum: differential regulation and independence from NMDA receptors." J Comp Neurol **367**(2): 165-176.

- Kemp, J. M. and T. P. Powell (1971). "The synaptic organization of the caudate nucleus." Philos Trans R Soc Lond B Biol Sci **262**(845): 403-412.
- Kim, D. S., R. D. Palmiter, A. Cummins and C. R. Gerfen (2006). "Reversal of supersensitive striatal dopamine D1 receptor signaling and extracellular signal-regulated kinase activity in dopamine-deficient mice." Neuroscience **137**(4): 1381-1388.
- Kim, D. S., M. S. Szczypka and R. D. Palmiter (2000). "Dopamine-deficient mice are hypersensitive to dopamine receptor agonists." J Neurosci **20**(12): 4405-4413.
- Kim, E. K. and E. J. Choi (2010). "Pathological roles of MAPK signaling pathways in human diseases." Biochim Biophys Acta **1802**(4): 396-405.
- Klein, C. (2014). "Genetics in dystonia." Parkinsonism Relat Disord **20 Suppl 1**: S137-142.
- Klein, C. and S. Fahn (2013). "Translation of Oppenheim's 1911 paper on dystonia." Mov Disord **28**(7): 851-862.
- Knappskog, P. M., T. Flatmark, J. Mallet, B. Ludecke and K. Bartholome (1995). "Recessively inherited L-DOPA-responsive dystonia caused by a point mutation (Q381K) in the tyrosine hydroxylase gene." Hum Mol Genet **4**(7): 1209-1212.
- Konradi, C., R. L. Cole, S. Heckers and S. E. Hyman (1994). "Amphetamine regulates gene expression in rat striatum via transcription factor CREB." J Neurosci **14**(9): 5623-5634.
- Kostrzewa, R. M. (1995). "Dopamine receptor supersensitivity." Neurosci Biobehav Rev **19**(1): 1-17.
- Kravitz, A. V., B. S. Freeze, P. R. Parker, K. Kay, M. T. Thwin, K. Deisseroth and A. C. Kreitzer (2010). "Regulation of parkinsonian motor behaviours by optogenetic control of basal ganglia circuitry." Nature **466**(7306): 622-626.

- Kurian, M. A., Y. Li, J. Zhen, E. Meyer, N. Hai, H. J. Christen, G. F. Hoffmann, P. Jardine, A. von Moers, S. R. Mordekar, F. O'Callaghan, E. Wassmer, E. Wraige, C. Dietrich, T. Lewis, K. Hyland, S. Heales, Jr., T. Sanger, P. Gissen, B. E. Assmann, M. E. Reith and E. R. Maher (2011). "Clinical and molecular characterisation of hereditary dopamine transporter deficiency syndrome: an observational cohort and experimental study." Lancet Neurol **10**(1): 54-62.
- Kuyper, D. J., V. Parra, S. Aerts, M. S. Okun and B. M. Kluger (2011). "Nonmotor manifestations of dystonia: a systematic review." Mov Disord **26**(7): 1206-1217.
- Largent, B. L., D. T. Jones, R. R. Reed, R. C. Pearson and S. H. Snyder (1988). "G protein mRNA mapped in rat brain by in situ hybridization." Proc Natl Acad Sci U S A **85**(8): 2864-2868.
- Laruelle, M., W. G. Frankle, R. Narendran, L. S. Kegeles and A. Abi-Dargham (2005). "Mechanism of action of antipsychotic drugs: from dopamine D(2) receptor antagonism to glutamate NMDA facilitation." Clin Ther **27 Suppl A**: S16-24.
- Lascaratos, J. and A. Damanakis (1996). "Ocular torticollis: a new explanation for the abnormal head-posture of Alexander the Great." Lancet **347**(9000): 521-523.
- LeDoux, M. S. (2011). "Animal models of dystonia: Lessons from a mutant rat." Neurobiol Dis **42**(2): 152-161.
- Lefkowitz, R. J. and S. K. Shenoy (2005). "Transduction of receptor signals by beta-arrestins." Science **308**(5721): 512-517.
- Lehericy, S., M. A. Tijssen, M. Vidailhet, R. Kaji and S. Meunier (2013). "The anatomical basis of dystonia: current view using neuroimaging." Mov Disord **28**(7): 944-957.

- Li, M., F. Niu, X. Zhu, X. Wu, N. Shen, X. Peng and Y. Liu (2015). "PRRT2 Mutant Leads to Dysfunction of Glutamate Signaling." Int J Mol Sci **16**(5): 9134-9151.
- Li, P., G. L. Snyder and K. E. Vanover (2016). "Dopamine Targeting Drugs for the Treatment of Schizophrenia: Past, Present and Future." Curr Top Med Chem **16**(29): 3385-3403.
- Lieberman, O. J., A. F. McGuirt, E. V. Mosharov, I. Pigulevskiy, B. D. Hobson, S. Choi, M. D. Frier, E. Santini, A. Borgkvist and D. Sulzer (2018). "Dopamine Triggers the Maturation of Striatal Spiny Projection Neuron Excitability during a Critical Period." Neuron **99**(3): 540-554 e544.
- Liskova, P., O. Ulmanova, P. Tesina, H. Melsova, P. Diblik, H. Hansikova, M. Tesarova and M. Votruba (2013). "Novel OPA1 missense mutation in a family with optic atrophy and severe widespread neurological disorder." Acta Ophthalmol **91**(3): e225-231.
- Liu, X., X. Luo and W. Hu (1992). "Studies on the epidemiology and etiology of moldy sugarcane poisoning in China." Biomed Environ Sci **5**(2): 161-177.
- Lohmann, K. and C. Klein (2017). "Update on the Genetics of Dystonia." Curr Neurol Neurosci Rep **17**(3): 26.
- Lorden, J. F., T. W. McKeon, H. J. Baker, N. Cox and S. U. Walkley (1984). "Characterization of the rat mutant dystonic (dt): a new animal model of dystonia musculorum deformans." J Neurosci **4**(8): 1925-1932.
- Maas, R. R., A. D. Marina, A. P. de Brouwer, R. A. Wevers, R. J. Rodenburg and S. B. Wortmann (2016). "SUCLA2 Deficiency: A Deafness-Dystonia Syndrome with Distinctive Metabolic Findings (Report of a New Patient and Review of the Literature)." JIMD Rep **27**: 27-32.

- Manvich, D. F., A. K. Petko, R. C. Branco, S. L. Foster, K. A. Porter-Stransky, K. A. Stout, A. H. Newman, G. W. Miller, C. A. Paladini and D. Weinshenker (2019). "Selective D2 and D3 receptor antagonists oppositely modulate cocaine responses in mice via distinct postsynaptic mechanisms in nucleus accumbens." Neuropsychopharmacology **44**(8): 1445-1455.
- Marano, M., F. Motolese, F. Consoli, A. De Luca and V. Di Lazzaro (2018). "Paroxysmal Dyskinesias in a PRRT2 Mutation Carrier." Tremor Other Hyperkinet Mov (N Y) **8**: 616.
- Marinissen, M. J. and J. S. Gutkind (2001). "G-protein-coupled receptors and signaling networks: emerging paradigms." Trends Pharmacol Sci **22**(7): 368-376.
- Marsden, C. D., J. A. Obeso, J. J. Zarranz and A. E. Lang (1985). "The anatomical basis of symptomatic hemidystonia." Brain **108 (Pt 2)**: 463-483.
- Masuho, I., H. Wakasugi-Masuho, E. N. Posokhova, J. R. Patton and K. A. Martemyanov (2011). "Type 5 G protein beta subunit (Gbeta5) controls the interaction of regulator of G protein signaling 9 (RGS9) with membrane anchors." J Biol Chem **286**(24): 21806-21813.
- Matamales, M. and J. A. Girault (2011). "Signaling from the cytoplasm to the nucleus in striatal medium-sized spiny neurons." Front Neuroanat **5**: 37.
- McGeorge, A. J. and R. L. Faull (1989). "The organization of the projection from the cerebral cortex to the striatum in the rat." Neuroscience **29**(3): 503-537.
- Mehta, S. H., J. C. Morgan and K. D. Sethi (2015). "Drug-induced movement disorders." Neurol Clin **33**(1): 153-174.
- Ming, L. (1995). "Moldy sugarcane poisoning--a case report with a brief review." J Toxicol Clin Toxicol **33**(4): 363-367.

- Mink, J. W. and W. T. Thach (1993). "Basal ganglia intrinsic circuits and their role in behavior." Curr Opin Neurobiol **3**(6): 950-957.
- Miura, S., H. Nakagawara, H. Kaida, M. Sugita, K. Noda, K. Motomura, Y. Ohyagi, M. Ayabe, H. Aizawa, M. Ishibashi and T. Taniwaki (2009). "Expansion of the phenotypic spectrum of SCA14 caused by the Gly128Asp mutation in PRKCG." Clin Neurol Neurosurg **111**(2): 211-215.
- Nagatsu, T., M. Levitt and S. Udenfriend (1964). "Tyrosine Hydroxylase. The Initial Step in Norepinephrine Biosynthesis." J Biol Chem **239**: 2910-2917.
- Nambu, A., H. Tokuno and M. Takada (2002). "Functional significance of the cortico-subthalamo-pallidal 'hyperdirect' pathway." Neurosci Res **43**(2): 111-117.
- Napolitano, F., M. Pasqualetti, A. Usiello, E. Santini, G. Pacini, G. Sciamanna, F. Errico, A. Tassone, V. Di Dato, G. Martella, D. Cuomo, G. Fisone, G. Bernardi, G. Mandolesi, N. B. Mercuri, D. G. Standaert and A. Pisani (2010). "Dopamine D2 receptor dysfunction is rescued by adenosine A2A receptor antagonism in a model of DYT1 dystonia." Neurobiol Dis **38**(3): 434-445.
- Naumann, M., W. Pirker, K. Reiners, K. W. Lange, G. Becker and T. Brucke (1998). "Imaging the pre- and postsynaptic side of striatal dopaminergic synapses in idiopathic cervical dystonia: a SPECT study using [123I] epidepride and [123I] beta-CIT." Mov Disord **13**(2): 319-323.
- Neer, E. J., J. M. Lok and L. G. Wolf (1984). "Purification and properties of the inhibitory guanine nucleotide regulatory unit of brain adenylate cyclase." J Biol Chem **259**(22): 14222-14229.

- Neve, K. A., J. K. Seamans and H. Trantham-Davidson (2004). "Dopamine receptor signaling." J Recept Signal Transduct Res **24**(3): 165-205.
- Newby, R. E., D. E. Thorpe, P. A. Kempster and J. E. Alty (2017). "A History of Dystonia: Ancient to Modern." Mov Disord Clin Pract **4**(4): 478-485.
- Neychev, V. K., R. E. Gross, S. Lehericy, E. J. Hess and H. A. Jinnah (2011). "The functional neuroanatomy of dystonia." Neurobiol Dis **42**(2): 185-201.
- Nibbeling, E. A., C. C. Delnooz, T. J. de Koning, R. J. Sinke, H. A. Jinnah, M. A. Tijssen and D. S. Verbeek (2017). "Using the shared genetics of dystonia and ataxia to unravel their pathogenesis." Neurosci Biobehav Rev **75**: 22-39.
- Nyhan, W. L., J. P. O'Neill, H. A. Jinnah and J. C. Harris (1993). Lesch-Nyhan Syndrome. GeneReviews((R)). M. P. Adam, H. H. Ardinger, R. A. Pagon et al. Seattle (WA).
- Oppenheim, H. (1911). "About a rare spasm disease of childhood and young age." Neurologische Centralblatt **30**: 1090-1107.
- Ostrem, J. L. and P. A. Starr (2008). "Treatment of dystonia with deep brain stimulation." Neurotherapeutics **5**(2): 320-330.
- Ozelius, L. J., J. W. Hewett, C. E. Page, S. B. Bressman, P. L. Kramer, C. Shalish, D. de Leon, M. F. Brin, D. Raymond, D. P. Corey, S. Fahn, N. J. Risch, A. J. Buckler, J. F. Gusella and X. O. Breakefield (1997). "The early-onset torsion dystonia gene (DYT1) encodes an ATP-binding protein." Nat Genet **17**(1): 40-48.
- Pearson, G., F. Robinson, T. Beers Gibson, B. E. Xu, M. Karandikar, K. Berman and M. H. Cobb (2001). "Mitogen-activated protein (MAP) kinase pathways: regulation and physiological functions." Endocr Rev **22**(2): 153-183.

- Pelosi, A., F. Menardy, D. Popa, J. A. Girault and D. Herve (2017). "Heterozygous Gnal Mice Are a Novel Animal Model with Which to Study Dystonia Pathophysiology." J Neurosci **37**(26): 6253-6267.
- Peterson, D. A., T. J. Sejnowski and H. Poizner (2010). "Convergent evidence for abnormal striatal synaptic plasticity in dystonia." Neurobiol Dis **37**(3): 558-573.
- Pisani, A., G. Bernardi, J. Ding and D. J. Surmeier (2007). "Re-emergence of striatal cholinergic interneurons in movement disorders." Trends Neurosci **30**(10): 545-553.
- Pizoli, C. E., H. A. Jinnah, M. L. Billingsley and E. J. Hess (2002). "Abnormal cerebellar signaling induces dystonia in mice." J Neurosci **22**(17): 7825-7833.
- Postuma, R. B., J. Anang, A. Pelletier, L. Joseph, M. Moscovich, D. Grimes, S. Furtado, R. P. Munhoz, S. Appel-Cresswell, A. Moro, A. Borys, D. Hobson and A. E. Lang (2017). "Caffeine as symptomatic treatment for Parkinson disease (Cafe-PD): A randomized trial." Neurology **89**(17): 1795-1803.
- Prosser, E. S., R. Pruthi and J. G. Csernansky (1989). "Differences in the time course of dopaminergic supersensitivity following chronic administration of haloperidol, molindone, or sulpiride." Psychopharmacology (Berl) **99**(1): 109-116.
- Prudente, C. N., E. J. Hess and H. A. Jinnah (2014). "Dystonia as a network disorder: what is the role of the cerebellum?" Neuroscience **260**: 23-35.
- Raike, R. S., H. A. Jinnah and E. J. Hess (2005). "Animal models of generalized dystonia." NeuroRx **2**(3): 504-512.
- Raike, R. S., C. E. Pizoli, C. Weisz, A. M. van den Maagdenberg, H. A. Jinnah and E. J. Hess (2013). "Limited regional cerebellar dysfunction induces focal dystonia in mice." Neurobiol Dis **49**: 200-210.

- Rascol, O., S. Perez-Lloret and J. J. Ferreira (2015). "New treatments for levodopa-induced motor complications." Mov Disord **30**(11): 1451-1460.
- Rashid, A. J., C. H. So, M. M. Kong, T. Furtak, M. El-Ghundi, R. Cheng, B. F. O'Dowd and S. R. George (2007). "D1-D2 dopamine receptor heterooligomers with unique pharmacology are coupled to rapid activation of Gq/11 in the striatum." Proc Natl Acad Sci U S A **104**(2): 654-659.
- Ravindran, K., N. Ganesh Kumar, D. J. Englot, T. J. Wilson and S. L. Zuckerman (2019). "Deep Brain Stimulation Versus Peripheral Denervation for Cervical Dystonia: A Systematic Review and Meta-Analysis." World Neurosurg **122**: e940-e946.
- Redgrave, P., M. Rodriguez, Y. Smith, M. C. Rodriguez-Oroz, S. Lehericy, H. Bergman, Y. Agid, M. R. DeLong and J. A. Obeso (2010). "Goal-directed and habitual control in the basal ganglia: implications for Parkinson's disease." Nat Rev Neurosci **11**(11): 760-772.
- Ren, K., B. Guo, C. Dai, H. Yao, T. Sun, X. Liu, Z. Bai, W. Wang and S. Wu (2017). "Striatal Distribution and Cytoarchitecture of Dopamine Receptor Subtype 1 and 2: Evidence from Double-Labeling Transgenic Mice." Front Neural Circuits **11**: 57.
- Renkema, G. H., S. B. Wortmann, R. J. Smeets, H. Venselaar, M. Antoine, G. Visser, T. Ben-Omran, L. P. van den Heuvel, H. J. Timmers, J. A. Smeitink and R. J. Rodenburg (2015). "SDHA mutations causing a multisystem mitochondrial disease: novel mutations and genetic overlap with hereditary tumors." Eur J Hum Genet **23**(2): 202-209.
- Richfield, E. K., J. B. Penney and A. B. Young (1989). "Anatomical and affinity state comparisons between dopamine D1 and D2 receptors in the rat central nervous system." Neuroscience **30**(3): 767-777.

- Robertson, G. S. and H. C. Fibiger (1992). "Neuroleptics increase c-fos expression in the forebrain: contrasting effects of haloperidol and clozapine." Neuroscience **46**(2): 315-328.
- Rose, S. J., T. F. Pack, S. M. Peterson, K. Payne, E. Borrelli and M. G. Caron (2018). "Engineered D2R Variants Reveal the Balanced and Biased Contributions of G-Protein and beta-Arrestin to Dopamine-Dependent Functions." Neuropsychopharmacology **43**(5): 1164-1173.
- Rose, S. J., X. Y. Yu, A. K. Heinzer, P. Harrast, X. Fan, R. S. Raike, V. B. Thompson, J. F. Pare, D. Weinshenker, Y. Smith, H. A. Jinnah and E. J. Hess (2015). "A new knock-in mouse model of l-DOPA-responsive dystonia." Brain **138**(Pt 10): 2987-3002.
- Sanberg, P. R. (1980). "Haloperidol-induced catalepsy is mediated by postsynaptic dopamine receptors." Nature **284**(5755): 472-473.
- Santini, E., C. Alcacer, S. Cacciatore, M. Heiman, D. Herve, P. Greengard, J. A. Girault, E. Valjent and G. Fisone (2009). "L-DOPA activates ERK signaling and phosphorylates histone H3 in the striatonigral medium spiny neurons of hemiparkinsonian mice." J Neurochem **108**(3): 621-633.
- Sarikcioglu, L., U. Altun, B. Suzen and N. Oguz (2008). "The evolution of the terminology of the basal ganglia, or are they nuclei?" J Hist Neurosci **17**(2): 226-229.
- Schiffmann, S. N., G. Fisone, R. Moresco, R. A. Cunha and S. Ferre (2007). "Adenosine A2A receptors and basal ganglia physiology." Prog Neurobiol **83**(5): 277-292.
- Schiffmann, S. N., O. Jacobs and J. J. Vanderhaeghen (1991). "Striatal restricted adenosine A2 receptor (RDC8) is expressed by enkephalin but not by substance P neurons: an in situ hybridization histochemistry study." J Neurochem **57**(3): 1062-1067.

- Schwarzschild, M. A., R. L. Cole and S. E. Hyman (1997). "Glutamate, but not dopamine, stimulates stress-activated protein kinase and AP-1-mediated transcription in striatal neurons." J Neurosci **17**(10): 3455-3466.
- Seeman, P., D. Weinshenker, R. Quirion, L. K. Srivastava, S. K. Bhardwaj, D. K. Grandy, R. T. Premont, T. D. Sotnikova, P. Boksa, M. El-Ghundi, F. O'Dowd B, S. R. George, M. L. Perreault, P. T. Mannisto, S. Robinson, R. D. Palmiter and T. Talerico (2005). "Dopamine supersensitivity correlates with D2High states, implying many paths to psychosis." Proc Natl Acad Sci U S A **102**(9): 3513-3518.
- Segawa, M. (2011). "Hereditary progressive dystonia with marked diurnal fluctuation." Brain Dev **33**(3): 195-201.
- Sethi, K. D., D. C. Hess and R. J. Harp (1990). "Prevalence of dystonia in veterans on chronic antipsychotic therapy." Mov Disord **5**(4): 319-321.
- Seyfried, N. T., E. B. Dammer, V. Swarup, D. Nandakumar, D. M. Duong, L. Yin, Q. Deng, T. Nguyen, C. M. Hales, T. Wingo, J. Glass, M. Gearing, M. Thambisetty, J. C. Troncoso, D. H. Geschwind, J. J. Lah and A. I. Levey (2017). "A Multi-network Approach Identifies Protein-Specific Co-expression in Asymptomatic and Symptomatic Alzheimer's Disease." Cell Syst **4**(1): 60-72 e64.
- Shakkottai, V. G., A. Batla, K. Bhatia, W. T. Dauer, C. Dresel, M. Niethammer, D. Eidelberg, R. S. Raike, Y. Smith, H. A. Jinnah, E. J. Hess, S. Meunier, M. Hallett, R. Fremont, K. Khodakhah, M. S. LeDoux, T. Popa, C. Gallea, S. Lehericy, A. C. Bostan and P. L. Strick (2017). "Current Opinions and Areas of Consensus on the Role of the Cerebellum in Dystonia." Cerebellum **16**(2): 577-594.

- Shaywitz, B. A., R. D. Yager and J. H. Klopfer (1976). "Selective brain dopamine depletion in developing rats: an experimental model of minimal brain dysfunction." Science **191**(4224): 305-308.
- Shen, W. W. (1999). "A history of antipsychotic drug development." Compr Psychiatry **40**(6): 407-414.
- Shiflett, M. W., R. A. Brown and B. W. Balleine (2010). "Acquisition and performance of goal-directed instrumental actions depends on ERK signaling in distinct regions of dorsal striatum in rats." J Neurosci **30**(8): 2951-2959.
- Sibley, D. R. and F. J. Monsma, Jr. (1992). "Molecular biology of dopamine receptors." Trends Pharmacol Sci **13**(2): 61-69.
- Simonyan, K., H. Cho, A. Hamzehei Sichani, E. Rubien-Thomas and M. Hallett (2017). "The direct basal ganglia pathway is hyperfunctional in focal dystonia." Brain **140**(12): 3179-3190.
- Sindreu, C. B., Z. S. Scheiner and D. R. Storm (2007). "Ca²⁺ -stimulated adenylyl cyclases regulate ERK-dependent activation of MSK1 during fear conditioning." Neuron **53**(1): 79-89.
- Siokas, V., A. M. Aloizou, Z. Tsouris, A. Michalopoulou, A. A. Mentis and E. Dardiotis (2018). "Risk Factor Genes in Patients with Dystonia: A Comprehensive Review." Tremor Other Hyperkinet Mov (N Y) **8**: 559.
- Skeberdis, V. A., V. Chevalyere, C. G. Lau, J. H. Goldberg, D. L. Pettit, S. O. Suadicani, Y. Lin, M. V. Bennett, R. Yuste, P. E. Castillo and R. S. Zukin (2006). "Protein kinase A regulates calcium permeability of NMDA receptors." Nat Neurosci **9**(4): 501-510.

- Smith, J. S. and S. Rajagopal (2016). "The beta-Arrestins: Multifunctional Regulators of G Protein-coupled Receptors." J Biol Chem **291**(17): 8969-8977.
- Smith, Y., D. V. Raju, J. F. Pare and M. Sidibe (2004). "The thalamostriatal system: a highly specific network of the basal ganglia circuitry." Trends Neurosci **27**(9): 520-527.
- Smrcka, A. V. (2008). "G protein betagamma subunits: central mediators of G protein-coupled receptor signaling." Cell Mol Life Sci **65**(14): 2191-2214.
- Soeder, A., B. M. Kluger, M. S. Okun, C. W. Garvan, T. Soeder, C. E. Jacobson, R. L. Rodriguez, R. Turner and H. H. Fernandez (2009). "Mood and energy determinants of quality of life in dystonia." J Neurol **256**(6): 996-1001.
- Sternweis, P. C. and J. D. Robishaw (1984). "Isolation of two proteins with high affinity for guanine nucleotides from membranes of bovine brain." J Biol Chem **259**(22): 13806-13813.
- Strzelczyk, A., K. Burk and W. H. Oertel (2011). "Treatment of paroxysmal dyskinesias." Expert Opin Pharmacother **12**(1): 63-72.
- Surmeier, D. J., J. Ding, M. Day, Z. Wang and W. Shen (2007). "D1 and D2 dopamine-receptor modulation of striatal glutamatergic signaling in striatal medium spiny neurons." Trends Neurosci **30**(5): 228-235.
- Svenningsson, P., M. Lindskog, F. Rognoni, B. B. Fredholm, P. Greengard and G. Fisone (1998). "Activation of adenosine A2A and dopamine D1 receptors stimulates cyclic AMP-dependent phosphorylation of DARPP-32 in distinct populations of striatal projection neurons." Neuroscience **84**(1): 223-228.

- Svenningsson, P., A. Nishi, G. Fisone, J. A. Girault, A. C. Nairn and P. Greengard (2004). "DARPP-32: an integrator of neurotransmission." Ann Rev Pharmacol Toxicol **44**: 269-296.
- Tadic, V., M. Kasten, N. Bruggemann, S. Stiller, J. Hagenah and C. Klein (2012). "Dopa-responsive dystonia revisited: diagnostic delay, residual signs, and nonmotor signs." Arch Neurol **69**(12): 1558-1562.
- Tepper, J. M. and J. P. Bolam (2004). "Functional diversity and specificity of neostriatal interneurons." Curr Opin Neurobiol **14**(6): 685-692.
- Thenganatt, M. A. and J. Jankovic (2014). "Treatment of dystonia." Neurotherapeutics **11**(1): 139-152.
- Thomas, G. M. and R. L. Huganir (2004). "MAPK cascade signalling and synaptic plasticity." Nat Rev Neurosci **5**(3): 173-183.
- Thomas, S. A., A. M. Matsumoto and R. D. Palmiter (1995). "Noradrenaline is essential for mouse fetal development." Nature **374**(6523): 643-646.
- Thompson, V. B., H. A. Jinnah and E. J. Hess (2011). "Convergent mechanisms in etiologically-diverse dystonias." Expert Opin Ther Targets **15**(12): 1387-1403.
- Threlfell, S. and A. R. West (2013). "Review: Modulation of striatal neuron activity by cyclic nucleotide signaling and phosphodiesterase inhibition." Basal Ganglia **3**(3): 137-146.
- Tiranti, V., C. Viscomi, T. Hildebrandt, I. Di Meo, R. Minerì, C. Tiveron, M. D. Levitt, A. Prelle, G. Fagiolarì, M. Rimoldi and M. Zeviani (2009). "Loss of ETHE1, a mitochondrial dioxygenase, causes fatal sulfide toxicity in ethylmalonic encephalopathy." Nat Med **15**(2): 200-205.

- Tolosa, E. and Y. Compta (2006). "Dystonia in Parkinson's disease." J Neurol **253 Suppl 7**: VII7-13.
- Traynelis, S. F., L. P. Wollmuth, C. J. McBain, F. S. Menniti, K. M. Vance, K. K. Ogden, K. B. Hansen, H. Yuan, S. J. Myers and R. Dingledine (2010). "Glutamate receptor ion channels: structure, regulation, and function." Pharmacol Rev **62**(3): 405-496.
- Trugman, J. M., R. Leadbetter, M. E. Zalis, R. O. Burgdorf and G. F. Wooten (1994). "Treatment of severe axial tardive dystonia with clozapine: case report and hypothesis." Mov Disord **9**(4): 441-446.
- Turner, M., H. S. Nguyen and A. A. Cohen-Gadol (2012). "Intraventricular baclofen as an alternative to intrathecal baclofen for intractable spasticity or dystonia: outcomes and technical considerations." J Neurosurg Pediatr **10**(4): 315-319.
- Ungerstedt, U. (1971). "Adipsia and aphagia after 6-hydroxydopamine induced degeneration of the nigro-striatal dopamine system." Acta Physiol Scand Suppl **367**: 95-122.
- Valjent, E., J. C. Corvol, C. Pages, M. J. Besson, R. Maldonado and J. Caboche (2000). "Involvement of the extracellular signal-regulated kinase cascade for cocaine-rewarding properties." J Neurosci **20**(23): 8701-8709.
- Valjent, E., V. Pascoli, P. Svenningsson, S. Paul, H. Enslen, J. C. Corvol, A. Stipanovich, J. Caboche, P. J. Lombroso, A. C. Nairn, P. Greengard, D. Herve and J. A. Girault (2005). "Regulation of a protein phosphatase cascade allows convergent dopamine and glutamate signals to activate ERK in the striatum." Proc Natl Acad Sci U S A **102**(2): 491-496.
- Vallone, D., R. Picetti and E. Borrelli (2000). "Structure and function of dopamine receptors." Neurosci Biobehav Rev **24**(1): 125-132.

- Vanhoutte, P., J. V. Barnier, B. Guibert, C. Pages, M. J. Besson, R. A. Hipskind and J. Caboche (1999). "Glutamate induces phosphorylation of Elk-1 and CREB, along with c-fos activation, via an extracellular signal-regulated kinase-dependent pathway in brain slices." Mol Cell Biol **19**(1): 136-146.
- Walaas, S. I., D. W. Aswad and P. Greengard (1983). "A dopamine- and cyclic AMP-regulated phosphoprotein enriched in dopamine-innervated brain regions." Nature **301**(5895): 69-71.
- Walsh, D. J., E. S. Sills, D. M. Lambert, N. Gregersen, F. D. Malone and A. P. Walsh (2010). "Novel ETHE1 mutation in a carrier couple having prior offspring affected with ethylmalonic encephalopathy: Genetic analysis, clinical management and reproductive outcome." Mol Med Rep **3**(2): 223-226.
- Wang, J. Q., E. E. Fibuch and L. Mao (2007). "Regulation of mitogen-activated protein kinases by glutamate receptors." J Neurochem **100**(1): 1-11.
- Warnke, P. C. (2015). "Selective peripheral denervation for cervical dystonia: a historical procedure in the age of deep brain stimulation?" J Neurol Neurosurg Psychiatry **86**(12): 1283.
- Watari, K., M. Nakaya and H. Kurose (2014). "Multiple functions of G protein-coupled receptor kinases." J Mol Signal **9**(1): 1.
- Westin, J. E., L. Vercaamen, E. M. Strome, C. Konradi and M. A. Cenci (2007). "Spatiotemporal pattern of striatal ERK1/2 phosphorylation in a rat model of L-DOPA-induced dyskinesia and the role of dopamine D1 receptors." Biol Psychiatry **62**(7): 800-810.

- Wichmann, T. (2008). "Commentary: Dopaminergic dysfunction in DYT1 dystonia." Exp Neurol **212**(2): 242-246.
- Wijemanne, S. and J. Jankovic (2015). "Dopa-responsive dystonia--clinical and genetic heterogeneity." Nat Rev Neurol **11**(7): 414-424.
- Wilson, C. J. and P. M. Groves (1980). "Fine structure and synaptic connections of the common spiny neuron of the rat neostriatum: a study employing intracellular inject of horseradish peroxidase." J Comp Neurol **194**(3): 599-615.
- Woisard, V., X. Liu, M. C. Bes and M. Simonetta-Moreau (2017). "Botulinum toxin injection in laryngeal dyspnea." Eur Arch Otorhinolaryngol **274**(2): 909-917.
- Xie, K. and K. A. Martemyanov (2011). "Control of striatal signaling by g protein regulators." Front Neuroanat **5**: 49.
- Yalcin-Cakmakli, G., S. J. Rose, R. M. Villalba, L. Williams, H. A. Jinnah, E. J. Hess and Y. Smith (2018). "Striatal Cholinergic Interneurons in a Knock-in Mouse Model of L-DOPA-Responsive Dystonia." Front Syst Neurosci **12**: 28.
- Yapo, C., A. G. Nair, J. Hellgren Kotaleski, P. Vincent and L. R. V. Castro (2018). "Switch-like PKA responses in the nucleus of striatal neurons." J Cell Sci **131**(14).
- Zeman, W., R. Kaelbling, B. Pasamanick and J. T. Jenkins (1959). "Idiopathic dystonia musculorum deformans. I. The hereditary pattern." Am J Hum Genet **11**(2 Part 1): 188-202.
- Zhang, Y., L. Li, W. Chen, J. Gan and Z. G. Liu (2017). "Clinical characteristics and PRRT2 gene mutation analysis of sporadic patients with paroxysmal kinesigenic dyskinesia in China." Clin Neurol Neurosurg **159**: 25-28.

Zhao, Y., N. Sharma and M. S. LeDoux (2011). "The DYT1 carrier state increases energy demand in the olivocerebellar network." Neuroscience **177**: 183-194.

Zhou, Q. Y. and R. D. Palmiter (1995). "Dopamine-deficient mice are severely hypoactive, adipsic, and aphagic." Cell **83**(7): 1197-1209.

Zhou, Q. Y., C. J. Quaife and R. D. Palmiter (1995). "Targeted disruption of the tyrosine hydroxylase gene reveals that catecholamines are required for mouse fetal development." Nature **374**(6523): 640-643.